EARTHQUAKE INDUCED DAMAGE ESTIMATION FOR STEEL BUILDINGS IN PUERTO RICO

by

Gustavo Cortés-Areizaga

A thesis submitted in partial fulfillment of the requirements for the degree of

MASTER OF SCIENCE
in
CIVIL ENGINEERING

UNIVERSITY OF PUERTO RICO
MAYAGÜEZ CAMPUS
2006

Approved by:

_____	_____
Ali Saffar, PhD Member, Graduate Committee	Date
_____	_____
Luis E. Suárez Colche, PhD Member, Graduate Committee	Date
_____	_____
Ricardo López Rodríguez, PhD President, Graduate Committee	Date
_____	_____
Pablo Cáceres Valencia, PhD Representative of Graduate Studies	Date
_____	_____
Ismael Pagán Trinidad, MSCE Chairperson of the Department	Date

ABSTRACT

This work presents a method for estimating the expected damage caused by an earthquake on steel buildings in Puerto Rico. Since Puerto Rico is located between a series of tectonic faults, buildings could suffer the damages caused by a major earthquake. The objective of this research is to develop the information needed for insurance companies to estimate the earthquake damage of steel buildings in a simple and practical way. Steel buildings typically found in Puerto Rico have been analyzed. The response of these buildings to many acceleration time histories have been recorded. With these recorded data, fragility curves which indicate the probability of a damage state to occur were created. A cost per square foot has been assigned to each damage state. This cost is then multiplied by the probability of damage for each damage state and the final expected cost for the total damage is obtained.

RESUMEN

Este trabajo presenta un método para estimar los daños causados por terremotos a estructuras de acero. Puerto Rico se encuentra rodeado de fallas tectónicas lo que hace que las estructuras estén propensas a sufrir los daños ocasionados por un terremoto. Nuestro objetivo es desarrollar la información necesaria para que las compañías de seguros puedan estimar el daño causado por un terremoto a estructuras de acero de una forma sencilla y práctica. Se investigaron estructuras típicas de acero construidas en Puerto Rico. Además, se consideró su respuesta a diferentes registros de aceleración. Con esto se han tomado los datos estadísticos y se han creado curvas que muestran la probabilidad de que algún estado de daño ocurra en la estructura. A cada estado de daño se le asigna un costo por pie cuadrado, el que luego será multiplicado por la probabilidad obtenida de las curvas para cada estado de daño y finalmente se obtiene el costo de daños para la estructura.

TO THE GIVER OF LIFE, GOD

TO MY FAMILY, IN SPECIAL TO MY MOM

TO MY DAD'S MEMORY

ACKNOWLEDGEMENTS

During the development of my graduate studies in the University of Puerto Rico, Mayagüez Campus, several persons and institutions collaborated directly and indirectly with my research. Without their support, it would have been impossible for me to finish my work. I wish to dedicate this section to recognize their support.

I want to gratefully acknowledge my advisor, Dr. Ricardo López for giving me the opportunity to research under his guidance and supervision. Special thanks I also owe to Dr. Luis Suárez and Dr. Ali Saffar for providing me with their supervision, and transmitted knowledge for the completion of my work.

Many companies dedicated to the fabrication of steel buildings in Puerto Rico provided typical plans of buildings they have built. That information was crucial for this research investigation and thus I wish to thank them. These companies are FCS Steel Corp., American Agencies Co, and Structural Steel Works Inc.

I also wish to thank Eng. John Gil and Dr. Vinay K. Goyal for providing their help and for encouraging me, when I needed the most.

Table of Contents

List of Tables

Tables **Page**

List of Figures

Figures **Page**

1 INTRODUCTION

The Civil Engineering and Surveying Department of the University of Puerto Rico, Mayagüez Campus is conducting research on the expected damages that civil structures would suffer if a natural disaster, such as an earthquake or hurricane occurs. The results obtained in this series of investigations will be utilized by the Insurance Commissioner of Puerto Rico. These investigations will develop a better understanding of the behavior of the different structures that are been built in Puerto Rico. At the same time it will provide the Insurance Commissioner of Puerto Rico useful tools to better estimate the risks associated with different structures. As part of the ongoing research, the behavior of the different structures will be studied accordingly to its structural type, occupancy and location.

Earthquakes are caused by the sudden slip of the Earth's crust at a fault. They include a violent shaking of the Earth that releases a large elastic strain energy and spreads through seismic waves that travel throughout the body and along the surface of the Earth. Structures are connected to the soil via a foundation system, which is the one that receives the acceleration and transmits it through the entire structure. Therefore, these structures try to remain in their original position due to the elastic forces acting on them. Hence, different structures will behave different to a same earthquake depending primary on the earthquake frequency content, amplitude, duration and the structures' flexibility and strength.

Puerto Rico is bounded by many faults; the two principal faults are the Great Northern Puerto Rico Fault Zone and the Great Southern Puerto Rico Fault Zone. There are a number of earthquakes that have affected Puerto Rico in the past. For example, in November 17, 1867, a 7.3 magnitude earthquake with an epicenter located at the Anegada Passage was

strongly felt in Puerto Rico. This earthquake caused most of its damages in the Eastern zone. Also, on October 11, 1918 the most devastating earthquake in the history of Puerto Rico occurred. It had an estimated magnitude of 7.3 on the Richter scale, and its origin was in the Mona Passage, about 50 km from the Northwestern coast of the Island. As a consequence, a tsunami that followed the earthquake affected the West side of Puerto Rico. The devastating earthquake left 116 people dead and the economical loss was estimated in over 4 million dollars at that time. The last earthquake felt in Puerto Rico occurred in August 4, 1946. Its epicenter was located in the Northeastern side of the Dominican Republic with an estimated 7.8 surface magnitude. However, only minor damages were reported in Puerto Rico.

The history of Puerto Rico's past earthquakes and the probability that more of these events may happen is a primary motivation for this investigation. Therefore, the purpose of this research is to estimate the structural damages a given building will suffer due to an earthquake. The building will be subjected to economical losses caused by different events and situations. These may include losses by damaged contents, removing debris, business interruption, renting alternative space, and moving to a new location, to list only a few examples. In addition to these, we may consider social losses such as injuries, deaths, and the need of emergency shelters. It is also possible that many other disasters may follow the earthquake, including land sliding, tsunamis, fires, and flooding. All these will generate additional damage to the structures, sometimes even worse than the ones caused by the earthquake itself.

Economic losses caused by earthquakes to the structural elements (force resisting elements) and to the non-structural elements are called Direct Losses; while other losses occurring from other disasters following the earthquake are called Indirect Losses. The

emphasis of this research will be given on calculating the Direct Losses to the structural elements of steel buildings.

1.1 Motivation and Objective

Are steel buildings in Puerto Rico capable of sustaining a large magnitude earthquake? How much damage a typical building will suffer if such event occurs? The need for answering these questions for a better understanding of the behavior of constructed steel buildings in Puerto Rico and their seismic behavior is the base for this thesis.

The objective of this thesis was to create fragility curves for the typical steel buildings found in Puerto Rico and to relate these curves to the expected damage cost.

1.2 Literature Review

A vast amount of researchers have been developing methods for estimating accurately the expected damages a certain structure will suffer if an earthquake occurs. Insurance Companies all around the globe are funding investigations for a better understanding of this phenomenon.

FEMA-355E (FEMA-351 2000) concludes that the Welded Steel Moment Frame (WSMF) is a relatively young structural system, and until the Northridge earthquake it had not been tested in large numbers by a real earthquake. The post-Northridge story offers compelling lessons as well. As connection damages were found, studied, and understood, engineers learned volumes about steel, welding, construction quality, fracture mechanics, and the demands of real earthquakes. It was after the 1994 Northridge earthquake that more attention was given to the estimation of damage in steel buildings and to the development of more rigorous procedures to predict the costs of damage.

Appendix B of the FEMA-351 presents a method for estimating the damage loss in structures using the results from a nonlinear static analysis (pushover analysis). A base shear versus displacement plot is obtained from the pushover analysis and is then transformed to spectral acceleration versus spectral displacement curve. The performance point is found from the intersection between the capacity curve and the demand curve. This point's abscise value is referred to as the spectral displacement and is used as the response parameter. Fragility curves correlating the spectral displacement with the expected damage are made on this basis. Finally, loss functions relating the damage to loss cost are made, and the final output is obtained.

The procedures utilized by FEMA-351 are compatible with the HAZUS methodology (NIBS 1997a). HAZUS is a complex collection of modules that work together to estimate casualties and economic impacts on a region due to an earthquake scenario. HAZUS was developed for FEMA by the National Institute of Building Sciences (NIBS) and is documented in a three-volume Technical Manual (NIBS, 1997b). One of the main components of the methodology estimates the probability of various states of structural and nonstructural damage to buildings. Other modules of the methodology use the damage state probabilities to estimate various types of building-related losses. HAZUS is intended primarily for use in estimating earthquake losses in regions with a large inventory of buildings represented by generic building types. In principle, this software could be used for Puerto Rico; however this research seeks to create more realistic fragility curves for the Island buildings.

Smyth et al. (2004) developed fragility curves to determine when retrofitting of structures would be a good option for Istanbul, Turkey. In their paper the authors created 4 models for

a 4 stories reinforced concrete building. In the first model the structure was modeled representing the actual state of the building. Three different alternatives of retrofitting for the building were also modeled: the building with cross bracing, with partial shear walls, and with full shear walls distributed along the corners. The authors used a nonlinear dynamic analysis to analyze the three different structural configurations. Fragility curves were then generated, and peak ground acceleration (PGA) was used as the abscise, instead of spectral displacement (Sd) which is used by FEMA-351. The authors concluded that in some cases it is cost effective to retrofit the building, while in other cases retrofitting the building is not a viable alternative.

Fragilities curves have been widely applied to the bridge retrofitting analysis. Shinozuka et al. (2001) used a method to create fragility curves empirically or analytically. In the examples given, they created empirical fragility curves using data from the 1994 Northridge earthquake and from the 1995 Kobe earthquake. They also developed analytical fragility curves for bridges in Memphis, Tennessee using non linear analyses. Shinozuka et al. used a Bernoulli type experiment in which only two options are possible, success or failure. The maximum likelihood method is employed in this work to find the two parameters that describe the fragility curves (median and log-standard deviation).

In a similar way, Karim and Yamazaki (2001) analyzed highway bridges analytically by modeling a typical bridge according to the seismic design provisions of Japan. They used strong motion records from Japan and the United States, and performed nonlinear analyses to obtain the damage indexes. They utilized a probabilistic logarithmic plot of the damage index versus the peak ground acceleration (PGA). The damage ratio was found by dividing the number of occurrence of each damage rank by the total number of records. Likewise, the

Bayesian probability method was employed to combine empirical results from past earthquakes with analytical models. Singhal and Kiremidjian (1998) used this method to update earthquake ground motion versus damage relationships in the form of fragility curves and for estimating confidence bounds on theses fragility curves.

Finally, Ellingwood et al. (2001) proposed a fragility curve methodology to asses the response of light-frame wood construction exposed to stipulated extreme windstorms and earthquakes. Their objective was to provide effective strategies for improving structural safety and performance and also, to mitigate social and economic losses from competing natural hazards.

1.3 Summary of the Following Chapters

Chapter 2 starts by introducing the history of steel buildings and the typical failure modes associated with them. It then explains the different methods available for analyzing the structures. Chapter 3 explains the methodology followed to estimate damage suffered by a typical steel building. It defines the response parameters, the damage states (DS), and the values utilized for each damage state. Chapter 4 explains the mechanical representation of steel buildings used for the nonlinear analysis, including the beam element, column element, panel zone element and footing element models. The five time history records used are also shown in this Chapter. Finally, the nonlinear model as well as the integration method for the nonlinear dynamic procedure is explained. Chapter 5 explains the procedure used to create fragility curves including an example for a four story commercial building. Also in this Chapter a simplified method is discussed. The study continues with a description of the generated models and its fragility curves on Chapter 6. The generated fragility curves with all the statistics involved for each type of building analyzed are also shown in this chapter.

Chapter uses the same example discussed in Chapter 5 to explain the development of the loss functions and its applications. Finally, Chapter 8 presents the conclusions, recommendations and the proposed future work.

2 THEORETICAL BACKGROUND

2.1 Introduction

This Chapter's objective is to provide with relevant background information needed to better understand this research. Section 2.2 describes the most common components of a steel building. A brief description of the evolution of steel as a material is found in Section 2.3 of this chapter. The typical failure modes found in steel buildings are discussed in Section 2.4. Section 2.5 discusses the different analysis methods and its selection criterion. Finally, Section 2.6 shows a series of PGA contour maps that were created by the United States Geological Survey (USGS).

2.2 Basic Components

Steel buildings are the product of a number of individual elements connected together. The global building's lateral stability is usually provided by moment resisting frames, braced frames, shear walls and/or other equivalent lateral load resisting system. In moment resisting frame systems the lateral stability is provided by the flexural stiffness of connected beams and columns. Braced frame or shear wall systems stability is obtained by the use of bracing or shear walls, respectively, connected to the frame.

Typical elements found in a structural steel building are:

- Columns – structural member which mainly resists axial loads
- Beams – structural member which mainly resists flexural forces

- Beam – column – structural member which resists both axial forces and flexural forces
- Connections – elements at joints used to transmit loads between two or more elements
- Panel Zone – web area of beam to column connection, transmitting moment through a shear panel
- Bracing – typically carries axial force, it is usually placed diagonally in braced frames to limit deflection in a building system
- Steel joists – secondary members which resist the gravity loads acting on a floor system
- Metal deck – thin membrane provided to resist the direct forces and transmit them uniformly among the structural members
- Cold formed sections – typical cold formed sections are c or z purlins
- Base plates – Plates at the base of the columns which transmit the concentrated load of the columns more uniformly to the columns
- Shear Studs – steel member embedded in concrete intended to transmit the shear forces at the interface of the two materials

Figure 2.1 shows some of the aforementioned components found in a typical Moment-Resisting Steel Frame.

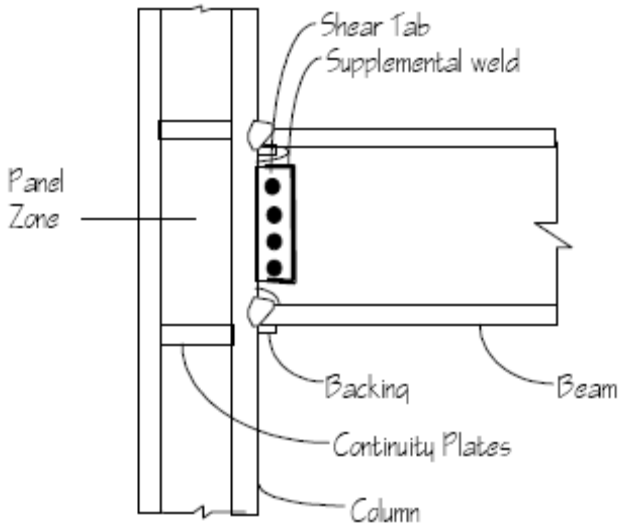

Figure 2.1 Basic components of a moment resisting frame connection

2.3 Steel Buildings History

Steel has been used in building construction for more than a century. At the beginning, construction designers used riveted connections as those illustrated in Figure 2.2. They were typically assumed as "pinned" connection for carrying gravity loads, and the stiffened connection was assumed "fixed" for lateral loads.

These early buildings used unreinforced masonry walls on the exterior frames. By the late 40's, curtain walls started to be used, and the need to design the steel frames to resist lateral loads emerged. Furthermore, design codes were improving its procedures and structures were required to resist more lateral loads. All this changed the way connections were designed and connections that allowed the beams to develop its full flexural capacity became the rule. When welding became very popular, connections used to be bolted to the beams web and welded to the columns flange.

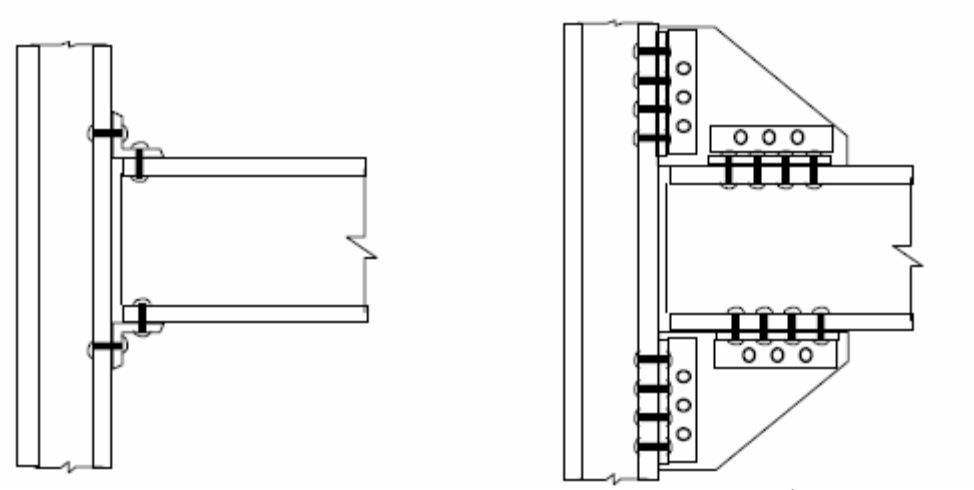

Figure 2.2 Typical early beam-column connections[1]

Many designers believed that steel buildings were not vulnerable to earthquake hazards until the 1994 Northridge earthquake. This earthquake changed that paradigm and revealed that steel buildings are as susceptible to damage as buildings made of any other material (FEMA-351 2000).

2.4 Failure Modes

FEMA-267 categorized the damages in steel buildings in accordance with the following classification: damage in the weld (W), girder (G), column (C), panel zone (P), or shear tab (S). Damage at a connection may be confined to one category or may include multiple types. The damaged welded steel moment frame (WSMF) may also exhibit global effects, such as permanent inter-story drifts (FEMA-351 2000). The next subsections briefly identify the different damages found after the 1994 Northridge earthquake; the table and figures where obtained from the FEMA-351 Manual.

[1] Figure taken from FEMA-351(SAC Joint Venture, 2000)

2.4.1 Typical damage

A. Girder Damage(G)

Type	Description
G1	Buckled flange (top or bottom)
G2	Yielded flange (top or bottom)
G3	Flange fracture in heat affected zone (HAZ) (top or bottom)
G4	Flange fracture outside heat affected zone (HAZ) (top or bottom)
G5	Flange fracture top and bottom (not used)
G6	Yielding or buckling of web
G7	Fracture of web
G8	Lateral torsional buckling of section

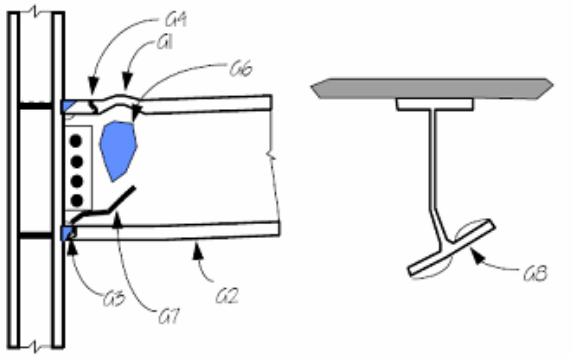

9

Figure 2.3 Girder damage[2]

B. Column Damage

Type	Description
C1	Incipient flange crack
C2	Flange tear-out or divot
C3	Full or partial flange crack outside heat-affected zone
C4	Full or partial flange crack in heat-affected zone
C5	Lamellar flange tearing
C6	Buckled flange
C7	Column splice failure

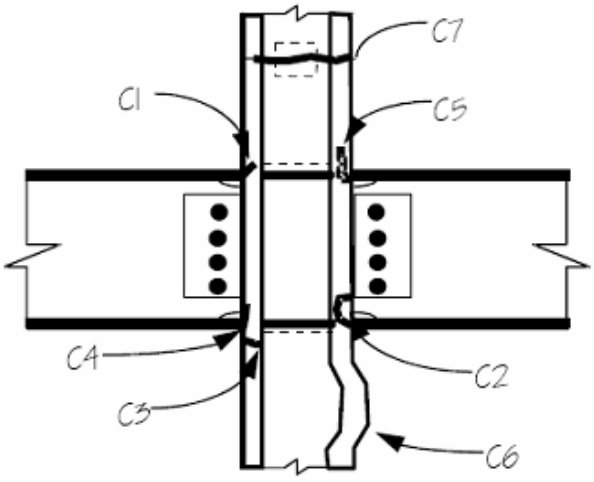

Figure 2.4 Column damage[2]

[2] Figure taken from FEMA-351(SAC Joint Venture, 2000)

C. Damage in the Weld

Type	Description
W2	Crack through weld metal thickness
W3	Fracture at column interface
W4	Fracture at girder flange interface

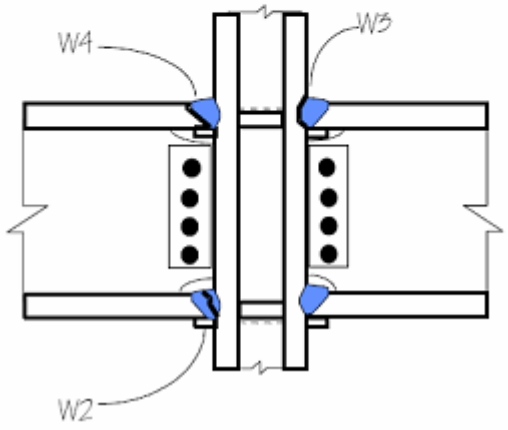

Figure 2.5 Weld damage types[3]

D. Shear tap damage

Type	Description
S1	Partial crack at weld to column
S2	Fracture of supplemental weld
S3	Fracture through tab at bolts or severe distortion
S4	Yielding or buckling of tab
S5	Loose, damaged or missing bolts
S6	Full length fracture of weld to column

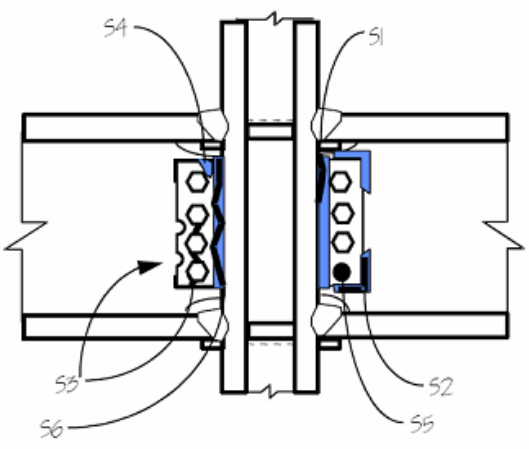

Figure 2.6 Shear tap damage[3]

[3] Figure taken from FEMA-351(SAC Joint Venture, 2000)

E. Panel Zone Damage

Type	Description
P1	Fracture, buckle or yield of continuity plate
P2	Fracture in continuity plate welds
P3	Yielding or ductile deformation of web
P4	Fracture of doubler plate welds
P5	Partial depth fracture in doubler plate
P6	Partial depth fracture in web
P7	Full or near full depth fracture in web or doubler
P8	Web buckling
P9	Severed column

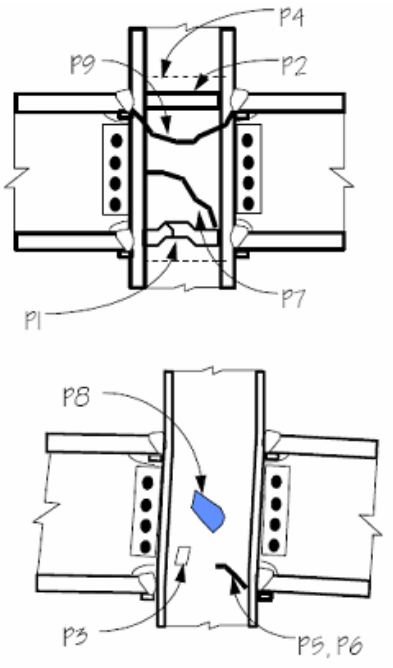

Figure 2.7 Panel zone damages[4]

2.4.2 Connections

Connections are responsible for transmitting the loads carried by the girders to the column elements. There are many types of connections; a designer may propose a connection to transmit moments and shear forces, or to transmit only shear forces. Buildings whose connections are intended to carry only the shear forces need other elements (bracing or shear walls) to resist the design lateral forces. Connections built before the 1994 Northridge earthquake are usually called Pre – Northridge connections, Figure 2.8 shows a typical Pre – Northridge connection.

[4] Figure taken from FEMA-351(SAC Joint Venture, 2000)

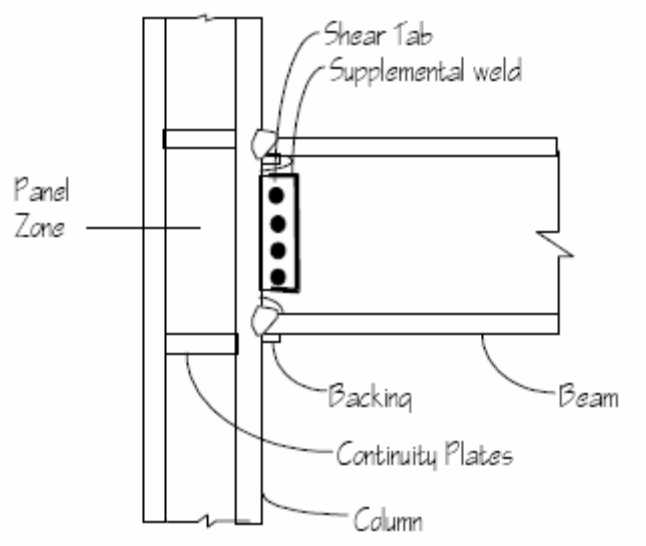

Figure 2.8 Typical Pre – Northridge connection[5]

After the 1994 Northridge earthquake building officials discovered the poor behavior of the connections and realized how vulnerable they were been designed and built. The urge to improve the design of such elements emerged. An improved connection that added cover plates to the beam, one over the top flange and one below the bottom flange became very common in practice. Figure 2.9 shows a typical Post – Northridge connection.

The new 2005 American Institute of Steel Construction (AISC) code includes the Seismic Provisions for Structural Steel Buildings. This Seismic Provisions state that the design of a member that is part of the seismic lateral resisting system shall be design such that a ductile limit state in either the connection or the member controls the design.

[5] Figure taken from FEMA-351(SAC Joint Venture, 2000)

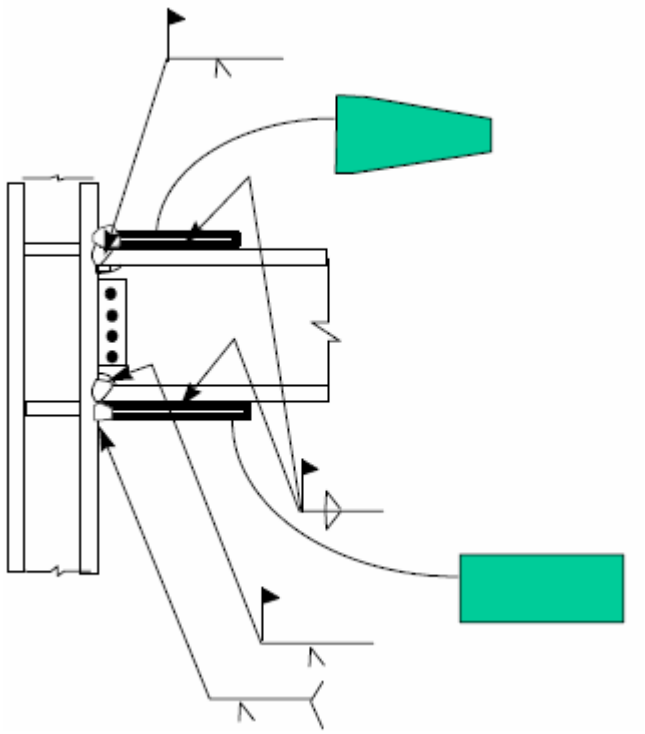

Figure 2.9 Typical moment connection after the 1994 Northridge earthquake[6]

2.5 Method Selection

As part of this research it is necessary to create mathematical models that represent the buildings, its structural features and its behavior. Structural analyses performed are intended to predict the values of key response parameters that are indicative of the structure's performance when it is subjected to ground motion. A decision regarding what analysis method should be used needs to be made. Four methods are commonly stated by the design codes; these methods are: (1) Linear Static Procedure (LSP), (2) Linear Dynamic Procedure

[6] Figure taken from FEMA-351(SAC Joint Venture, 2000)

(LDP), (3) Non Linear Static Procedure (NSP), and (4) Non Linear Dynamic Procedure (NDP). The following subsections briefly discuss the different methods aforementioned.

2.5.1 Linear Static Procedure

A linear static procedure is the method typically used by design professionals when designing a new structure. Earthquake forces are determined from Newton's 2nd law:

$$F = ma \qquad \textbf{(2.1)}$$

where:

F = force [Newtons, lb-f, kips],

m = mass of the system [kg, lb-m], and

a = acceleration [m/s^2, ft/s^2].

Thus, depending on the mass and the earthquake acceleration, floor accelerations are estimated and corresponding forces are assigned as static loads to the building. A base shear is calculated and then distributed along the building stories.

Although the linear static procedure is very commonly used in the design of new buildings, it does not account for the nonlinearities found in the structures. Not accounting for the nonlinearities tend to overestimate the forces assigned to the structure; therefore, this method was not be used here.

2.5.2 Linear Dynamic Procedure

Under the linear dynamic procedure, inertial seismic forces, their distribution over the height of the building, and the corresponding internal forces and system displacements are determined using a linearly elastic, response spectrum analysis. The linear dynamic procedure is very similar to the dynamic non-linear procedure; and for structures with an elastic behavior it tends to work very well.

As explained in section 2.5.1 a linear analysis does not take into account the different nonlinearities expected on the structures. Therefore, a linear method for analyzing the structures is not desirable for the purpose of this research.

2.5.3 Non Linear Static Procedure (Push-Over Analysis)

A push over analysis is a nonlinear static method in which deformations are induced by monotonically increasing lateral loads. Buildings are evaluated by using a series of incremental elastic analyses that are sequentially degraded to represent the effects of the structural nonlinearity.

The output of the push-over analysis is a base force versus displacement plot. The resulting graph gives us the capacity curve which is needed to find the peak building response. A coordinate transformation from coordinates of base shear and roof displacement to coordinates of spectral acceleration and spectral displacement must be made. This coordinate transformation is done by using equations 2.2 and 2.3 shown below (FEMA-351 2000).

$$S_{Ai} = \frac{\left(V_i / W\right)}{\alpha_1} \quad \textbf{(2.2)}$$

$$S_{Di} = \alpha_2 \Delta_i \quad \textbf{(2.3)}$$

where:

α_1 = fraction of building weight effective in the fundamental mode in the direction under consideration,

α_2 = fraction of building height at the elevation where the fundamental-mode displacement is equal to spectral displacement,

Δ_i = displacement at point "i" on the pushover curve,

V_i = base shear force at point "i" on the pushover curve, and

W = building weight.

As stated in Section 1.2, this methodology has been used by FEMA and it's the base for HAZUS. Although the nonlinear static procedure seems to work very well on estimating the damages, it has limitations. The method only takes into account the first mode of vibration, which means that it should not be used in structures where higher modes of vibration contribute significantly to the response. An example of this procedure is found in Appendix A.

2.5.4 Non Linear Dynamic Procedure (NDP)

A NDP, also known as a Non Linear Time History Analysis, is a step-by-step analysis of a structure subjected to loads that vary with time, such as an earthquake. The dynamic equilibrium equation is solved at every time step (Chopra 2001):

$$M\,a(t) + C\,v(t) + K\,u(t) = r(t) \qquad \textbf{(2.4)}$$

where:

M = diagonal mass matrix,

C = damping matrix,

K = stiffness matrix, and

r(t) = the applied load (or acceleration).

In the NDP an acceleration record is input at the base of the structure. The internal forces on the structure elements try to bring back the structure to equilibrium. This method accounts for the nonlinear effects found in the structure by changing the stiffness matrix after every acceleration increment.

2.5.5 Method Selection

A nonlinear dynamic analysis was selected and used to analyze all buildings in this research. This method seems to be the most reliable; however, using this method requires more computational effort and time. Under the NDP the distribution of the inertial seismic forces over the height of the building, the corresponding inertial forces, and the system displacements are determined by using an inelastic response dynamic analysis. With this method the design displacements are not established using a target displacement, as in a NSP, but instead they are determined using suites of ground motion records.

In the NDP the numerical model accounts directly for effects of material inelasticity. Using this procedure the response of the building is determined through numerical

integration of the equations of motion of the building. The building stiffness is altered during the analysis to conform to nonlinear hysteretic models of the building components. Material nonlinearities are taken into account by placing plastic springs at the beam and column elements. The P-Δ effects (Geometric Nonlinearity) were also considered in the model.

Table 2.1 shows the limitations found in the different methods. The NDP is the only one permitted for any case; it can be used regardless of both, the natural period (T) and the ratios of Column to Beam Strength of the building. Furthermore, the structure can be regular or irregular.

Table 2.1 Analysis Procedure Selection Criteria (Table 3-3 FEMA-351)[7]

Structural Characteristics				Analytical Procedure			
Performance Level	Fundamental Period, T	Regularity	Ratio of Column to Beam Strength	Linear Static	Linear Dynamic	Nonlinear Static	Nonlinear Dynamic
Immediate Occupancy	$T \leq 3.5T_s$[1]	Regular or Irregular	Any Conditions	Permitted	Permitted	Permitted	Permitted
	$T > 3.5\ T_s$[1]	Regular or Irregular	Any Conditions	Not Permitted	Permitted	Not Permitted	Permitted
Collapse Prevention	$T \leq 3.5T_s$[1]	Regular[2]	Strong Column[3]	Permitted	Permitted	Permitted	Permitted
			Weak Column[3]	Not Permitted	Not Permitted	Permitted	Permitted
		Irregular[2]	Any Conditions	Not Permitted	Not Permitted	Permitted	Permitted
	$T > 3.5T_s$	Regular	Strong Column[3]	Not Permitted	Permitted	Not Permitted	Permitted
			Weak Column[3]	Not Permitted	Not Permitted	Not Permitted	Permitted
		Irregular[2]	Any Conditions	Not Permitted	Not Permitted	Not Permitted	Permitted

[7] SAC Joint Venture, 2000

2.5.6 Method Comparison

Figure 2.10 displays the capacity curve (Base Shear vs. Displacement) for a one story steel building subjected to the artificial earthquake for the City of Mayagüez (Irizarry 1999). This building was analyzed using a linear procedure; straight lines are representative of this analysis case. A pushover analysis with and without the P-Δ effects was also performed to the same building, the chart is also plotted in Figure 2.10. Finally, a nonlinear dynamic analysis, considering and not considering the P-Δ effects was performed.

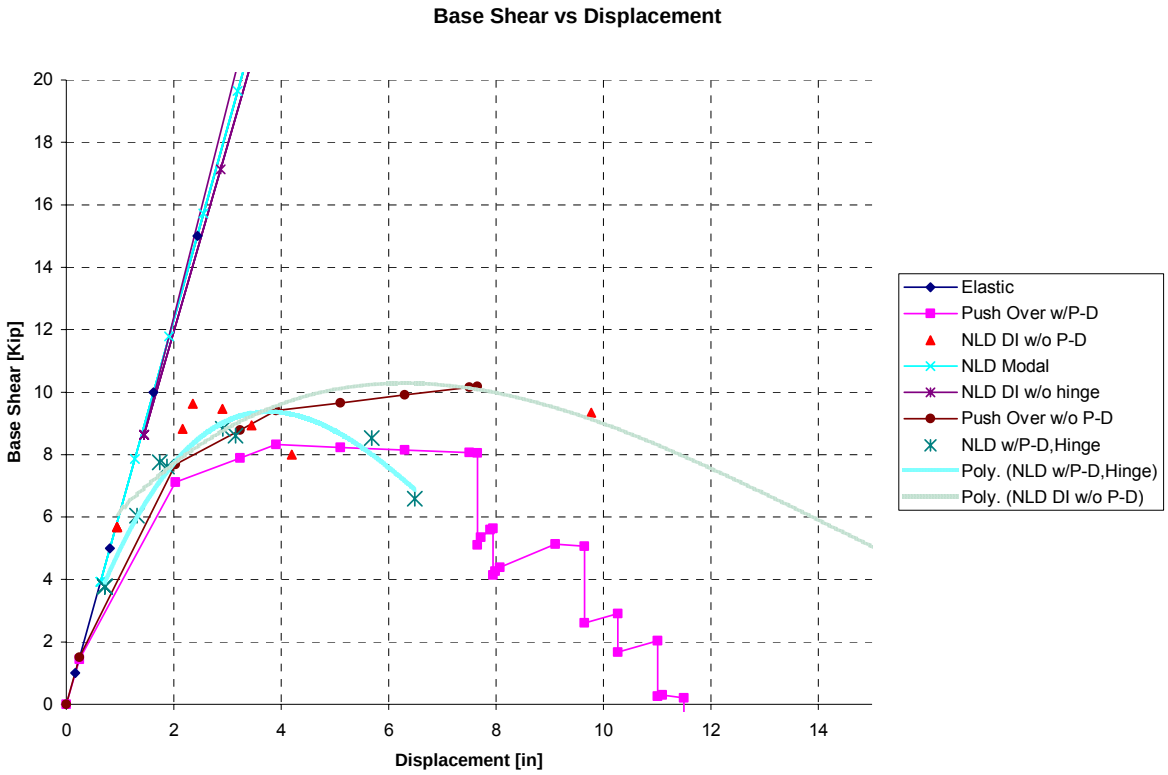

Figure 2.10 Capacity curve obtained with different methods

From figure 2.10 it can be seen that the nonlinear dynamic procedure capacity curve follows a path very close to the linear case until the structure is subjected to moments that exceed the yield capacity of its members. Up to that point, the structure behaves linear, and the stiffness

remains constant. When the moments exerted in the structure exceed the yield moment capacity of the different members, the building behaves nonlinear, and the stiffness of those members is reduced. We can also see that the capacity curve obtained for the push-over analysis is similar to that obtained for the nonlinear dynamic analysis. This was expected since the analyzed structure is a one story building.

2.6 PGA Values

The peak ground acceleration (PGA) has been taken as the earthquake intensity measure used for this research. This value represents the maximum acceleration of the ground recorded in an acceleration record for a certain earthquake. Figure 2.11 shows how the PGA value obtained. The PGA value for such record is 0.8080g (312 in/sec^2) occurring at 14.13 seconds.

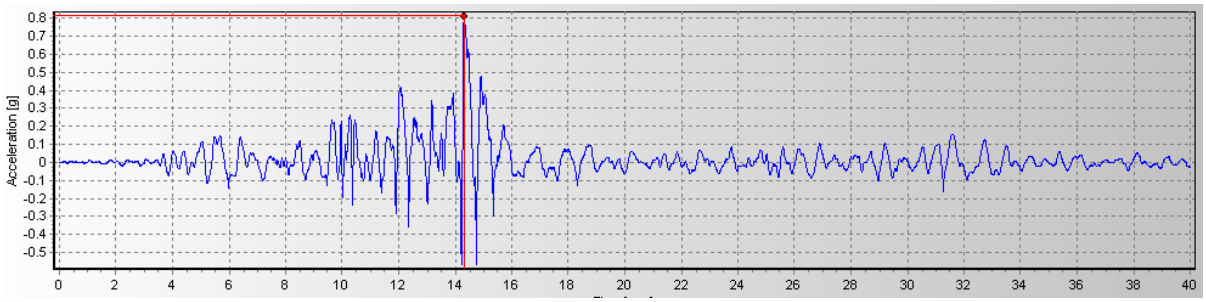

Figure 2.11 Earthquake record for the Chi Chi, Taiwan earthquake.[8]

Although the PGA used in this research as the intensity measure does not describe the frequency content of the earthquake, it is widely used by the engineering community. In

[8] University of California at Berkeley, 2000

order to account for the different frequency content and duration of different earthquakes, five earthquake records were used.

For Puerto Rico and the US Virgin Islands, the USGS Agency has developed a series of PGA contour maps. These maps give the expected PGA intensity values for different recurrent times and probabilities of occurrence. These maps are shown in Figures 2.12 to 2.14.

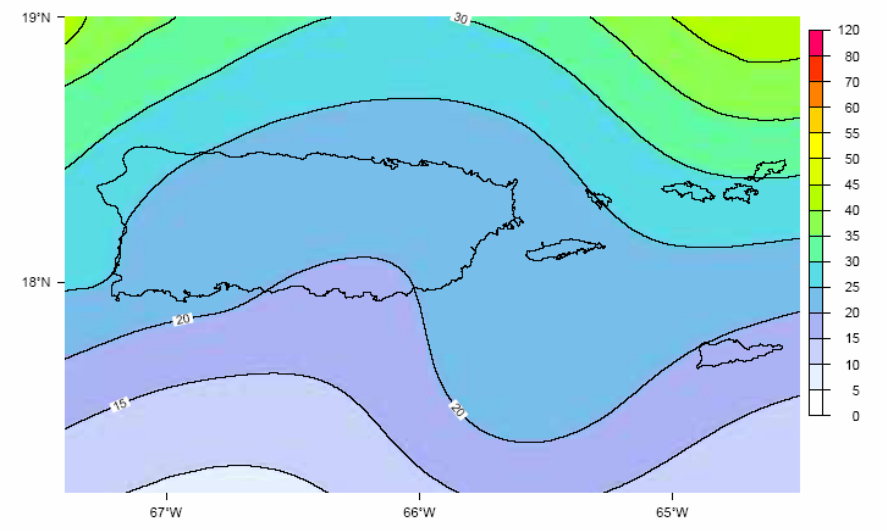

Figure 2.12 PGA(%g) with probability of exceedance in 50 years from all modeled sources.[9]

[9] United States Geological Survey, 2003

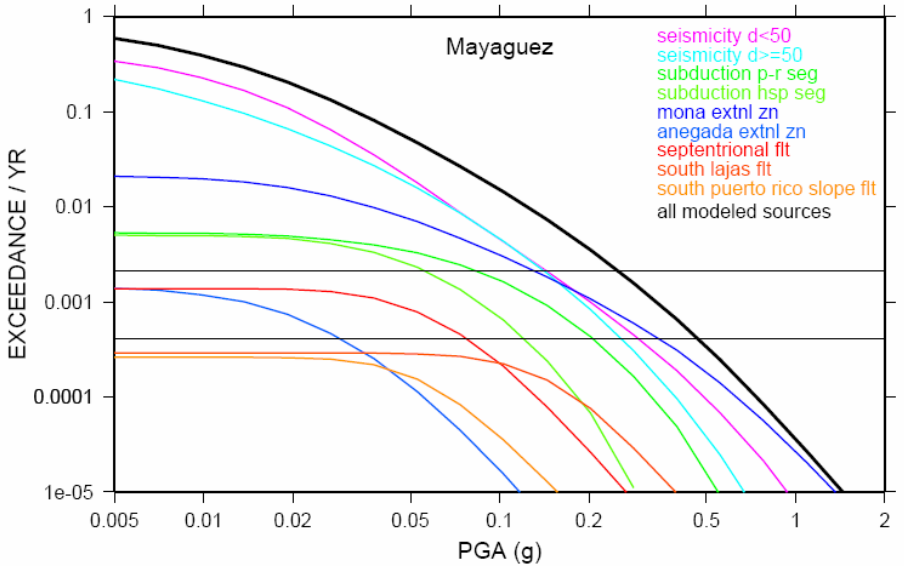

Figure 2.13 PGA hazard curves for Mayagüez[10]

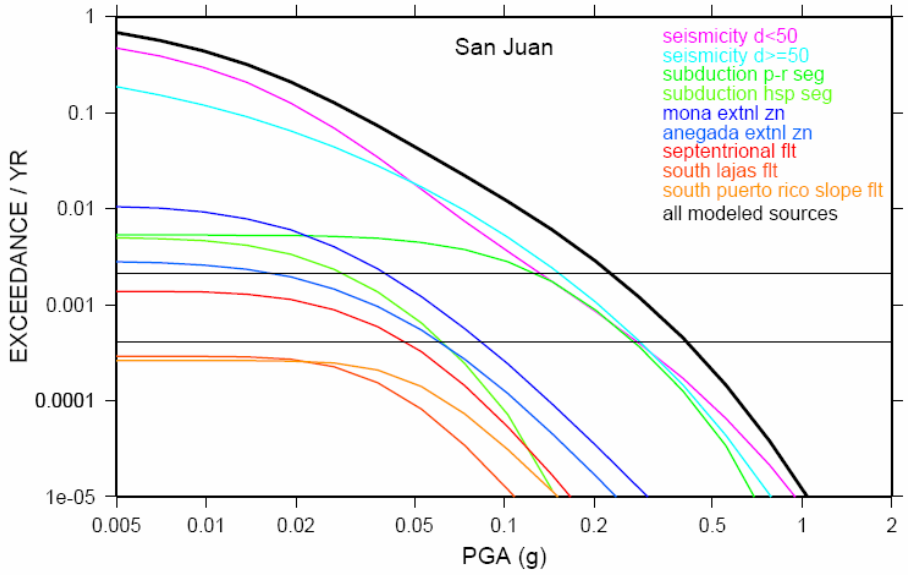

Fig.13a: PGA hazard curves for San Juan.

Figure 2.14 PGA hazard curves for San Juan[10]

[10] United States Geological Survey, 2003

3 Methodology

3.1 Introduction

This chapter discusses the methodology used to estimate the damages in a typical steel building. Although the method may apply to buildings of any type, the focus of this research is on steel buildings. It also includes a brief discussion of how is the non linear dynamic procedure utilized to obtain the buildings response parameter, and how it is related to loss functions.

3.2 Procedure

3.2.1 Categorization

Different building categories must be considered in order to take into account different structural behaviors. By categorizing the buildings a more homogeneous sample is created. A first division was made depending on the building occupancy. This is important because the code requirements depend on the building occupancy. The categories in this division are: Commercial & Offices Buildings, Industrial Buildings, and Storage Buildings. Knowing that buildings behavior depends on its height, a second division based on the number of stories was considered. The categories for the second subdivision are: buildings with three or less stories (low-rise buildings), buildings with four to seven stories (mid-rise buildings), and buildings with eight or more stories (high-rise buildings).

Fragility curves for each of the aforementioned categories were created and they are shown in Chapter 7. Also, a general curve including the statistics obtained for all models has

been created. The purpose of this curve is to provide a general idea of what the damage would be.

3.2.2 Analysis

The most important step in order to estimate the damage induced to the buildings is to create a mathematical model to analyze them. This was done with the help of the computer software RAM Performance 2D. Once the building is modeled, a nonlinear dynamic analysis is performed, and the building's response parameters are obtained. A short explanation of the nonlinear dynamic analysis was provided in Chapter 2.

Five earthquake records were used. Records from past earthquakes that occurred in San Salvador, California, and the two expected earthquakes for Puerto Rico were used. Chapter 4 thoroughly explains the mathematical model and the different aspects of the analysis procedure.

3.2.3 Response Parameter

From the ground motion acceleration time histories applied to the building, the maximum inter-story drift (δ_i) was found and used as the response parameter. Inter-story drift has been selected as the response parameter because it is an excellent parameter for judging the ability of a structure to resist P-Δ instability and collapse. Inter-story drift is also closely related to plastic rotation demand, or drift angle demand, on individual beam-column connection assemblies, and it is therefore a good predictor of the performance of beams, columns and connections. The peak inter-story drift represents the maximum displacement of one floor relative to any adjacent floor (see Figure 3.1) divided by the story height.

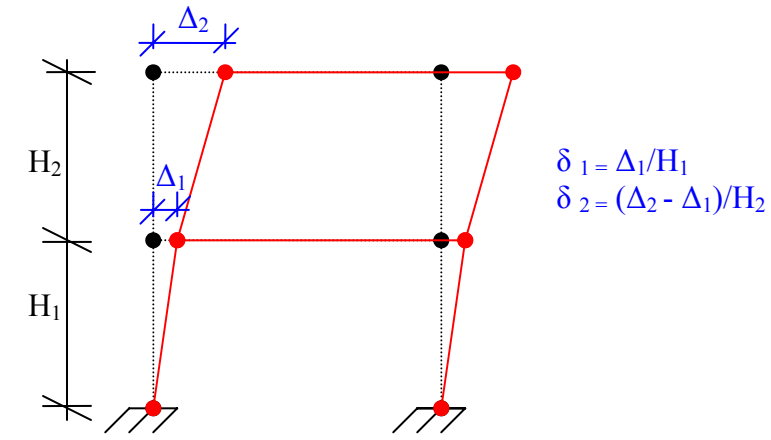

Figure 3.1 Inter-story drift definition

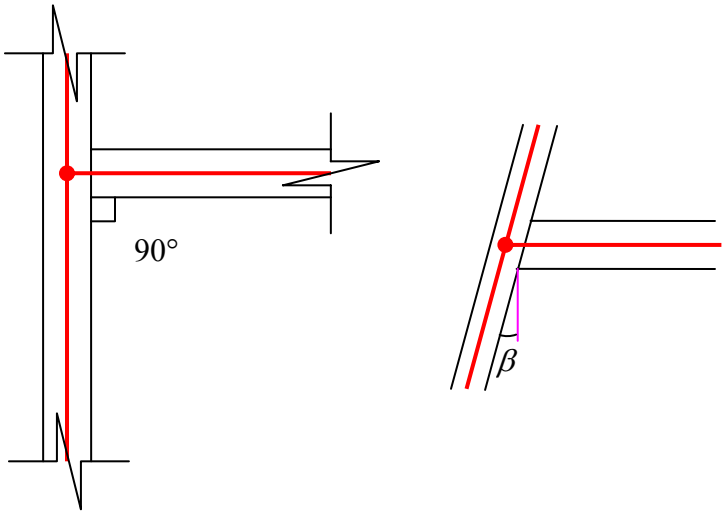

Figure 3.2 Connection Rotation

Figure 3.2 (left) displays the initial state of a typical column at an angle of 90° to the beam. Figure 3.2 (right) shows the same beam-column connection with an additional rotation called β, which can be expressed as:

$$\beta = \tan^{-1}\left(\frac{\Delta_{i+1} - \Delta_i}{H_{i+1}}\right). \qquad \textbf{(3.1)}$$

For small angles it is accepted that:

$$\tan(\alpha) = \alpha . \qquad \textbf{(3.2)}$$

By applying the small angles simplification, equation 3.1 becomes:

$$\beta = \left(\frac{\Delta_{i+1} - \Delta_i}{H_{i+1}} \right). \qquad \textbf{(3.3)}$$

Equation 3.3 gives the additional rotation in the connection. This equation is exactly the same as the previously equation shown for estimating the inter-story drift.

The inter-story drift has been obtained at every time step of the earthquake acceleration time history. The earthquake has been divided in intervals of 0.02 seconds, which means that for a ground motion history with duration of 10 seconds there will be 500 time step values of every response parameter. The displacement for every floor is taken at every time step, from these displacements, the inter-story drift is obtained for every floor at each time step.

3.2.4 Damage States

The next step, once the building's response is known, is to classify the damage. The buildings structural damage is described by damage states. Five damage states are considered: no damage, slight, moderate, extensive, and complete damage. Note that damage varies as a continuous function of the earthquake demand; however, it was discretized in order to establish the procedure. The following table gives the description for each of the damage states:

Table 3.1. Damage State description (Table B-2, FEMA-351)[11]

Damage State	Buildings with Pre-Northridge Connections	Buildings with Post-Northridge Connections
Slight structural damage	No permanent inter-story drift. Minor deformations in some connection elements and fractures in less than 10% of the connections at any floor level.	No permanent inter-story drift. Minor deformation in some connection elements. No fractures in connections.
Moderate structural damage	Permanent inter-story drift as large as 0.5%. Perhaps as many as 25% of the connections on any floor level have experienced fracture.	Permanent inter-story drift as large as 0.5%. Moderate amounts of yielding and distortion of some column panel zones. Minor buckling of some girders.
Extensive structural damage	Many connections have failed with a number of fractures extending into and across column panel zones. Some connections may have lost ability to support gravity load, resulting in partial local collapse. Large permanent inter-story drift occurs in some stories.	Many steel members have exceeded their yield capacity, resulting in significant permanent lateral deformation of the structure. Some structural members or connections may have major permanent member rotations at connections, buckled flanges and failed connections. Some connections may have lost ability to support gravity load, resulting in partial local collapse.
Complete structural damage	A significant portion of the structural elements have exceeded their ultimate capacities and/or many critical structural elements or connections have failed resulting in dangerous permanent lateral displacement, partial collapse or collapse of the building. Approximately 15% (of the total square footage) of all WSMF buildings with complete damage are expected to have collapsed.	

[11] SAC Joint Venture, 2000

Table 3.2. Inter Story Drift (able B-7, FEMA-351)[12]

Connection Condition, Building Height and Location	Structural Damage State			
	Slight	Moderate	Extensive	Complete
Pre-Northridge–All Heights/Locations	0.010	0.015	0.025	0.040
Post-Northridge–3-Story–Los Angeles	0.010	0.020	0.040	0.100
Post-Northridge–9-Story–Los Angeles	0.010	0.020	0.040	0.080
Post-Northridge–20-Story–Los Angeles	0.010	0.020	0.040	0.060
Post-Northridge–3-Story–Seattle	0.010	0.0175	0.030	0.080
Post-Northridge–9-Story–Seattle	0.010	0.0175	0.030	0.060
Post-Northridge–20-Story–Seattle	0.010	0.0175	0.030	0.050
Post-Northridge–All Heights–Boston	0.010	0.015	0.025	0.040

For this analysis the Pre-Northridge connection condition will be used. The parameters are chosen from Table 3.2 for buildings of all heights and all locations,

E1 = slight damage $\delta/h \geq 0.010$

E2 = moderate damage $\delta/h \geq 0.015$

E3 = extensive damage $\delta/h \geq 0.025$

E4 = complete damage $\delta/h \geq 0.040$

3.2.5 Fragility Curve Generation

After the response parameter is determined for a building, it is compared with the damage state limits at every scaled earthquake PGA value. If the inter-story drift corresponding to a PGA value exceeds a damage state, a value of one (1) is plotted; otherwise, a value of cero (0) is plotted. This procedure was proposed by Shinozuka and it is explained in Chapter 5. The output of this procedure is a Fragility Curve or the probability of being in or exceeding a

[12] SAC Joint Venture, 2000

certain damage state. The purpose of a fragility curve is to give the probability of damage for a building when it is subjected to an earthquake with certain intensity (PGA).

3.2.6 Loss Functions

Loss Functions are needed to estimate the economic loss. The damage probability of each damage state is multiplied by a relative cost assigned to each damage state. FEMA defines the structural cost for steel buildings as 20% of the total cost. The repair cost of slight damage is assumed to be zero on the basis that any incidental damage under this category will not require to be repaired. For the Moderate and Extensive structural damage the cost of repair is assumed to be 10% and 50% of the structural cost, respectively. A 100% of the structural cost is assumed for the Complete Structural Damage State. Table 3.4 shows the assigned cost for each damage state for a building with an estimated structural cost per square foot of $25.00 ($25.00/ft^2).

Table 3.3. Cost of Damage State DS

	Structural Damage State			
Damage State	Slight	Moderate	Extensive	Complete
Mean Loss Ratio	0%	10%	50%	100%
Mean Loss Rate [$/SF]	$0.00	$2.50	$12.50	$25.00

A more extensive discussion of Loss Functions is presented in Chapter 7.

4 Mechanical Model

4.1 Introduction

This Chapter explains in detail the elements used as part of the mechanical model. Each building was analyzed using beam elements, column elements, panel zone elements, and footing elements. Each of this element models is explained in this chapter. A matrix analysis of each of the buildings has been performed. A 2-D model was used since the buildings analyzed are generally symmetric, and torsional effects are sufficiently small to be neglected. The program RAM Performance has been used to create and analyze such models.

As shown in Figure 4.1, elements have been modeled using center to center distances. In many of the buildings analyzed, a lightly reinforced concrete slab has been placed over the metal deck. For such cases, following the code recommendations, the story is assumed to behave as a rigid diaphragm. This is modeled by adding a diaphragm constraint at each node of the story. This ensures that every node in a certain story is subjected to the same deformation.

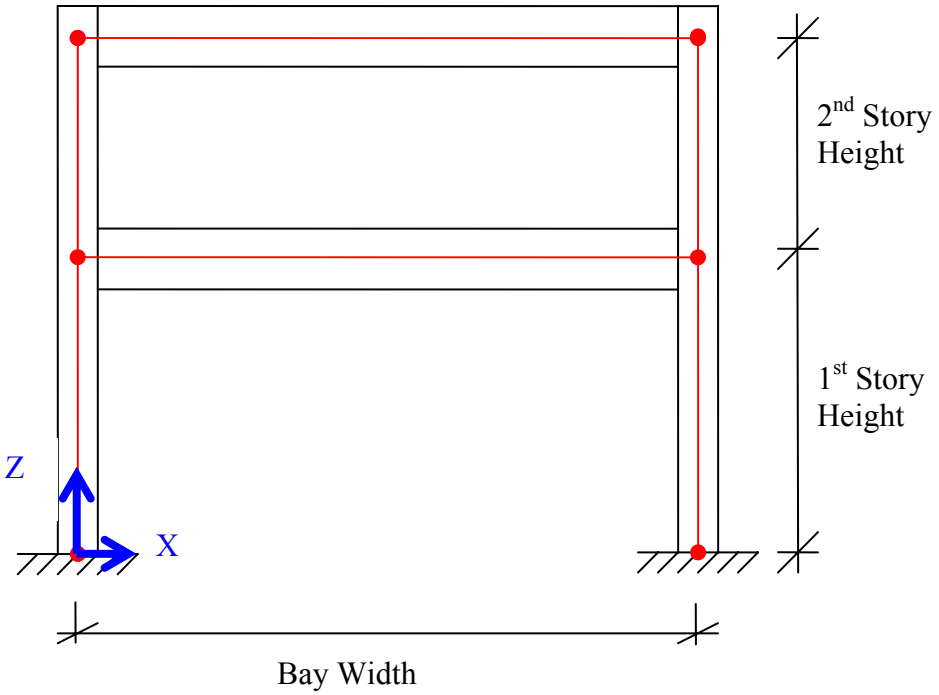

Figure 4.1 Model of a typical frame

4.2 Elements

4.2.1 Beam Element Model

To model the beams, a non linear element proposed in a FEMA publication (FEMA-273 1997) has been used. At every corner the beam element has a stiff end zone which behaves elastic (Figure 4.2). The beam is composed of two plastic springs, one at each end, the remaining part of the beam is essentially elastic. A chord deflection method, which assumes an inflection point at mid-span, is used; a graphical representation of this method is shown in Figure 4.3.

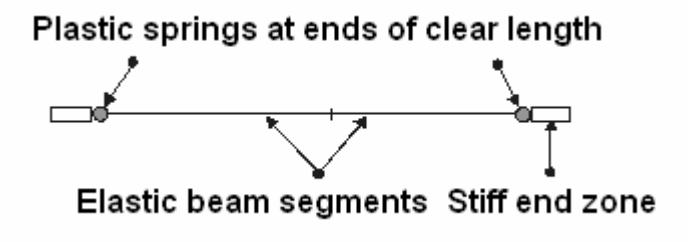

Figure 4.2 Implementation of the chord rotation method by RAM Performance 2D.

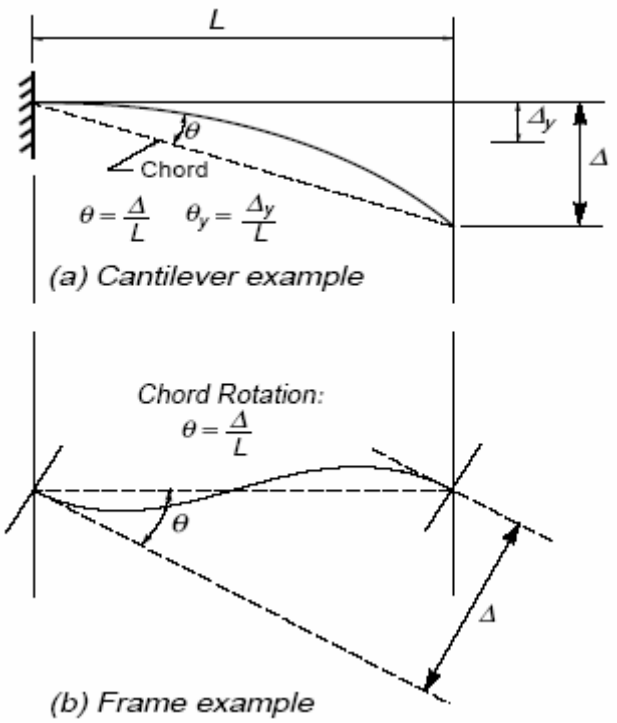

Figure 4.3 Chord deflection method

This method provides for a reasonable estimate of the non linear behavior of the steel beams in the buildings analyzed. The mathematical derivation is shown next.

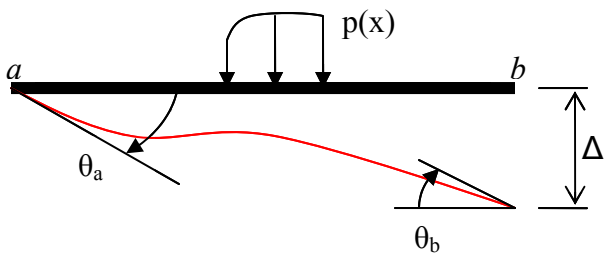

Figure 4.4 Beam deflection model

The rotation at point *a* is defined by adding the rotation caused by the moments at each end, by the contribution of the loads, and by the rotation caused due to a displacement (Δ).

$$\theta_a = \theta_a^{M_{ab}} + \theta_a^{M_{ba}} + \theta_a^{loads} + \theta_a^{\Delta} \quad \textbf{(4.1)}$$

with,

$$\theta_a^{\Delta} = \frac{\Delta}{L} \quad \textbf{(4.2)}$$

$$\theta_a^{M_{ab}} = \frac{M_{ab}L}{3EI} \quad \textbf{(4.3)}$$

$$\theta_a^{M_{ba}} = -\frac{M_{ba}L}{6EI} \quad \textbf{(4.4)}$$

where:

θ_a = Rotation at point *a* of the beam,

θ_a^{Mab} = Rotation at point *a* of the beam caused by the moment at *a*,

$\theta_a^{M_{ba}}$ = Rotation at point *a* of the beam caused by the moment at *b*,

$\theta_a^{load\,s}$ = Rotation at point *a* of the beam caused by the applied loads, and

θ_a^{Δ} = Rotation at point *a* of the beam caused by the deflection Δ.

The chord rotation method proposed by FEMA, and used here, has the following assumptions:

1. The loads do not cause the beam to rotate.
2. The moment at each end have the same magnitude.
3. Point *a* and *b* stay in the same elevation, so that Δ is cero.

Substituting equations 4.3 and 4.4 into equation 4.1 and applying the assumptions aforementioned, equation 4.1 yields:

$$\theta_a = \frac{M_{ab}L}{3EI} - \frac{M_{ba}L}{6EI} + \cancel{\theta_a^{loads}} + \cancel{\theta_a^{\Delta}} = \frac{M_{ab}L}{3EI} - \frac{M_{ba}L}{6EI} = \frac{M_{ab}L}{6EI} = \frac{ZF_{ye}L}{6EI}$$

Based on the point of inflection at mid-span, and the aforementioned assumptions, the yielding rotation of the plastic hinge is taken as,

$$\theta_y = \frac{ZF_{ye}L_b}{6EI_b}. \qquad \textbf{(4.5)}$$

For the beam elements, $Q_{CE} = M_{CE} = ZF_{ye}$

where:

Z = Plastic Section Modulus,

F_{ye} = Expected yield strength of the material,

E = Modulus of Elasticity,

I_b = Moment of Inertia of the beam,

L_b = Beam length, and

θ_y = Yield Rotation, radians.

4.2.2 Column Element Model

The inelastic column elements have been modeled as elastic elements with rotational springs to account for the inelastic behavior. The axial force – bending moment (P-M) interaction has been taken into consideration for the columns non linear rotational spring behavior. Figure 4.5 shows the model used for the mathematical representation.

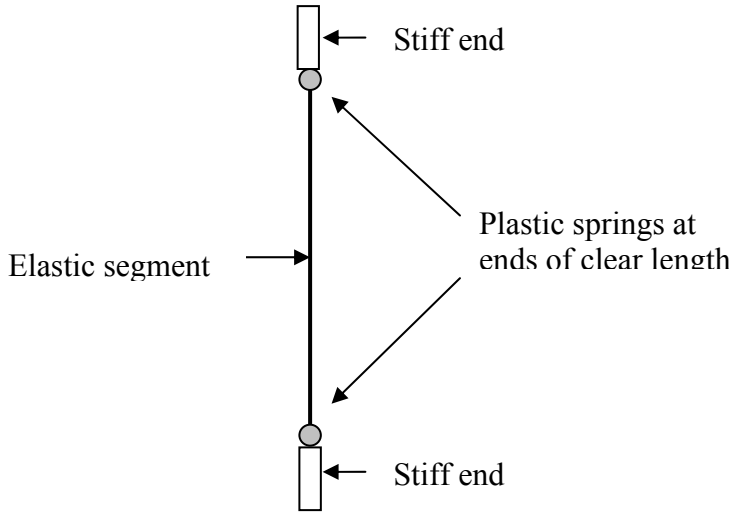

Figure 4.5 Inelastic column model

An elastic perfectly plastic (E-P-P) behavior has been assumed for the non linear springs in the column sections. Section 4.2.7 explains the E-P-P concept in more detail.

4.2.3 Panel Zone Element Model

Sometimes the flange of a column itself can not resist the shear induced by beam flanges. When this happens, the panel zone needs to be reinforced. This additional strength required by the column web in the panel zone is provided by either adding plates of by adding stiffeners. A graphic representation of this phenomenon is shown in figure 4.6. Buildings whose connections included some sort of reinforcement at the panel zone have been modeled considering their reinforcement.

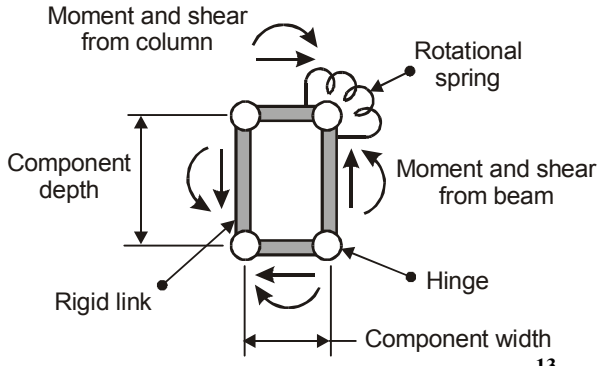

Figure 4.6 Model for panel zone[13]

The Krawinkler model which consists of four rigid links hinged at the corners is used by the software program RAM Performance 2D. Figure 4.6, shows the rigid links configuration and how they are attached to the hinges. The width and depth is taken as 95% of the column width and the beam depth, respectively. The rotational spring also shown in Figure 4.7 provides the connection strength and stiffness; it may behave linearly or nonlinearly.

Equations 4.6, 4.7 and 4.8 are used to calculate the initial stiffness of the spring, the yielding strength, and the hardening stiffness respectively.

[13] RAM International, L.L.C., 2002

$$Initial\ stiffness\ of\ rotational\ spring = 0.95 d_b d_c t_p G \quad \textbf{(4.6)}$$

$$Strength\ at\ Y\ point = 0.55 F_y t_p 0.95 d_b d_c \quad \textbf{(4.7)}$$

$$\text{Hardening stiffnes} = 1.04 b_{fc} t_{fc}^2 G \quad \textbf{(4.8)}$$

where:

d_b = beam depth,

d_c = column depth,

t_p = panel zone thickness,

b_{fc} = column flange width,

t_{fc} = column flange thickness,

G = shear modulus, and

F_y = yield stress.

4.2.4 Footings Element Model

Most of the columns have been assumed to be fixed to the footings. In other words, a stiffness value of infinity has been assumed in the connection of the building to the ground. The soil-structure interaction may affect significantly the stresses in the building. This effect should be considered in a future research. Figure 4.7 shows a typical footing detail. Figure 4.8 shows the model idealization with stiffness K.

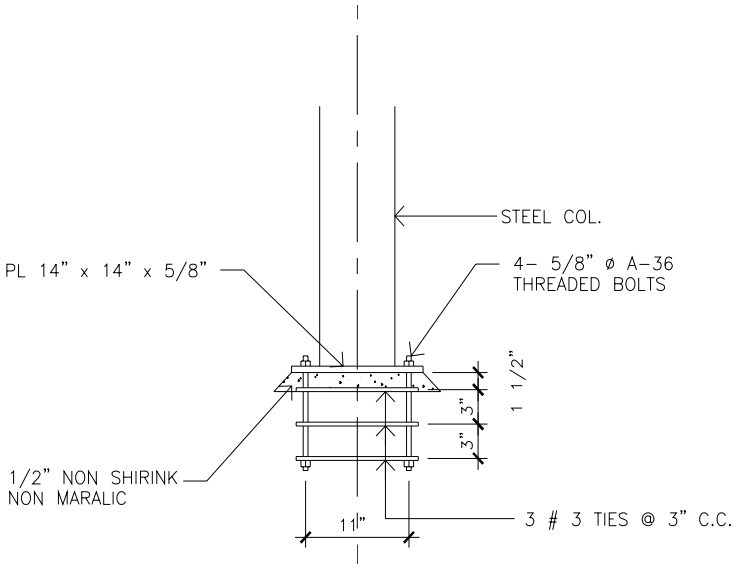

Figure 4.7 Typical column-footing connection detail

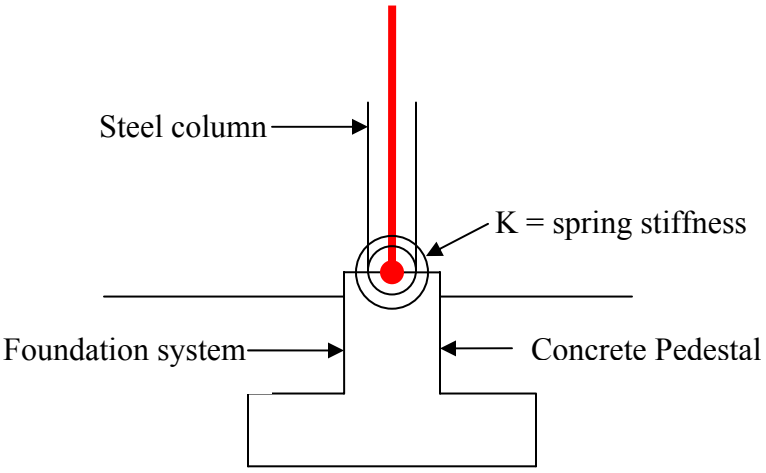

Figure 4.8 Model idealization of column-footing connection

4.2.5 2D versus 3D Model

All the buildings have been modeled as 2D. All the buildings analyzed are symmetrical; therefore, the effects of torsion have been neglected. A representative moment resisting frame is selected and all the analyses are carried using a 2D model. In general, a 3D model

should be realistic, but the computational time and effort would too much for the purpose of this research.

4.2.6 External Forces

The building is initially subjected to dead loads and live loads. The Dead Load consists of the self weight of the structural and nonstructural components of the building. As stated in the UBC 97, Live Loads are those loads produced by the use and occupancy of the building or other structure and do not include dead load, construction load, or environmental loads such as: wind load, snow load, rain load, earthquake load, or flood load.

After the dead loads and live loads are applied, earthquake forces are applied to the model. The earthquake forces are dynamic forces in the form of acceleration applied at the base of the buildings. Figure 4.9 shows the typical behavior of buildings subjected to earthquake forces.

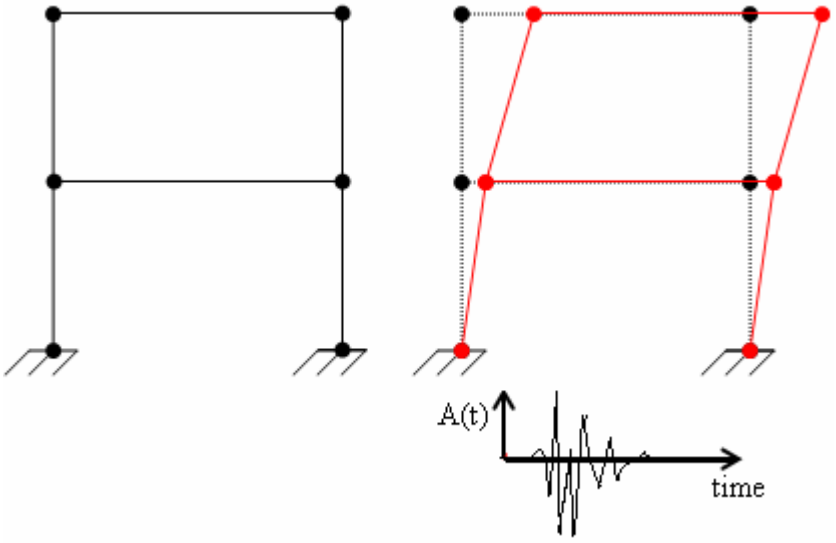

Figure 4.9 Acceleration at the building's base

The main idea of the dynamic procedure is to shake the structure at the base with records of acceleration time histories from past earthquakes or generated earthquakes. Figures 4.10 to 4.13 show the acceleration time histories that have been used for this research. The acceleration time histories have been scaled; its PGA values were varied starting from 0.1g up to 1.0g. This set of 10 acceleration time histories for each of the 5 earthquakes considered were introduced in RAM Performance 2D, and a nonlinear dynamic analysis of each building was performed.

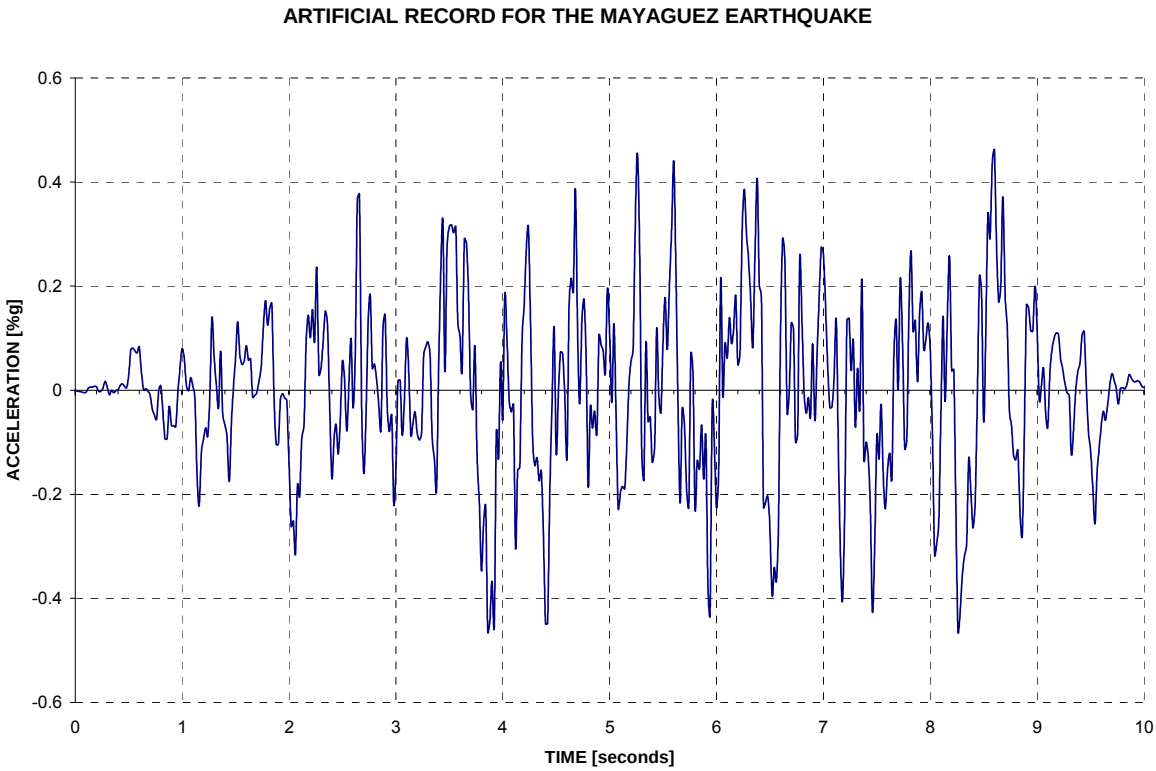

Figure 4.10 Acceleration time history for the artificial earthquake for the City of Mayagüez (Irizarry 1999).

Figure 4.10 shows the expected acceleration time history for Mayagüez and its surrounding cities (Irizarry 1999). This acceleration time history has a peak ground acceleration of 0.46 g occurring at 3.86 seconds.

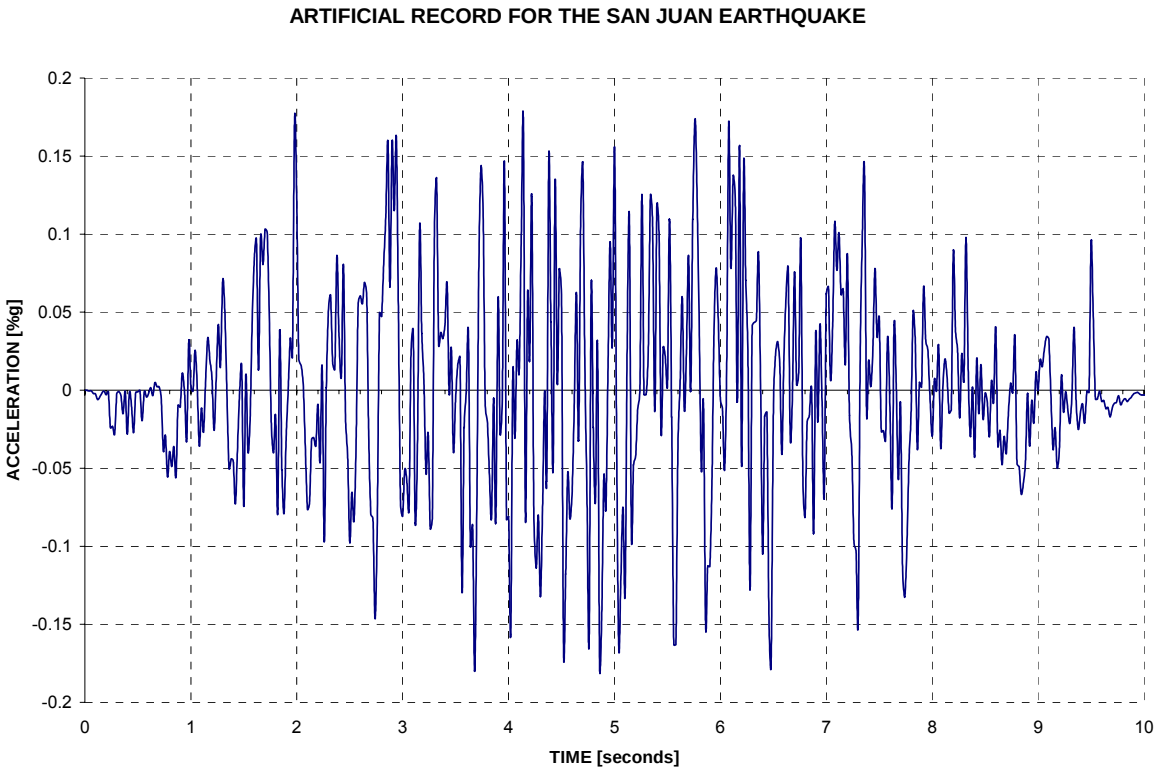

Figure 4.11 Acceleration time history for the artificial earthquake for the City of San Juan (Irizarry 1999).

The acceleration time history for the San Juan earthquake is shown in Figure 4.11 (Irizarry 1999). This acceleration time history has a peak ground acceleration of 0.18 g, it occurs at 3.68 seconds.

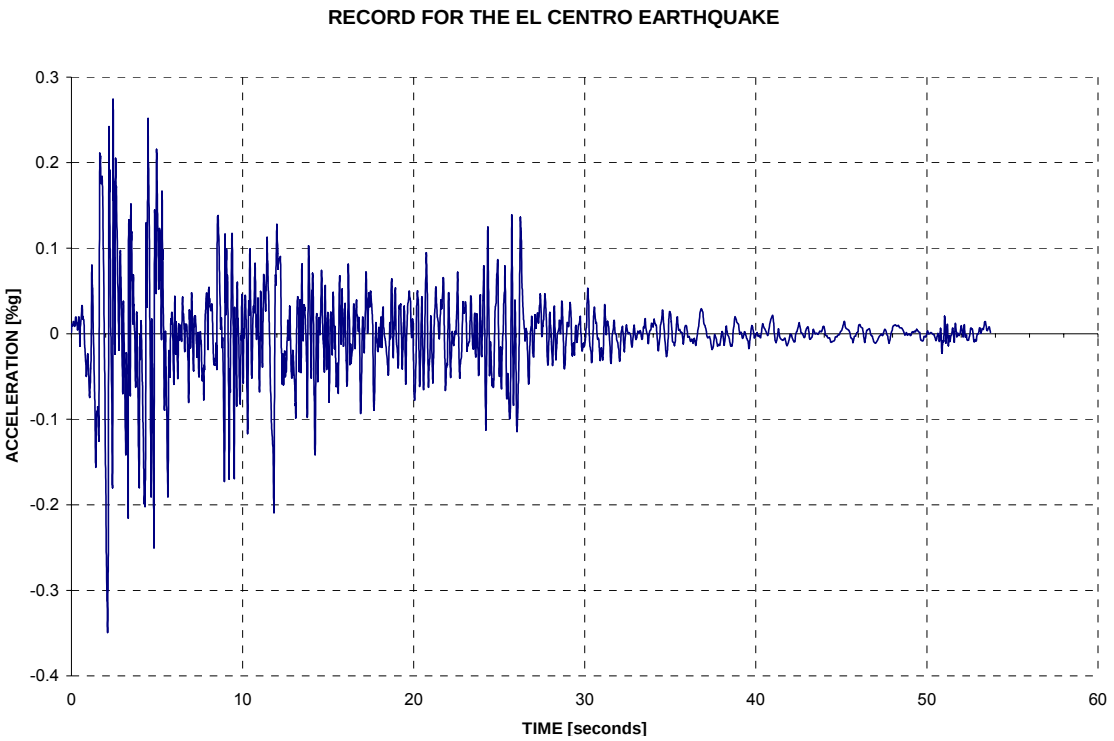

Figure 4.12 Acceleration time history from the 1940 Imperial Valley Earthquake at the El Centro Station (PGA=0.348)

The acceleration time history for the Imperial Valley Earthquake of 1940 at the El Centro station is shown in Figure 4.12. This record has a PGA of 0.348 g. Additional information regarding this earthquake is shown in Table 4.1.

Table 4.1. 1940 Imperial Valley Earthquake Facts

Time	May 18, 1940 / 8:37 pm, PST
Location	32° 44' N, 115° 30' W 8 km (5 miles) north of Calexico 145 km (90 miles) east of San Diego
Magnitude	M_W6.9
Type of faulting	probably right-lateral strike-slip
Fault ruptured	Imperial Fault
Rupture length	at least 40 km (25 miles)
Maximum offset	at least 4.5 meters (15 feet)
Deaths	9
Injured	20
Damage ($)	$6 million

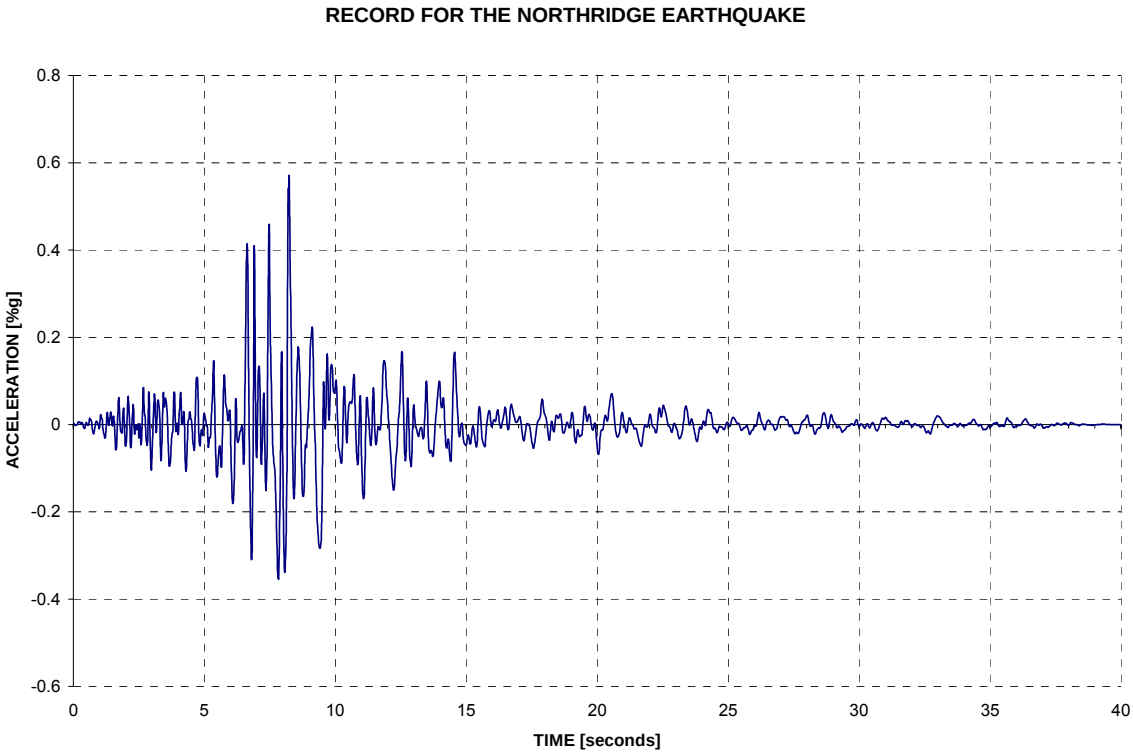

Figure 4.13 Acceleration time history record for the 1994 N-S Northridge earthquake measured at the Castaic Station. (PGA = 0.568g)

The acceleration time history for the North-South component of the 1994 Northridge earthquake at the Castaic Station is shown in Figure 4.13. The peak ground acceleration for this earthquake is 0.568 g. Additional information is shown in Table 4.2.

Table 4.2 1994 Northridge Earthquake Facts

Date / Time	January 17, 1994 / 4:30:55 am PST
Location	34° 12.80' N, 118° 32.22' W 20 miles west-northwest of Los Angeles 1 mile south-southwest of Northridge
Magnitude	M_W6.7
Type of Faulting	blind thrust
Faults Involved	Northridge Thrust (also known as Pico Thrust). Several other faults experienced minor rupture, rupture during large aftershocks
Depth	18.4 km
Deaths	51
Injured	9,000+
Duration	40 seconds
Damage ($)	44 billion

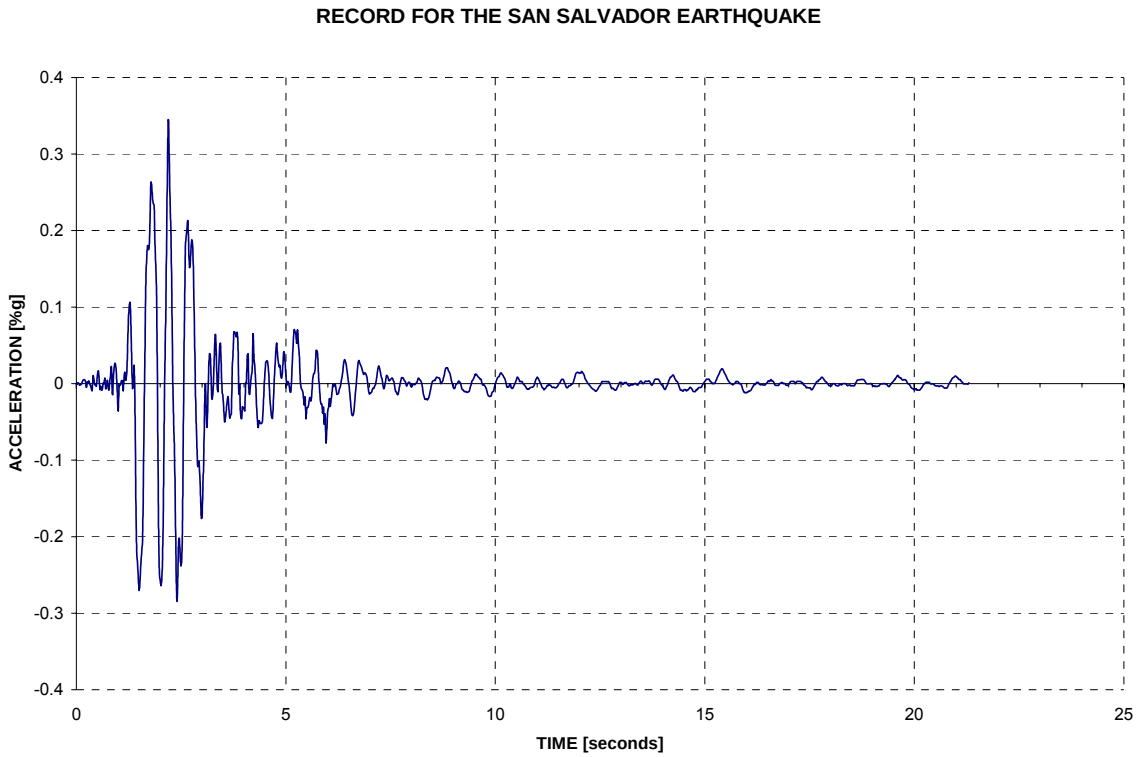

Figure 4.14 1986 San Salvador acceleration record (E-W direction)

The acceleration time history for the 1986 San Salvador earthquake in the East-West direction is shown in Figure 4.14. This record was measured at the Hotel Camino Real station. It has a peak ground acceleration magnitude of 0.345g.

Table 4.3. 1986 San Salvador Earthquake Facts

Time	October 10, 1986 17:49
Location	13.67° N 89.19° O
Magnitude	M_s 5.5
Depth	7.3
Deaths	1,500
Injured	10,000
Duration	22 seconds

All five records were used in this research investigation. Each record was scaled from 0.1g to 1.0g, meaning that 10 earthquakes were created from each earthquake record. Figure

4.15 shows the response spectra for the earthquakes used after they were scaled to 0.36g. The UBC-97 design spectrum for a zone 3 and soil type Sd is also plotted in Figure 4.15 to allow a comparison between the five earthquakes and the design code provisions.

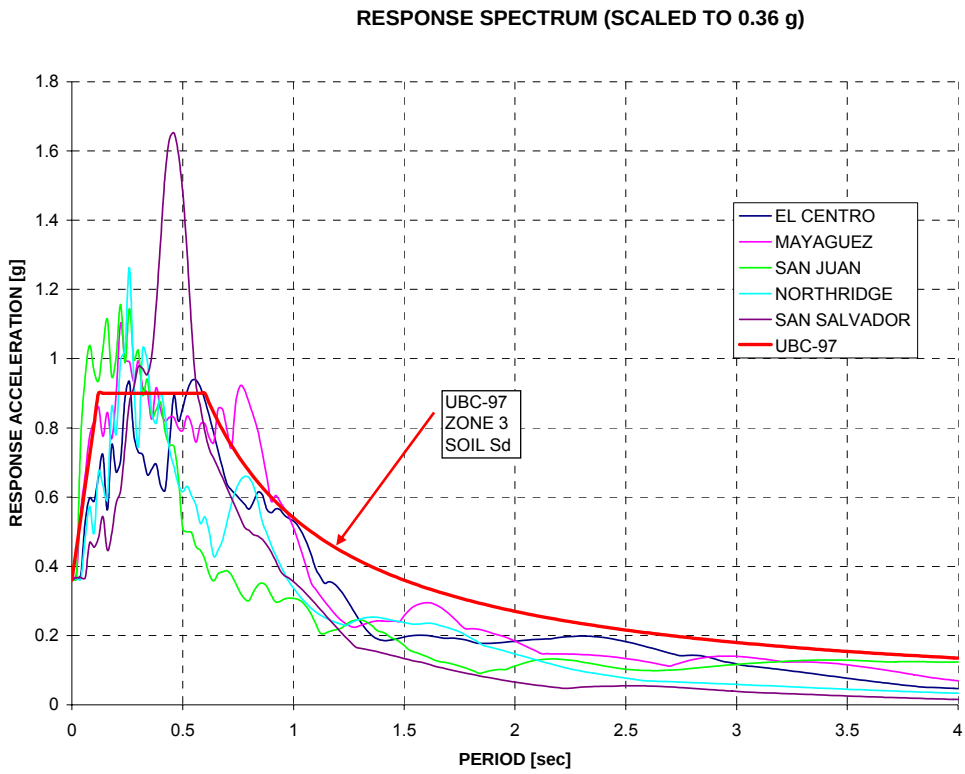

Figure 4.15 Response spectrum for the 5 earthquakes scaled to a 0.36 g.

Note that for periods larger than one second the UBC-97 Response Spectrum has larger acceleration values. Figure 4.15 was created for illustration purposes; it is important to have in mind that the PGA values were scaled from 0.1g up to 1.0g.

Figure 4.16 shows the response spectrum for each of the ten earthquakes created from the Northridge earthquake as well as the UBC-97 response spectrum. Note that up to 0.4g the Northridge response spectrum curve falls under the UBC-97 spectrum curve, which has a PGA of 0.36g.

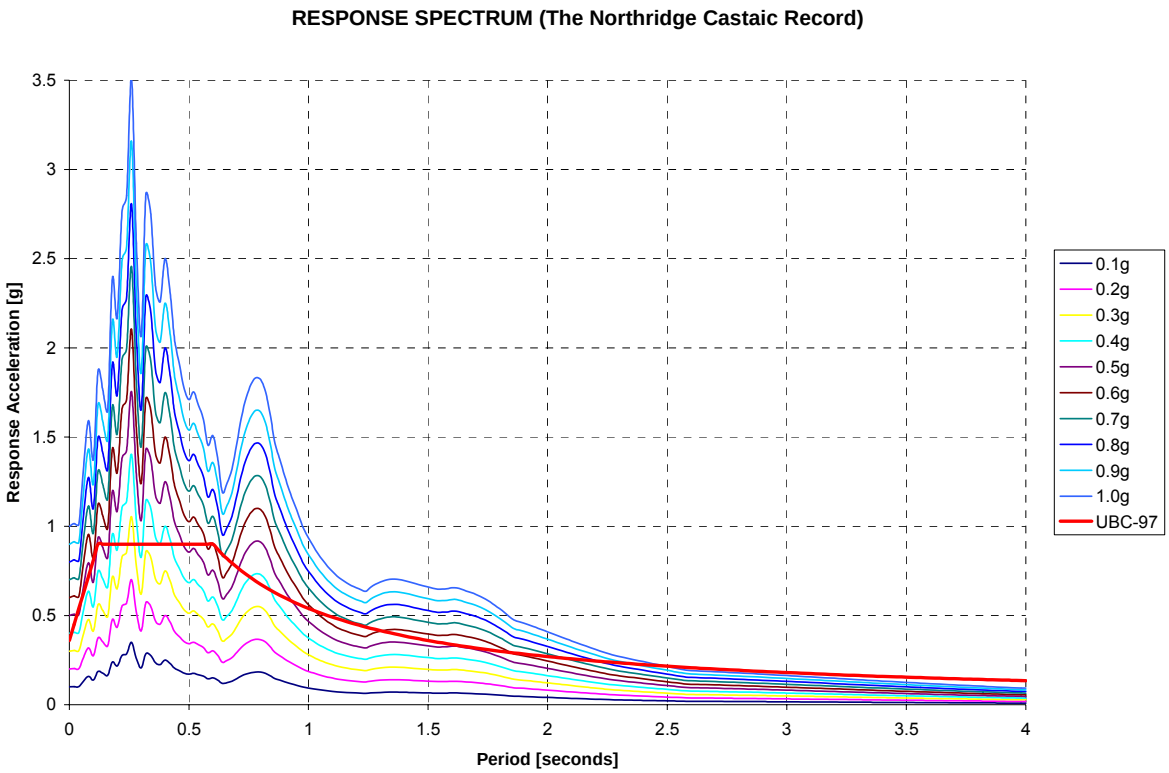

Figure 4.16 Response spectrum for the Northridge Castaic record.

Table 4.4. Earthquakes Summary

Earthquake	PGA [%g]	Duration [s]
Mayagüez	0.460	10
San Juan	0.180	10
Northridge	0.568	40
El Centro	0.348	54
San Salvador	0.345	22

Table 4.4 shows a summary of the five earthquakes used in this research. It also shows the duration and the peak ground acceleration intensity of each earthquake.

Five different earthquake records were used to include the frequency content variation.

4.2.7 Nonlinearity

Before the elastic limit is reached, the building behaves linearly elastic and the stiffness of the members remain unchanged. In the NDP the numerical model accounts directly for the

effects of material nonlinearity. Using this procedure, the response of the structure is determined through numerical integration of the equations of motion of the building. The building's stiffness is altered during the analysis to conform to nonlinear hysteretic models of its components. Figure 4.18 shows the elastic-perfectly-plastic (e-p-p) model that has been used for the beam models. After the yield moment of the element has been exceeded, the stiffness of that element remains constant. Also, when a plastic hinge is formed at a member, the member end moment can not increase, therefore, the additional forces are redistributed to other elements. This process goes on until more and more plastic hinges are formed at the elements, and a collapse mechanism finally occurs. The non linear behavior of the beam elements was accounted for by rotational springs with an e-p-p behavior without strength degradation.

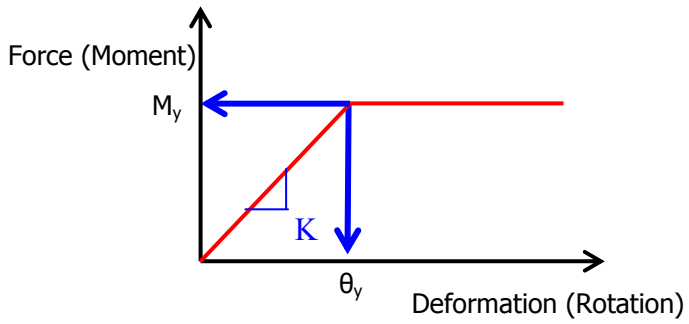

Figure 4.18 Force deformation relationship

Figure 4.19 shows the moment-rotation behavior of a W21X62 beam. Figure 4.20 shows the hysteretic loop for the same beam subjected to the Northridge earthquake with an intensity of 0.6 PGA.

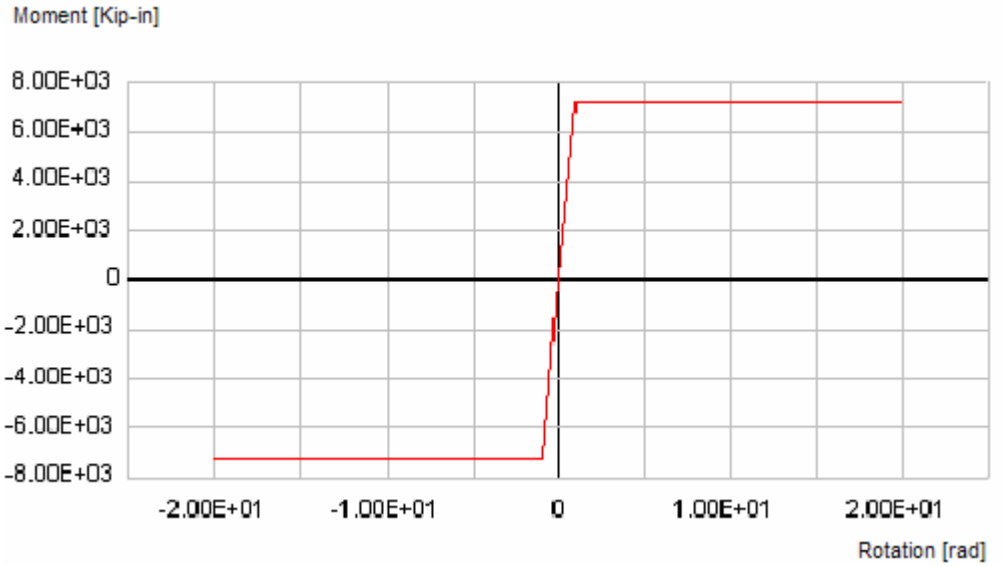

Figure 4.19 Moment-rotation relationship for a W21X62 beam

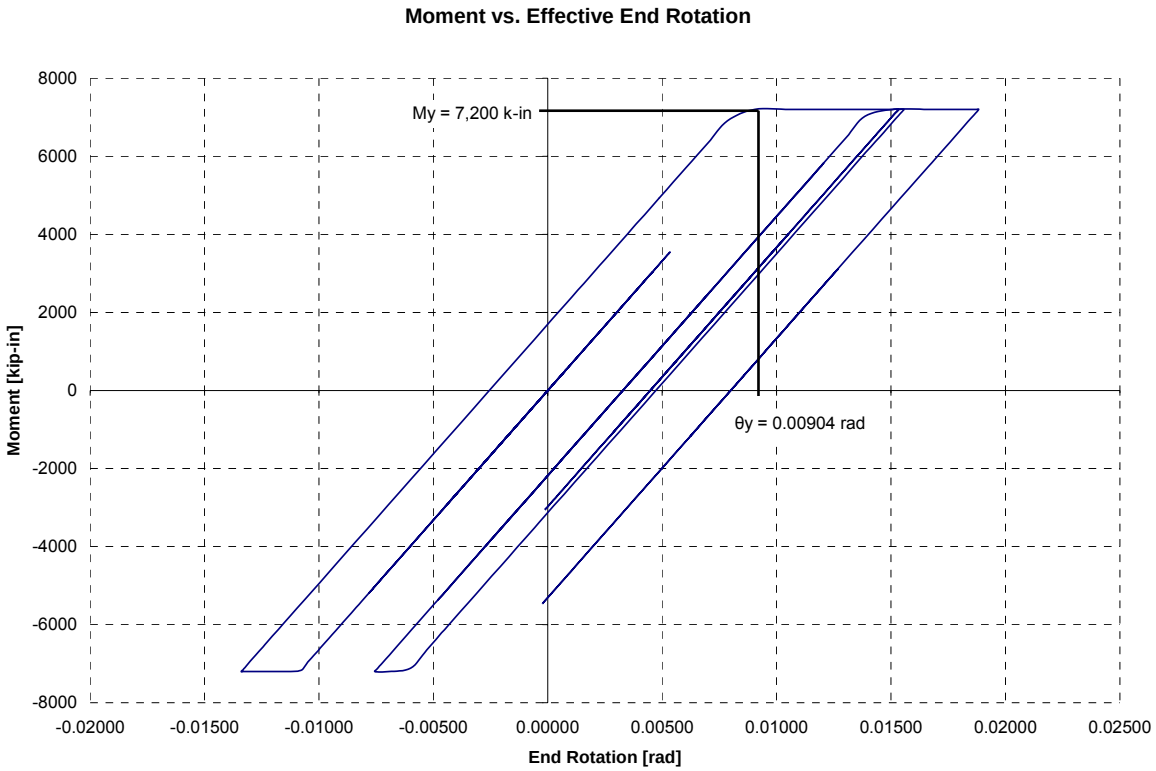

Figure 4.20 Hysteresis loop for the W21X62 beam subjected to the 0.8g Mayagüez earthquake.

A geometric nonlinearity known as the P – Δ effect was also considered. The P – Δ effect caused by gravity loads may be critical in the seismic performance. Steel moment frame buildings tend to be flexible; therefore, they are usually subjected to large lateral displacements increasing the P- Δ effects. Following the recommendations of the FEMA-351 Publication, a building at any story i should be checked to ensure that Ψ_i is less than or equal to 0.1.

$$\psi_i = \frac{P_i \delta_i}{V_{yi} h_i} \qquad \textbf{(4.9)}$$

Where:

P_i = portion of the total weight of the structure including dead, permanent live load and 25% of the transient live loads acting on all of the columns within story level *i*,

V_i = total plastic lateral shear in the direction under consideration,

h_i = height of story *i*, and

δ_i = lateral inter-story drift of story *i*.

If the value of Ψ_i in equation 4.7, is less than 0.1, no other check is required. Otherwise, P – Δ effects need to be considered. For the purpose of this research, P– Δ effects were considered in all the analyses.

4.2.8 Direct Integration Method

A direct numerical integration of the dynamic equilibrium equations is used to find the dynamic response of the structural systems. The method consists in finding the dynamic equilibrium at discrete points in time. RAM Performance 2D uses the constant average acceleration method, which is also know as the trapezoid rule. This method is the same as the Newmark method with a factor β=1/4.

The basis of this method is the following. The solution of the equation of motion:

$$M\ddot{u}_t + C\dot{u}_t + Ku_t = F_t \qquad \textbf{(4.10)}$$

can be expressed as follows, with the help of the Taylor Series,

$$u_\tau = u_{t-\Delta t} + \tau \dot{u}_{t-\Delta t} + \frac{\tau^2}{2}\ddot{u}_{t-\Delta t} + \frac{\tau^3}{6}\dddot{u}_{t-\Delta t} + \ldots \qquad \textbf{(4.11)}$$

$$u_\tau \approx u_{t-\Delta t} + \tau \dot{u}_{t-\Delta t} + \frac{\tau^2}{2}\left(\frac{\ddot{u}_{t-\Delta t} + \ddot{u}_t}{2}\right) \qquad \textbf{(4.12)}$$

The velocity is obtained by differentiating equation 4.12,

$$\dot{u}_{\tau} = \dot{u}_{t-\Delta t} + \tau\left(\frac{\ddot{u}_{t-\Delta t} + \ddot{u}_{t}}{2}\right) \qquad \textbf{(4.13)}$$

There are 3 unknown values $(u, \dot{u}, \ddot{u})$ and 3 equations (4.10, 4.12 and 4.13), therefore, the system can be solved and the three unknown values obtained at every time step of the acceleration time history.

4.2.9 Damping

Structures that are essentially elastic dissipate energy by various mechanisms; however, energy dissipation is typically modeled using viscous damping. In the common practice for linear analyses a 5% of critical viscous damping in each natural mode of vibration is used. In a nonlinear analysis, damping is taken as the sum of the elastic energy dissipation and the inelastic energy dissipation. The elastic energy dissipation used by RAM Perform-2D uses the "αM + βK" model (RAM Performance 2-D User Manual), it assumes an essentially constant damping matrix [C] defined as:

$$\mathbf{C = \alpha M + \beta K} \qquad \textbf{(4.14)}$$

where:

C = damping matrix,

M = mass matrix, and

K = Initial elastic stiffness.

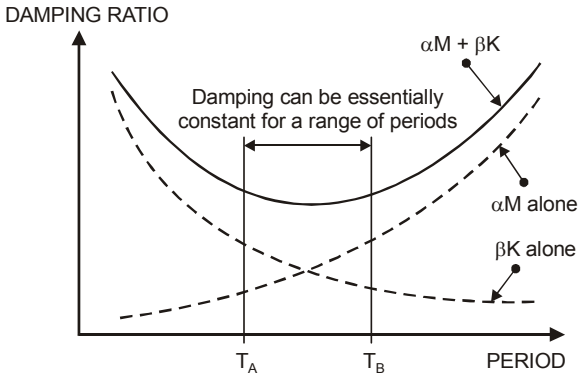

Figure 4.21 Variation of damping with period

Alpha (α) and beta (β) are two multiplying factors; the values used are 0.11828 and 0.0065763 respectively. Applying the model shown in Figure 4.21 allows assigning a damping ratio essentially constant for a very large range of periods. A 3% elastic damping was used in this thesis.

5 FRAGILITY CURVES

5.1 Introduction

Fragility curves define the probability of being in or exceeding a certain damage state for a given ground motion intensity. Fragility curves can be determined empirically, with the aid of damage data from past earthquakes, analytically, by creating computer models and performing either nonlinear static analyses or nonlinear dynamic analyses to the models. Furthermore, the empirical method could be combined with analytical models. In Puerto Rico, due to the lack of information from past earthquakes it would not be possible to create fragility curves empirically; therefore, fragility curves were created analytically from nonlinear dynamic analyses of typical buildings. Fragility curves were plotted for every building analyzed using a nonlinear optimization code. This chapter explains in detail how fragility curves were obtained.

5.2 Development

Fragility curves indicate the probability of reaching or exceeding a previously defined damage state. As previously stated, five damage states were used, these are: no damage,

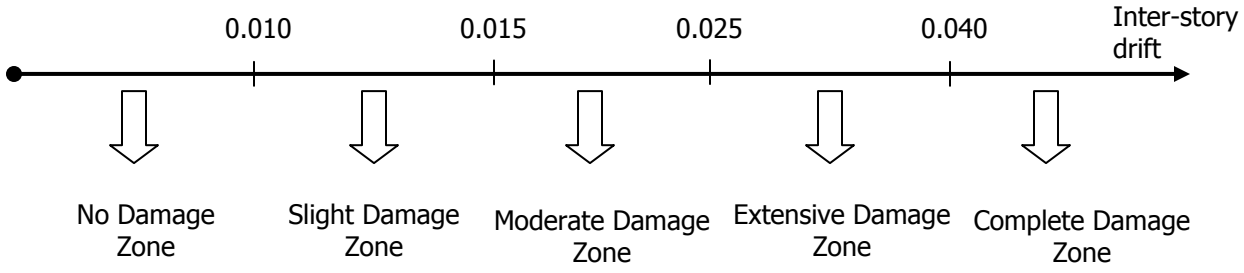

Figure 5.1 Graphical representation of the damage states.

slight, moderate, extensive and complete damage. Figure 5.1 shows the damage states and its values.

From the computer code RAM Performance, an inter story drift vs. time is obtained for each input record at each floor. An example of such chart is shown in Figure 5.2. From that chart, the maximum inter-story drift is found at each floor, for each PGA value. Each of the maximum inter-story drifts obtained at each PGA value for each floor is compared, the maximum value is used for the entire building. It is important to note that only absolute values are used, since the sign only tells the direction to which the structure was deformed at that specific moment.

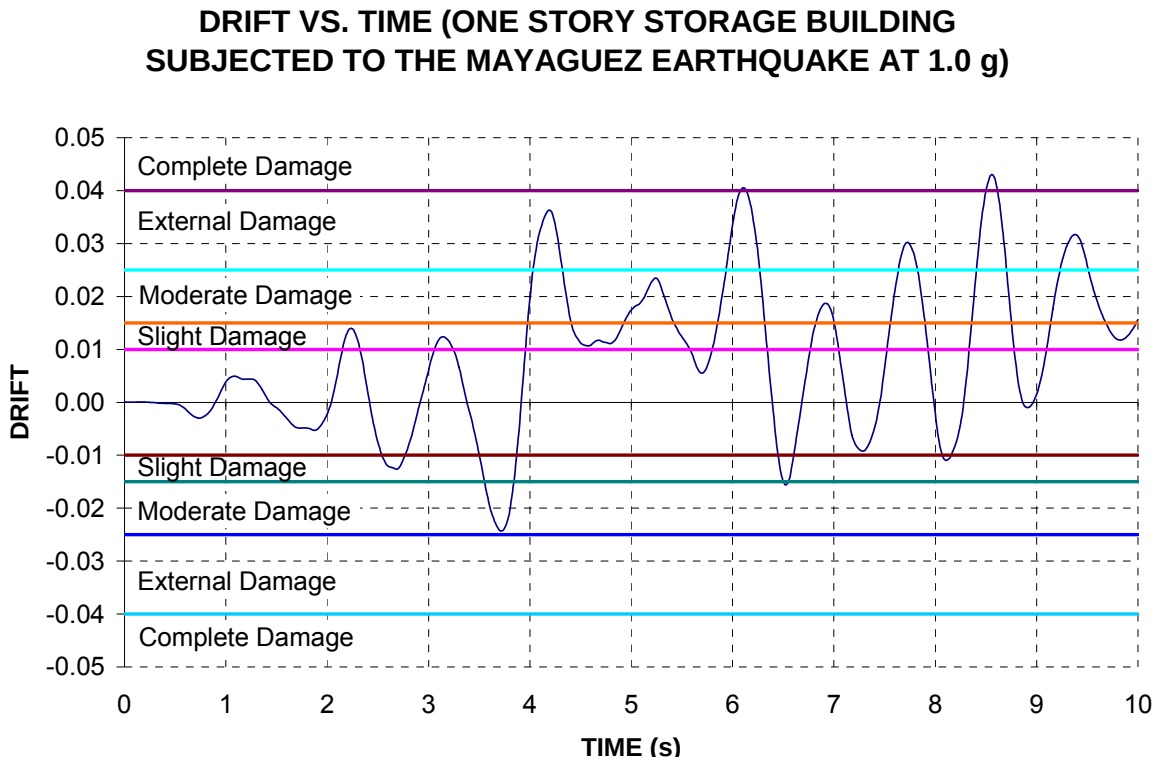

Figure 5.2 Example of a drift time history at roof level.

Once the maximum drift value is obtained at each PGA, the damage state is obtained. When a damage state occurs, a 1 is written; otherwise a 0 is written to indicate that the inter-story

drift value has not reached the specific damage state. Table 5.1 shows an example of a table created to count the number of times each damage state occurs.

Table 5.1. Occurrence worksheet

PGA	Max drift	slight	moderate	extensive	complete
0.1	0.004	0	0	0	0
0.2	0.008	0	0	0	0
0.3	0.012	1	0	0	0
0.4	0.015	1	0	0	0
0.5	0.019	1	1	0	0
0.6	0.027	1	1	1	0
0.7	0.039	1	1	1	0
0.8	0.059	1	1	1	1
0.9	0.067	1	1	1	1
1.0	0.067	1	1	1	1

After completing this process at each PGA value for each earthquake and for all models of a similar building type, the number of occurrences is added and written in a summary table such as Table 5.2. The cumulative distribution for each damage state is shown in Table 5.2 for the entire population of the 8 models subjected to 5 earthquakes, resulting in a total of 40 cases.

Table 5.2. Cumulative damage state occurrence

PGA [%g]	S	M	E	C
0.1	0	0	0	0
0.2	0	0	0	0
0.3	12	0	0	0
0.4	35	1	0	0
0.5	40	20	0	0
0.6	40	32	1	0
0.7	40	38	3	0
0.8	40	40	9	1
0.9	40	40	18	3
1	40	40	30	5

Table 5.2 tells the number of buildings that reached a damage state at each PGA value. For an earthquake having an intensity of 0.6g 32 buildings are subjected to moderate damage. Now, it is a matter of dividing each damage state by the total cases studied (40) for this example. The results are shown in Table 5.3.

Table 5.3. Cumulative probability data

PGA [%g]	S	M	E	C
0.1	0.00%	0.00%	0.00%	0.00%
0.2	0.00%	0.00%	0.00%	0.00%
0.3	30.00%	0.00%	0.00%	0.00%
0.4	87.50%	2.50%	0.00%	0.00%
0.5	100.00%	50.00%	0.00%	0.00%
0.6	100.00%	80.00%	2.50%	0.00%
0.7	100.00%	95.00%	7.50%	0.00%
0.8	100.00%	100.00%	22.50%	2.50%
0.9	100.00%	100.00%	45.00%	7.50%
1	100.00%	100.00%	75.00%	12.50%

With the values in Table 5.3, a probability plot was created; it is shown in Figure 5.3.

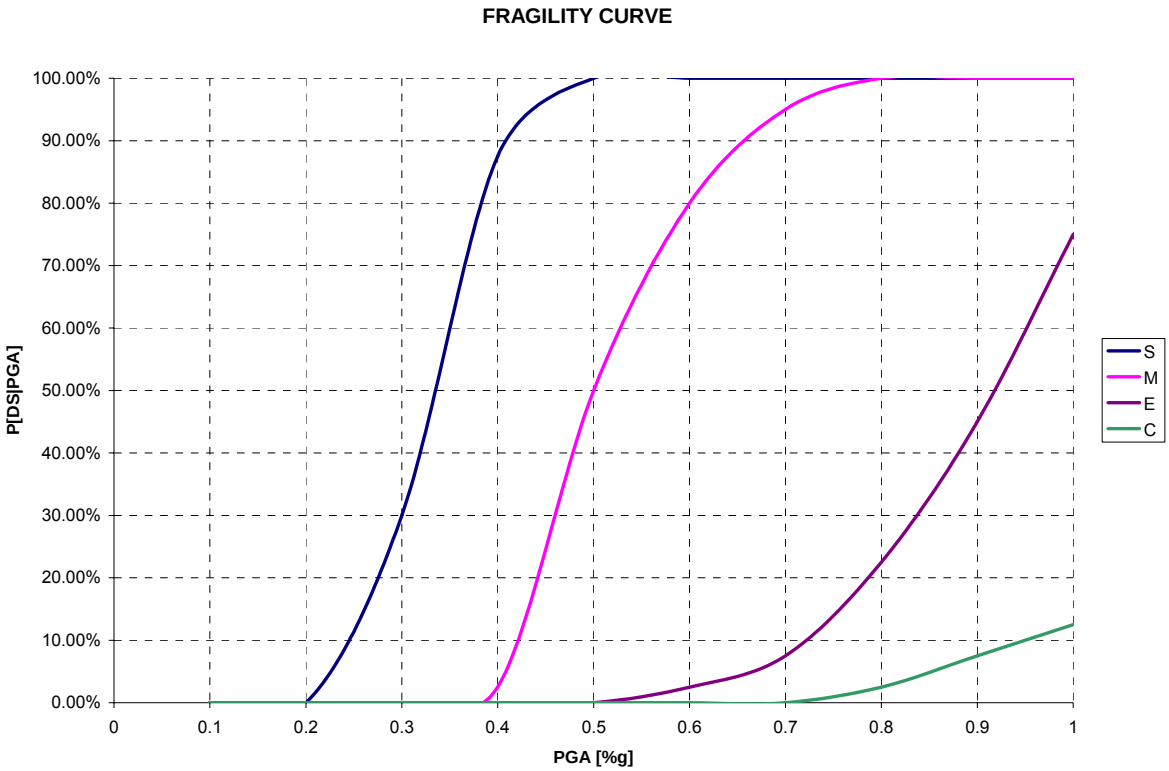

Figure 5.3 Probability plot for the example four story office building.

A two parameter log normal cumulative distribution has been used to represent the observed values. The log-normal distribution has a probability density function:

$$f(x \mid \mu,\sigma) = \frac{1}{x\sigma\sqrt{2\pi}} e^{-\left(\frac{(Ln(x)-\mu)^2}{2\sigma^2}\right)} \qquad \textbf{(5.1)}$$

where:

x = is the value at which is evaluated the function,

μ = is the median value of the PGA, and

σ = is the log-standard deviation.

The cumulative log-normal distribution is obtained by integration of the area below the density function; it is shown in equation 5.2.

$$f(x \mid \mu,\sigma) = \frac{1}{\sigma\sqrt{2\pi}} \int_0^x \frac{e^{-\left(\frac{(Ln(x)-\mu)^2}{2\sigma^2}\right)}}{t} dt \qquad \textbf{(5.2)}$$

In order to obtain the two parameters that define the log-normal distribution (μ,σ), the Microsoft Excel® Solver tool was used. Microsoft Excel® applies the Generalized Reduced Gradient (GRG2)[14] nonlinear optimization code. The following procedure was utilized:

1. Define a preliminary value for the median and standard deviation (μ,σ).
2. Plot the values obtained from the data (Table 5.4 for this example).
3. Calculate the cumulative log-normal distribution using the two preliminary values of μ and σ.
4. Calculate the sum of the differences between the probability found from the log-normal probability plot constructed in step 3 and the probability plot constructed in step 2.
5. Perform the optimization code included in Microsoft Excel®.
6. Repeat this procedure for each damage state.

[14] Developed by Leon Nelson, University of Texas at Austin and by Allan Warre, Cleveland State University.

Table 5.4. Table created to implement the optimization code for the extensive damage state.

DATA			
PGA [%g]	Probability (extensive damage)	Probabilty (Log-normal Distribution)	Difference
0.1	0	2.37013E-45	2.37E-45
0.2	0	2.67009E-22	2.67E-22
0.3	0	9.43415E-13	9.43E-13
0.4	0	1.00368E-07	1E-07
0.5	0	8.21562E-05	8.22E-05
0.6	0.025	0.004664508	0.020335
0.7	0.075	0.053513582	0.021486
0.8	0.225	0.224882186	0.000118
0.9	0.45	0.499657993	0.049658
1	0.75	0.749993427	6.57E-06
			0.091687

μ	-0.10523
σ	0.156014

The first two columns of Table 5.4 show the PGA intensity and the probability (from Table 5.3), respectively. The third column shows the probability values obtained using the cumulative log-normal equation (equation 5.2). Column four shows the absolute values of the difference between column 3 and column 2. The last cell in column 4 represents the sum of column 4. By minimizing this cell, the values in column 3 get closer to the real values of column 2. This process is done by the Microsoft Excel optimization code.

Figures 5.4 to 5.7 show the fragility curve of each damage state. Figure 5.8 shows the fragility curve for all damage states. The data points were also plotted to show how close the log-normal distribution is to the real probability data. In the same manner, the median and standard deviation were found for all buildings.

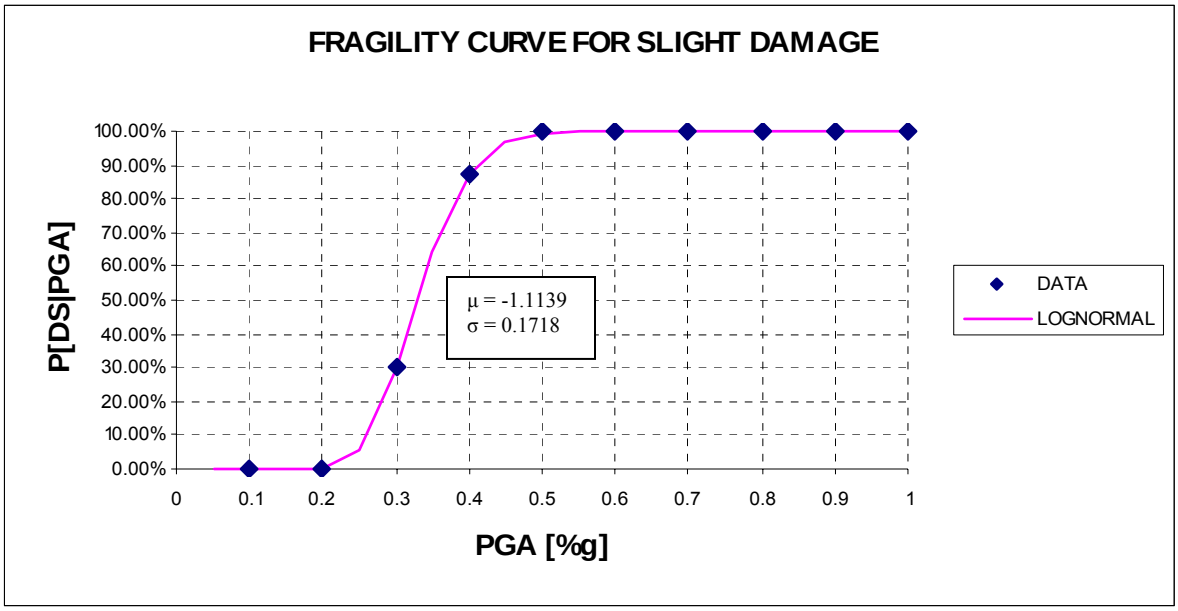

Figure 5.4 Fragility Curve for the slight damage state

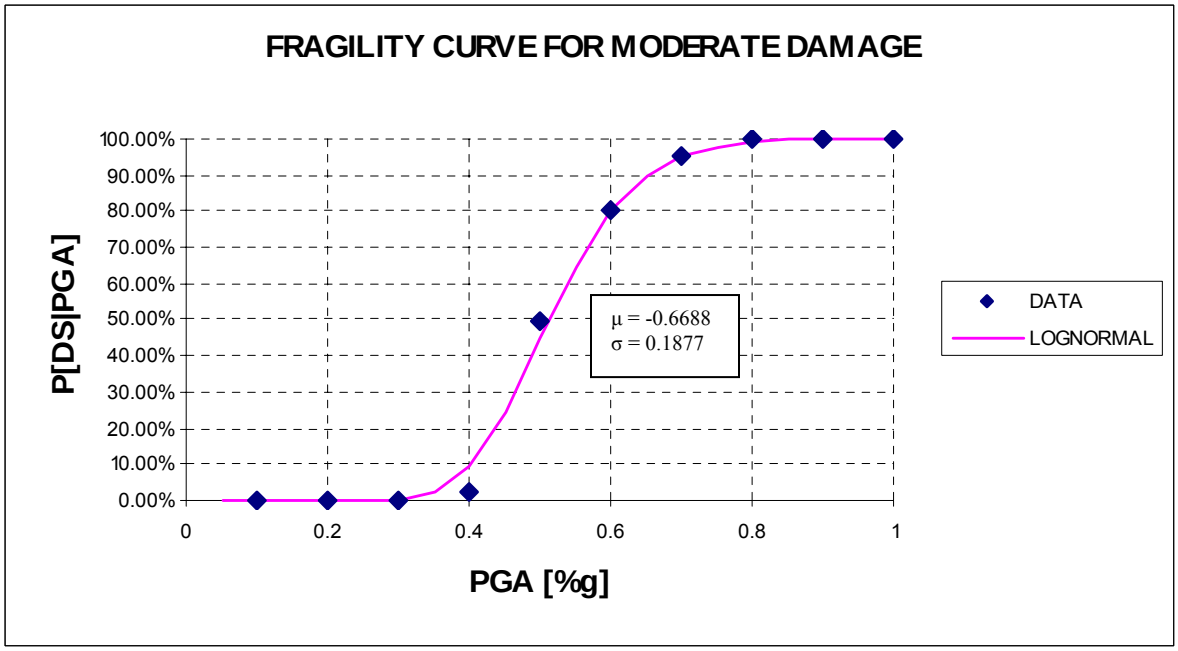

Figure 5.5 Fragility Curve for the moderate damage state

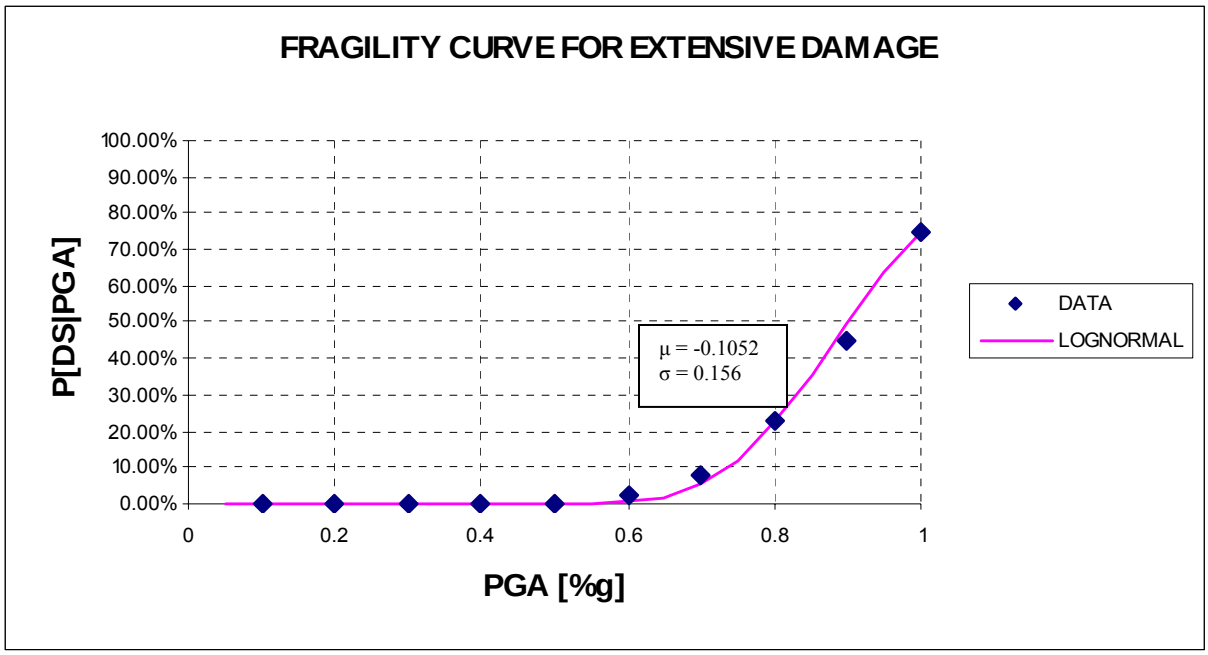

Figure 5.6 Fragility Curve for the extensive damage state

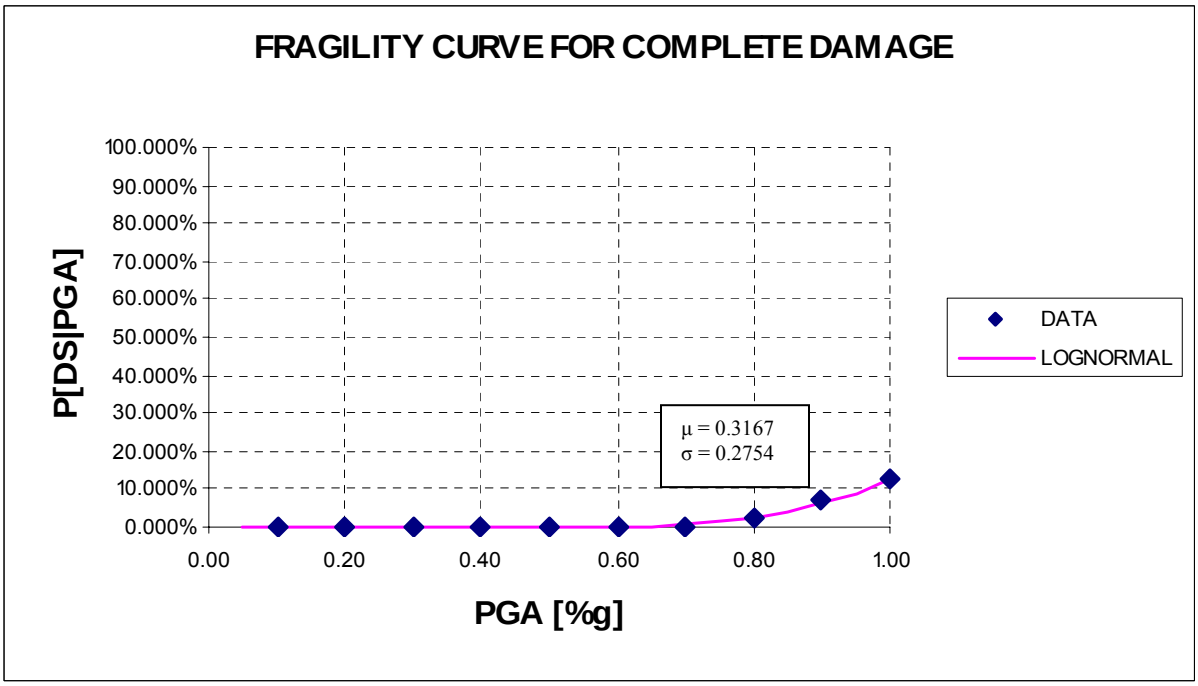

Figure 5.7 Fragility Curve for the complete damage state

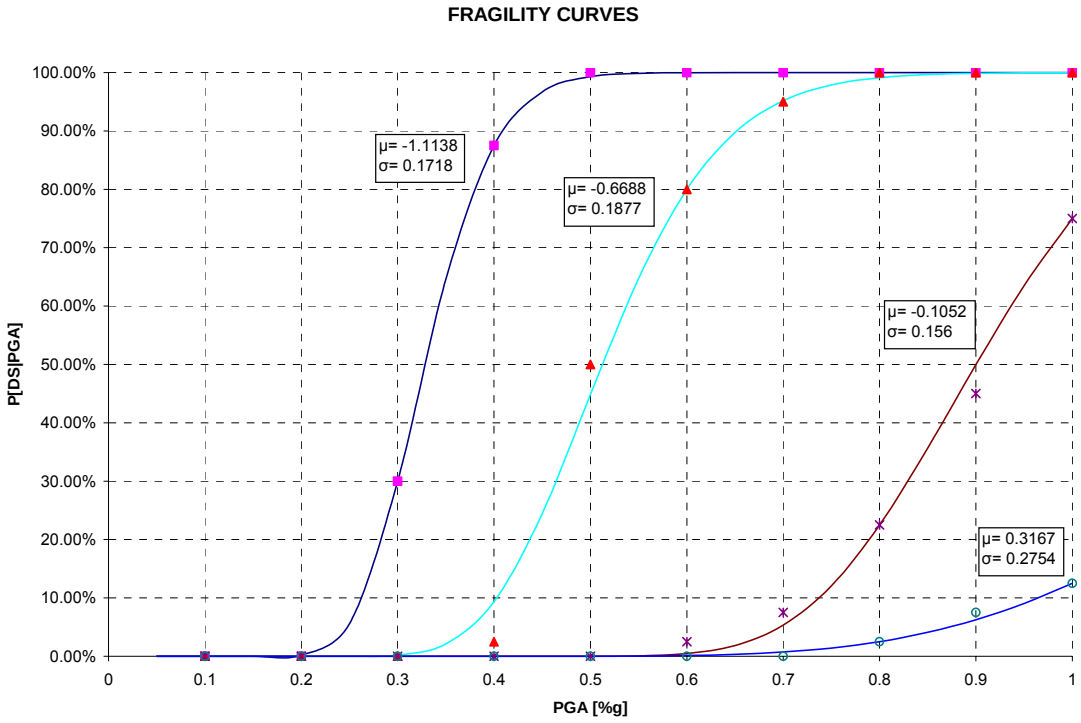

Figure 5.8 Fragility curves for all four damage states.

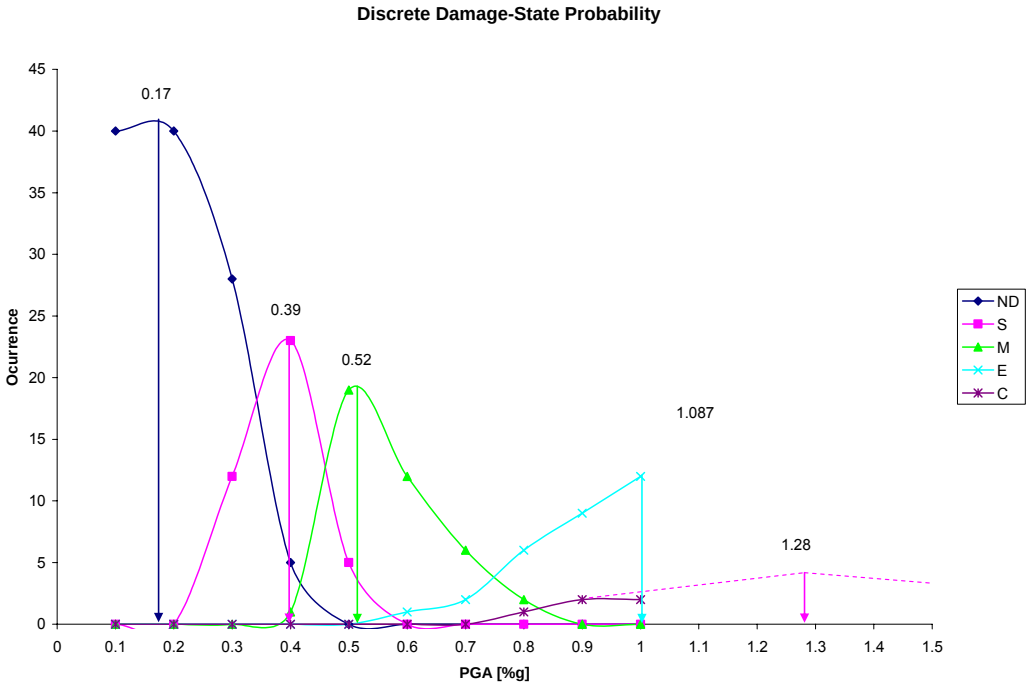

Figure 5.9 Discrete damage-state probability curves

In Figure 5.9 the discrete number of occurrence of each damage state was plotted against the PGA values. From this plot the median PGA value can be found by taking the natural logarithm of the values obtained:

$$\mu_S = Ln(0.39) = -0.94 \quad \textbf{(5.3)}$$

$$\mu_M = Ln(0.52) = -0.654 \quad \textbf{(5.4)}$$

$$\mu_E = Ln(1.085) = 0.08158 \quad \textbf{(5.5)}$$

$$\mu_C = Ln(1.28) = 0.247 \quad \textbf{(5.6)}$$

These values are very close to those obtained by the first method.

A fragility curve has been created for each building type. These fragility curves are shown in Chapter 6.

As it has been explained, fragility curves are cumulative density functions (CDF), however, it is necessary to convert these curves to discrete damage-state probability curves[15]. The discrete damage-state probability curves are obtained by taking the difference in probability between adjacent damage state fragility curves. From Figure 5.10 it can be seen that the discrete slight probability is obtained by subtracting the slight damage state to the moderate damage state at each pga value. The same is done for each damage state curve, and Figure 5.11 is obtained on this basis.

[15] SAC Joint Venture, 2000 (Appendix B, FEMA-351)

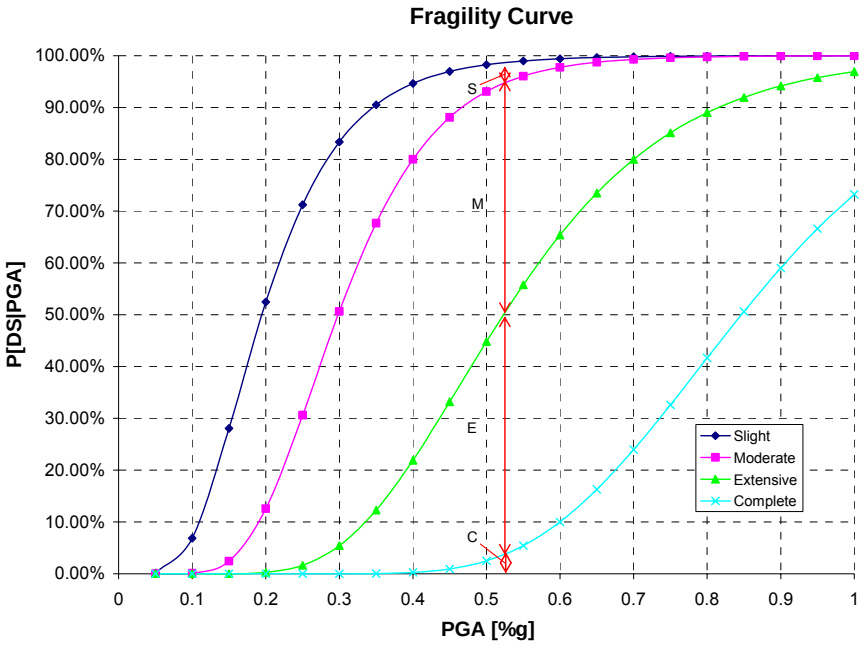

Figure 5.10. How to obtain the discrete damage-state probability curves from the fragility curves

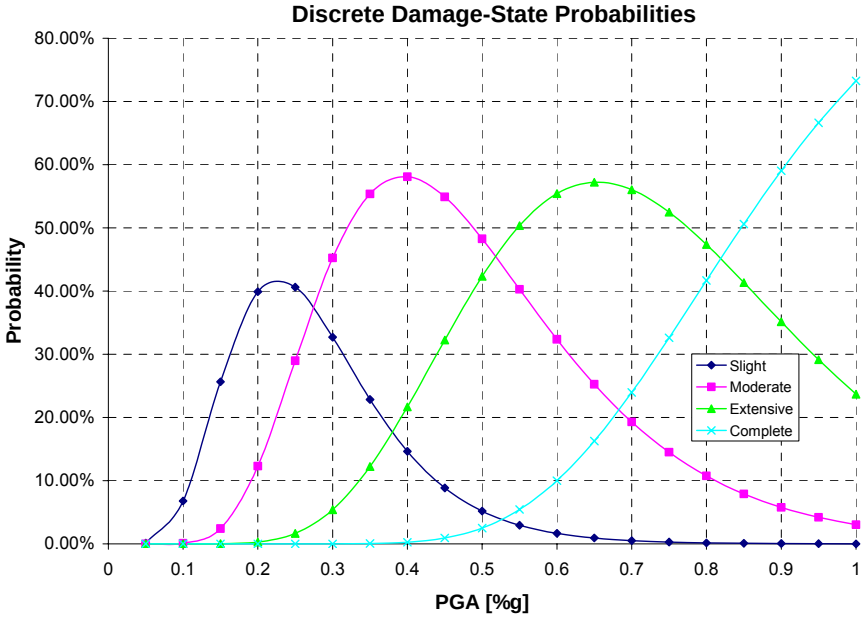

Figure 5.11. Discrete damage-state probability curves

5.3 Simplified Method

This method seeks to estimate the expected damage on a building in a simple way. It can be used to get an initial descriptive estimate of how much damage is expected. The idea of the method is that a linear regression can be plotted for the maximum drift vs. PGA ordinates of the average taken from all model variations for each building type.

Figure 5.12 shows the maximum drift vs. PGA charts for the eight 4 story buildings analyzed. Also, the average drift curve is plotted.

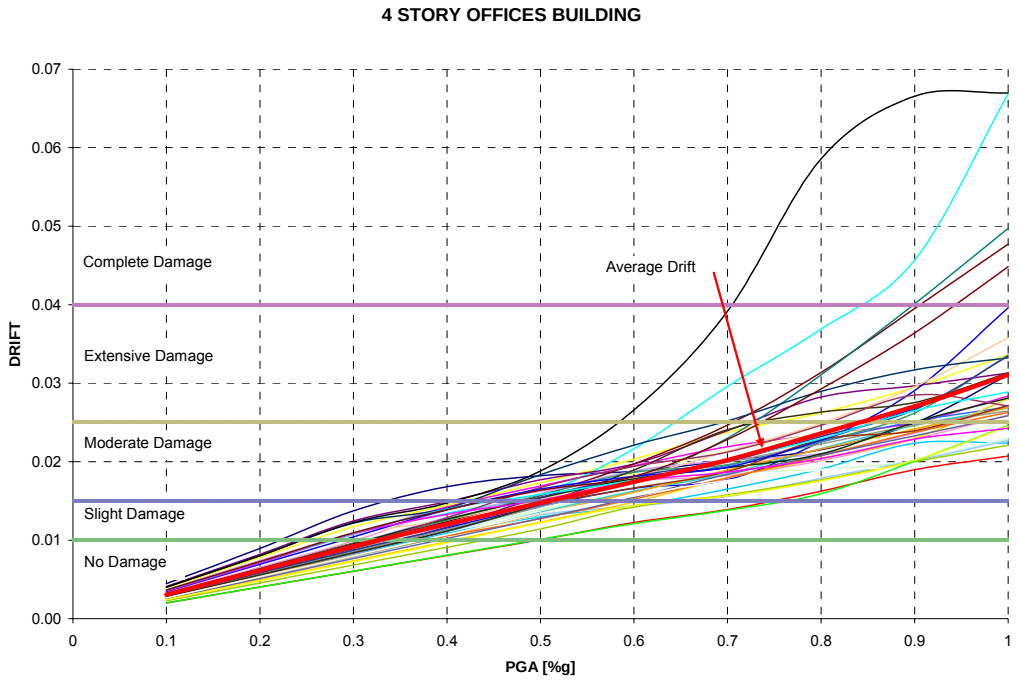

Figure 5.12 Inter-story drift vs. PGA chart for the four story offices building.

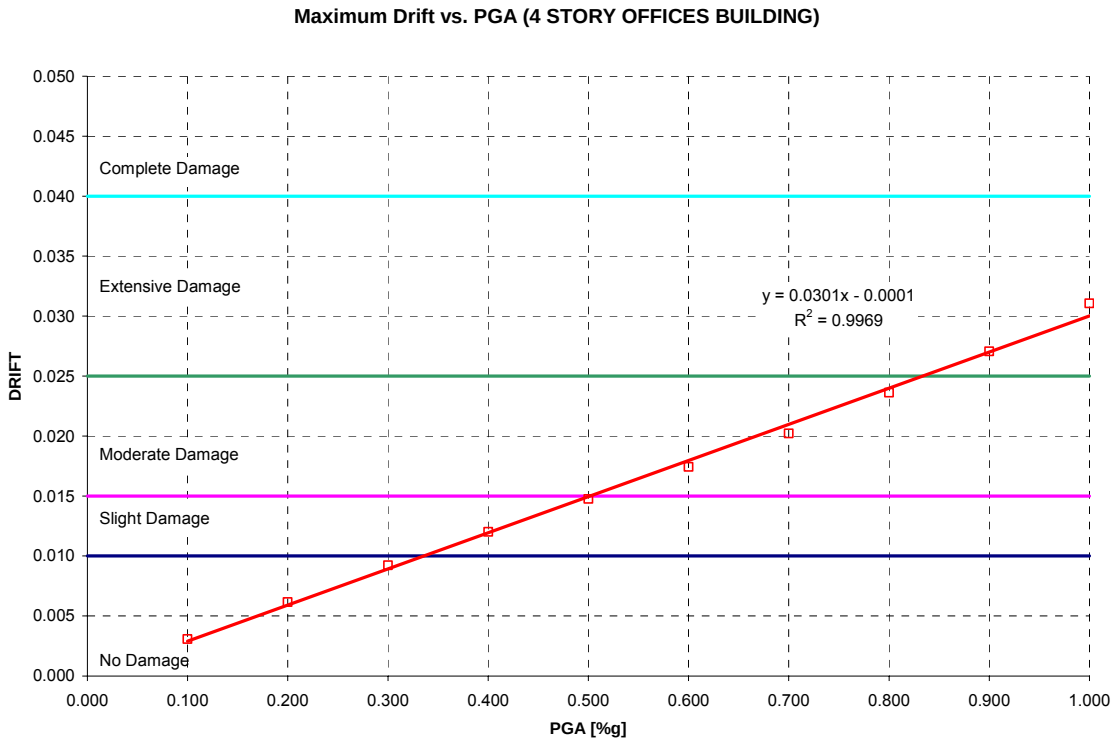

Figure 5.13 Linear regression fit for the average drift vs. PGA values.

From the linear regression of the data, the equation of the line is:

$$Drift = 0.0301(PGA) - 0.0001 \quad \textbf{(5.7)}$$

Applying this equation to the example in Section 5.2 one obtains,

$$Drift = 0.0301(0.6) - 0.0001 = 0.01796 \quad \textbf{(5.8)}$$

According to the damage states previously defined in Table 3.2, a drift value of 0.01796 would cause moderate damage to the building. If the building analyzed used Pre-Northridge connections, this amount of drift would cause fracture on as many as 25% of the connections on any floor level (Table 3.1). If Post-Northridge connections were used in the building, only moderate amounts of yielding and distortion of some column panel zones and minor buckling of some girders would be expected.

Letting the slope of the line be equal to a_0 and the y intercept equal to b_0, a table containing these values for the different building types was created and is presented in Appendix B. Equation 5.9 shows the final equation used to approximate the damage in a building.

$$Drift = a_0(PGA) - b_0 \quad \textbf{(5.9)}$$

Where:

a_0 = slope of the linear regression obtained from the average drift values in the maximum drift vs. PGA plot.

b_0 = y intercept of the linear regression obtained from the average drift values in the maximum drift vs. PGA plot.

6 Generation of Models and Fragility

6.1 Introduction

The main objective of this thesis is to create functions that can predict the probability of damage in steel buildings produced by an earthquake. Considering that a statistical analysis is fundamental to create such probability functions, it is essential to have as many models as possible so that a more realistic sample population is used. This chapter explains how the approach of generating more models is accomplished.

6.2 Models from the drawings

A search for plans of steel buildings already constructed and to be constructed in Puerto Rico was done. A general idea of the predominant way of designing steel buildings in Puerto Rico was obtained from these plans. From all the plans obtained, a selection was made accounting for the different occupancies, these selected steel buildings were used for the analysis. From these selected buildings additional building models were created according to the typical parameters observed in the plans collected.

6.2.1 Parameter Variation

To account for the fact that many models are needed, eight to twelve variations were made from the original models. A total of 435 buildings were obtained and modeled. The span length, the height of the stories, and the tributary length have been varied. The next sections show the original model as well as the parameters that have been varied from each original model.

6.2.2 Procedure

Since new models were created from the original ones, it was necessary to design the new generated buildings. A linear analysis using SAP2000 was performed to each of the generated models. Gravity loads were used to assign the new sections depending on the variation. The design codes used in Puerto Rico are the UBC-97, and the AISC LRFD. The program SAP 2000 has a quick method for linearly designing the steel structures. This procedure is explained next.

Steps:

1. Draw the geometry of the building (since 2D models are being considered here, the geometry becomes that of a plane frame).
2. Assign a list of possible sections to each beam and column section (typically W sections or HSS Sections).
3. Assign the dead and live loads to each member.
4. Create the load combinations (as indicated by the UBC-97). These are:
    1) 1.4D
    2) 1.2D + 1.6L
5. Run the analysis.
6. Run the steel design feature. (included in SAP 2000)
7. Verify the proposed design.

After the elastic design is performed, the building model is created in the program RAM Performance, and a NDP is performed. For details on how the NDP is done, see Chapter 4.

6.2.3 Industrial Buildings

6.2.3.1 One Story Industrial Building

A one story industrial building with an area of 10,800 square feet was analyzed. Figure 6.1 shows a sectional view of the Industrial building.

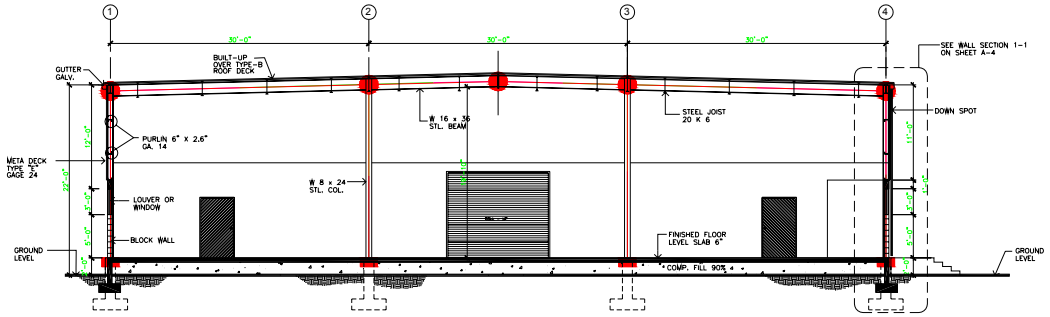

Figure 6.1 One story factory

Figure 6.2 represents the model created for the matrix analysis of the industrial building. The masses are concentrated in the joints according to their tributary area. The first column (from left to right) on Figure 6.2 has a mass of 1/6 M. This means that it accounts for 1/6 of the total mass carried by such frame.

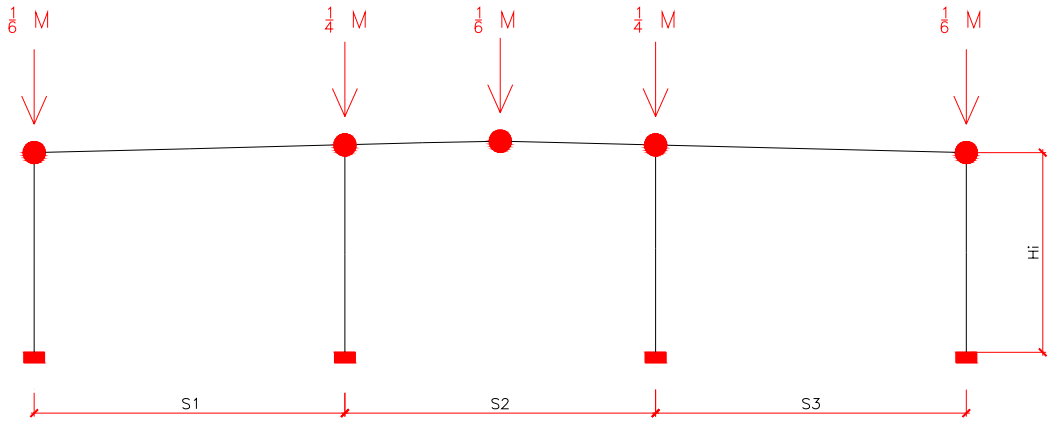

Figure 6.2 Typical frame found in the one story industrial building.

The fundamental period for the models analyzed range from 0.76 seconds to 1.71 seconds. Table 6.1 shows the different variations made to the original model, and the values used for each modification.

Table 6.1. Parameter Variation for the Factory Classification

		PARAMETERS VARIATION				
MODEL	REMARK	S1[ft]	S2[ft]	S3[ft]	Hi[ft]	Ltrib[ft]
1	Orig.	30	30	30	19.5	30
2		30	30	30	25	30
3		30	30	30	19.5	35
4		30	30	30	25	35
5		30	30	30	19.5	40
6		30	30	30	25	40
7		40	40	40	19.5	30
8		40	40	40	25	30
9		40	40	40	19.5	35
10		40	40	40	25	35
11		40	40	40	19.5	40
12		40	40	40	25	40

Table 6.2. Masses added to the different models

			Distributed		Mass		M/4		M/6	
MODEL	Ltrib (ft)	S (ft)	DL	LL	DL	LL	DL	LL	DL	LL
1	30	30	0.6	0.6	54	54	13.5	13.5	9	9
2	30	30	0.6	0.6	54	54	13.5	13.5	9	9
3	35	30	0.7	0.7	63	63	15.75	15.75	10.5	10.5
4	35	30	0.7	0.7	63	63	15.75	15.75	10.5	10.5
5	40	30	0.8	0.8	72	72	18	18	12	12
6	40	30	0.8	0.8	72	72	18	18	12	12
7	30	40	0.6	0.6	72	72	18	18	12	12
8	30	40	0.6	0.6	72	72	18	18	12	12
9	35	40	0.7	0.7	84	84	21	21	14	14
10	35	40	0.7	0.7	84	84	21	21	14	14
11	40	40	0.8	0.8	96	96	24	24	16	16
12	40	40	0.8	0.8	96	96	24	24	16	16

The span length was varied using S = 30 ft and S = 40ft. The eave height has been modeled using H = 19.5ft and H = 25 ft. The third and last variation is the tributary length, where three values were used, L_{trib} = 30ft, 35ft and 40ft. Increasing the tributary length increases

the tributary loads and; therefore, the mass applied to the frame. Table 6.2 also shows how the loads and the masses are affected by the change in the tributary length (L_{trib}). By combining the 2 span variations with the 2 height variations and with the 3 tributary length variations, a total of 12 variations is obtained. The next flowchart (Figure 6.3) explains the combinations that were used.

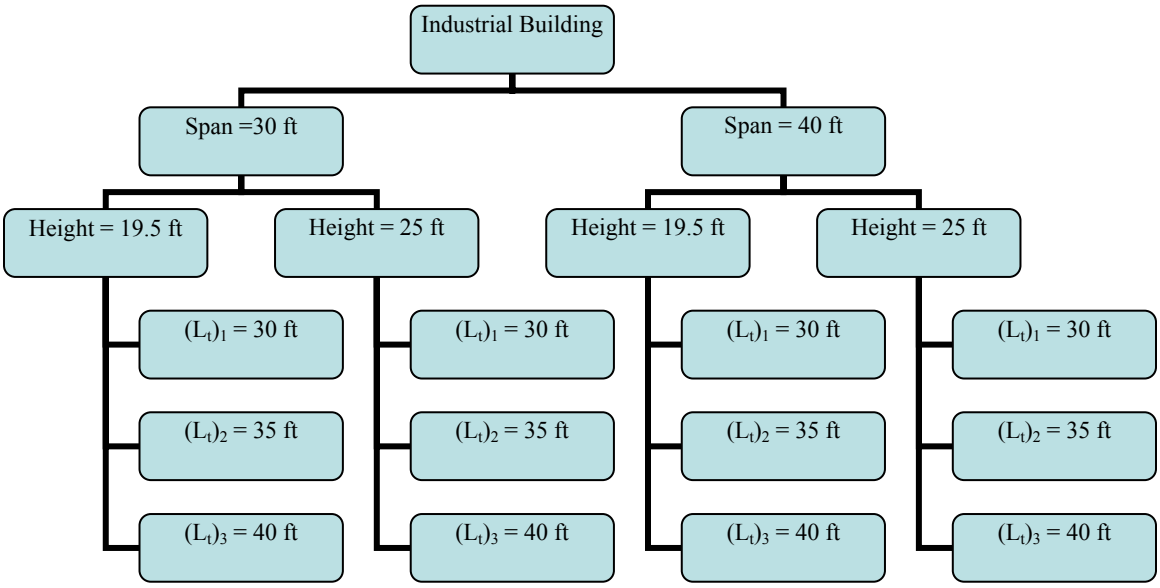

Figure 6.3 Flowchart of the model variations

The inter-story drift for each model has been obtained for each PGA value. Figure 6.4 shows the corresponding drift values for each PGA value.

In Table 6.3 the maximum drift obtained at every 0.05g for all 12 models is shown. The table also shows the mean and the standard deviation values for the 12 models at every 0.05g.

Table 6.3. Maximum inter story drift values for each PGA

PGA	model 1	model 2	model 3	model 4	model 5	model 6	model 7	model 8	model 9	model 10	model 11	model 12	mean	std dev
0.05	0.003394	0.003814	3.20E-03	0.003957	3.67E-03	0.003877	3.65E-03	0.00366	3.53E-03	0.003685	2.64E-03	0.00375	3.57E-03	3.59E-04
0.1	0.006786	0.007629	6.40E-03	0.007916	7.34E-03	0.007755	7.30E-03	0.007322	7.07E-03	0.007372	5.28E-03	0.007502	7.14E-03	0.000716
0.15	0.010178	0.011444	9.60E-03	0.011875	1.10E-02	0.011633	1.10E-02	0.010984	1.06E-02	0.011058	7.93E-03	0.011254	1.07E-02	0.001073
0.2	0.013571	1.53E-02	1.28E-02	1.58E-02	1.47E-02	1.55E-02	1.46E-02	1.46E-02	1.38E-02	1.47E-02	1.06E-02	1.50E-02	1.43E-02	0.001435
0.25	0.016963	1.91E-02	1.60E-02	1.98E-02	1.75E-02	1.94E-02	1.83E-02	1.83E-02	1.63E-02	1.84E-02	1.32E-02	1.88E-02	1.77E-02	0.001832
0.3	0.020114	2.29E-02	1.92E-02	2.38E-02	1.84E-02	2.33E-02	2.20E-02	2.20E-02	1.89E-02	2.21E-02	1.54E-02	2.25E-02	2.09E-02	0.002482
0.35	0.023708	0.026746	2.24E-02	0.027777	1.98E-02	0.02721	2.35E-02	0.025667	2.17E-02	0.02585	1.77E-02	0.025462	2.40E-02	0.003098
0.4	0.026971	0.030829	2.47E-02	0.032046	2.27E-02	0.031375	2.42E-02	0.029528	2.30E-02	0.029714	2.02E-02	0.02867	2.70E-02	0.003915
0.45	0.027028	0.033938	2.50E-02	0.034091	2.47E-02	0.032449	2.49E-02	0.030512	2.27E-02	0.030756	2.23E-02	0.030306	2.82E-02	0.00429
0.5	0.026297	0.035775	2.73E-02	0.035413	2.63E-02	0.033448	2.56E-02	0.031482	2.54E-02	0.031737	2.34E-02	0.03172	2.95E-02	0.00424
0.55	0.029471	0.037752	3.04E-02	0.037043	2.91E-02	0.034876	2.63E-02	0.032493	2.81E-02	0.032888	2.54E-02	0.033199	3.14E-02	0.003974
0.6	0.032933	0.040288	3.37E-02	0.039003	3.20E-02	0.03635	2.60E-02	0.03373	3.11E-02	0.034198	2.79E-02	0.034976	3.35E-02	0.004077
0.65	0.036606	0.043759	3.71E-02	0.042442	3.41E-02	0.039633	2.65E-02	0.037077	3.36E-02	0.037957	3.07E-02	0.036108	3.63E-02	0.004757
0.7	0.040482	0.04915	4.03E-02	0.047386	3.69E-02	0.044271	2.77E-02	0.042475	3.58E-02	0.04339	3.29E-02	0.035038	3.96E-02	0.006237
0.75	0.043444	0.055184	4.20E-02	0.05254	4.22E-02	0.049031	2.99E-02	0.047709	3.80E-02	0.049138	3.52E-02	0.039307	4.36E-02	0.007415
0.8	0.044786	0.061871	4.42E-02	0.060192	4.83E-02	0.055208	3.25E-02	0.054829	3.97E-02	0.056452	4.02E-02	0.043784	4.85E-02	0.009145
0.85	0.046341	0.065933	4.59E-02	0.066167	5.24E-02	0.061902	3.62E-02	0.062173	4.12E-02	0.063339	4.57E-02	0.0486	5.30E-02	0.010442
0.9	0.048276	0.066163	4.75E-02	0.066019	5.55E-02	0.065576	4.08E-02	0.063718	4.25E-02	0.063615	5.40E-02	0.054164	5.57E-02	0.009363
0.95	0.049588	0.066161	4.91E-02	0.06631	5.59E-02	0.065872	4.59E-02	0.064438	4.39E-02	0.06344	5.53E-02	0.05936	5.71E-02	0.008353
1	0.050928	0.066407	5.18E-02	0.066805	5.56E-02	0.066462	5.10E-02	0.064549	4.59E-02	0.064241	5.61E-02	0.063209	5.86E-02	0.007495

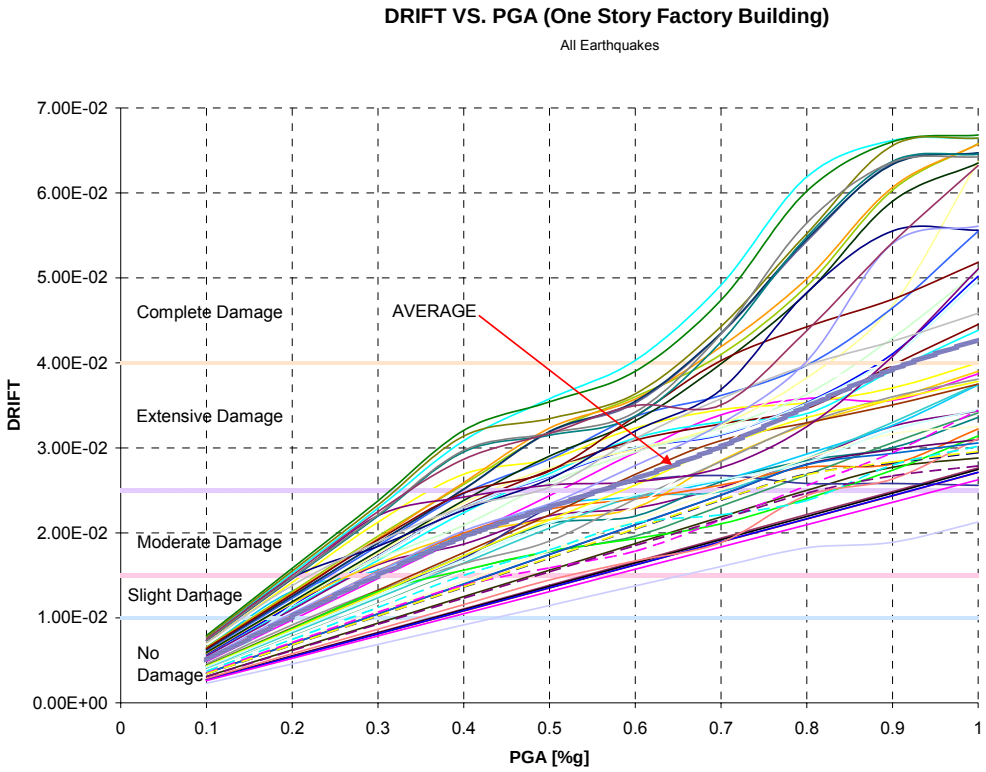

Figure 6.4 Maximum drift values for all the earthquakes

From Figure 6.4 it can be seen that an earthquake with intensity of 0.15g will cause slight damage in this type of structures. The intensities that will cause moderate, extensive and

complete damage are 0.2, 0.36 and 0.7, respectively. After performing the non linear analysis for the 12 variations, for the 5 earthquakes, a total of 60 points was obtained. Table 6.4 shows the cumulative occurrence distribution for one story industrial buildings.

Table 6.4. Cumulative occurrence distribution

PGA [%g]	S	M	E	C
0.1	0	0	0	0
0.2	30	4	0	0
0.3	51	30	0	0
0.4	59	44	12	0
0.5	60	53	25	0
0.6	60	59	31	1
0.7	60	60	41	11
0.8	60	60	50	15
0.9	60	60	54	22
1	60	60	59	27

The occurrence distribution is shown in Figure 6.5. Figure 6.6 shows the fragility curves.

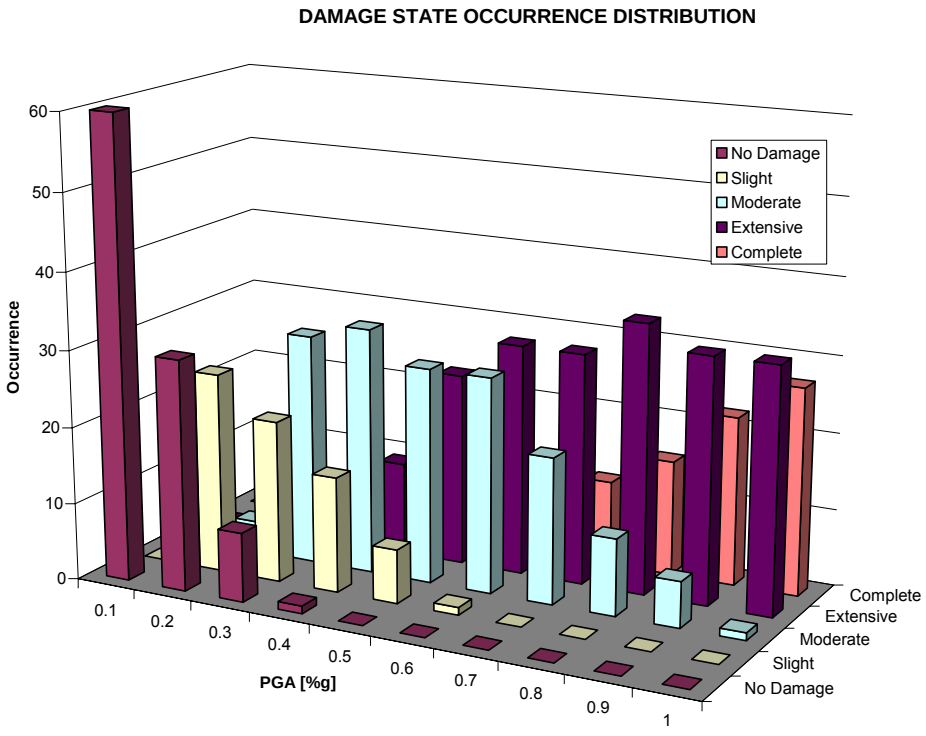

Figure 6.5 Occurrence distribution for each damage state at each PGA value

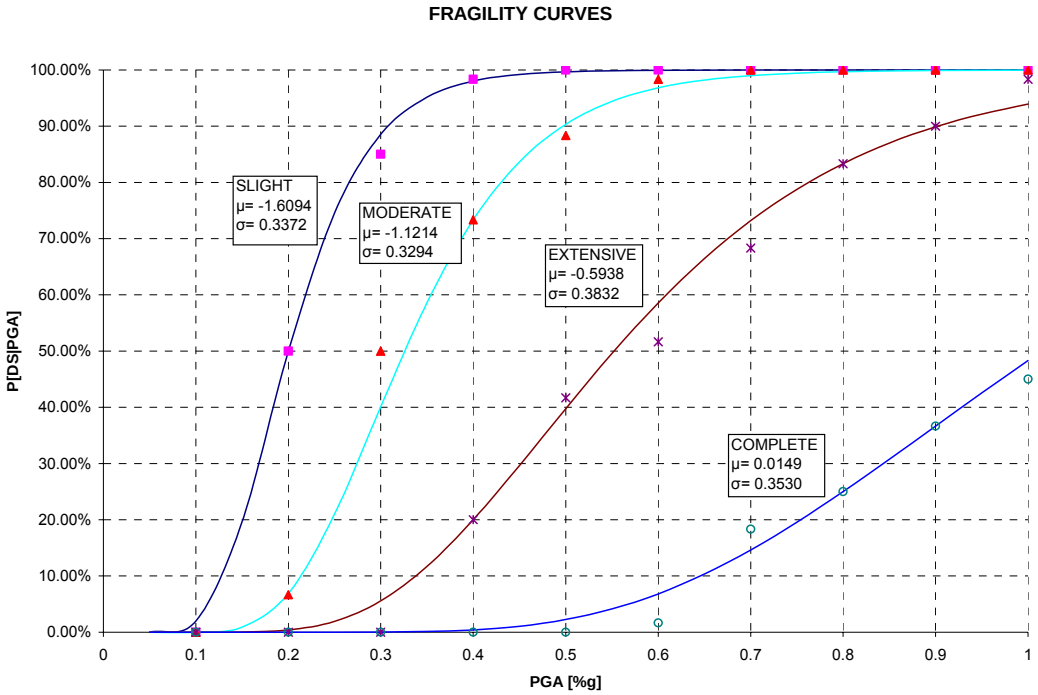

Figure 6.6 Fragility curve for a one story factory building

6.2.3.2 Two Story Industrial Building

The second factory studied is a two story building having an area of 76,800 square feet. Figure 6.7 shows a typical frame of this building. The fundamental period for the models analyzed range from 0.68 seconds to 1.36 seconds.

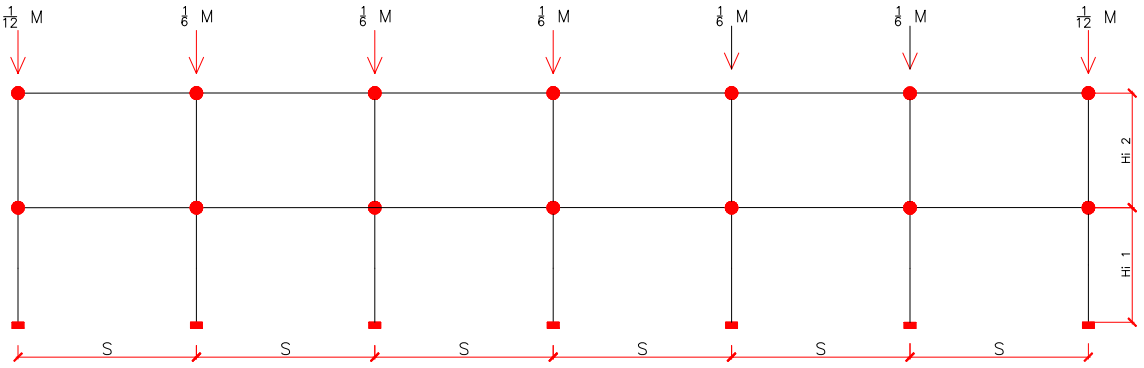

Figure 6.7 Typical frame modeled for a 2 story industrial building

Twelve variations have been made to this model: the span length, the story height, and the tributary length. Figure 6.8 shows a flowchart with the twelve resulting combinations.

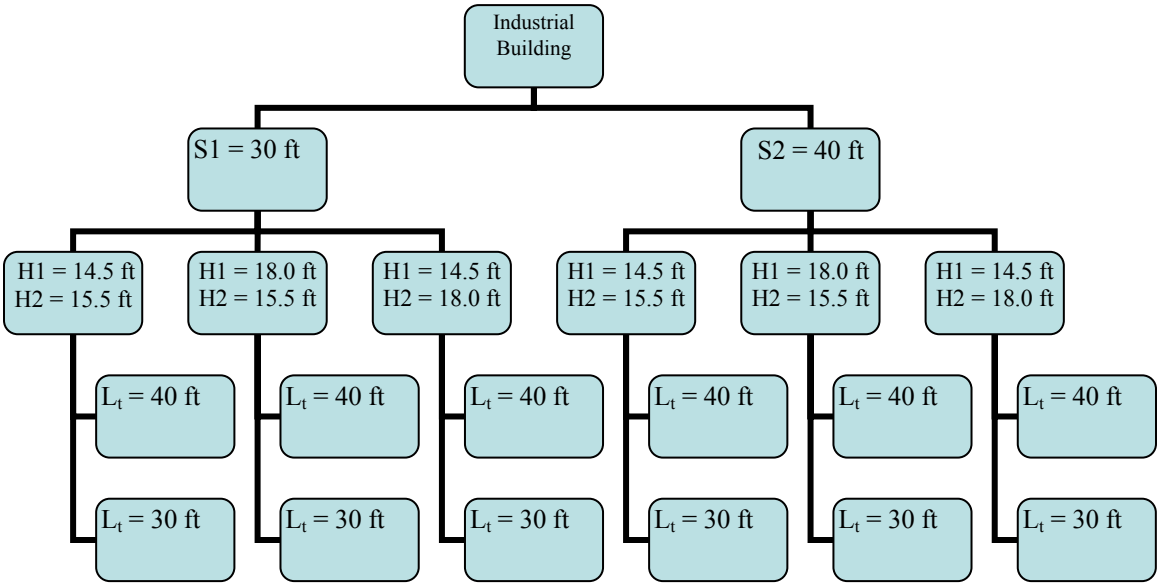

Figure 6.8 Flowchart of the variation of industrial buildings

Table 6.5. Parameters Variation

	PARAMETERS VARIATION			
MODEL	S[ft]	Hi 1[ft]	Hi 2[ft]	Ltrib[ft]
1	40	14.5	15.5	40
2	40	14.5	15.5	30
3	40	18	15.5	40
4	40	18	15.5	30
5	40	14.5	18	40
6	40	14.5	18	30
7	30	14.5	15.5	40
8	30	14.5	15.5	30
9	30	18	15.5	40
10	30	18	15.5	30
11	30	14.5	18	40
12	30	14.5	18	30

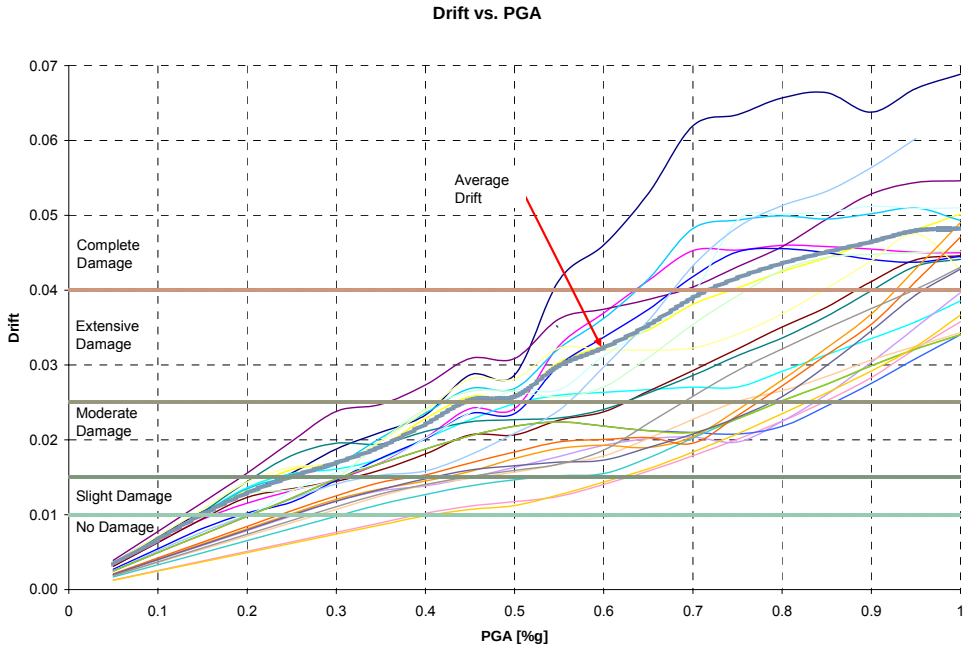

Figure 6.9 Maximum drift vs. PGA for the 12 models of the 2 story industrial building

Table 6.5 shows the different configurations used for the 12 models in a tabular way. Figure 6.9 shows the maximum drift values for each PGA value. The average drift value is also plotted in the same chart. From the average curve, it can be seen that until 0.2g no damage is expected. This plot also shows that an earthquake whose intensity ranges from 0.2g to 0.45g will cause only moderate damage. From 0.45g to 0.72g extensive damage is expected. Complete damage to the building is expected after 0.72g.

The discrete damage distribution is shown in Figure 6.10. The fragility curves for this type of buildings are shown in Figure 6.11.

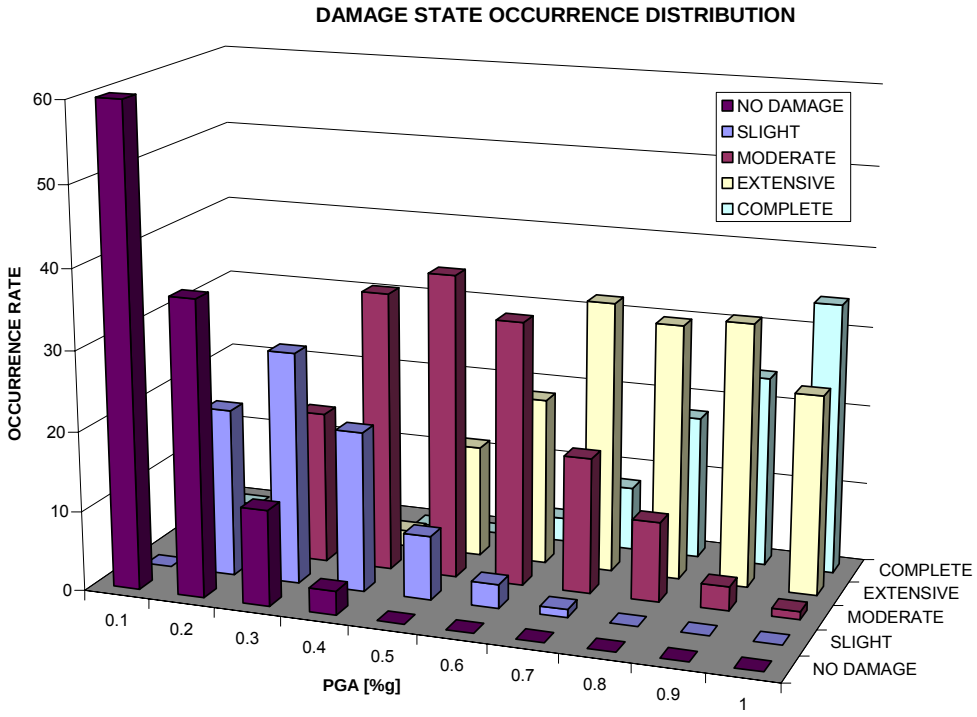

Figure 6.10 Occurrence distribution for each damage state

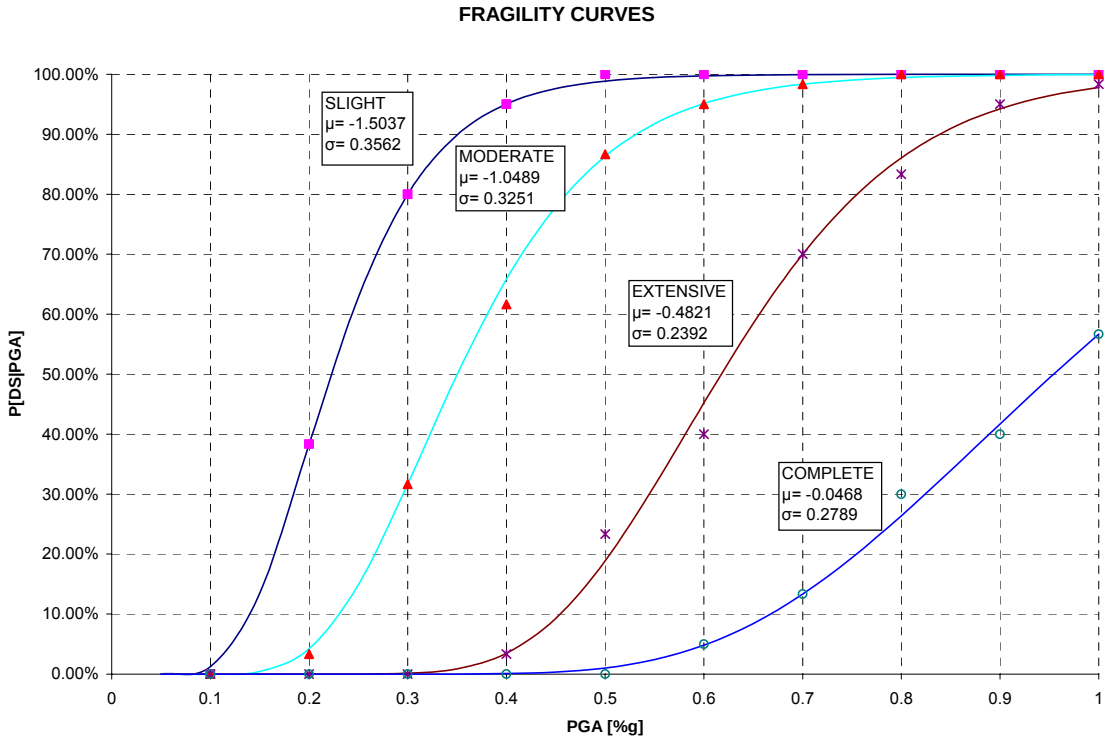

Figure 6.11 Fragility Curve for the two story industrial buildings

6.2.3.3 Industrial Building's Combined Fragility Curves

After performing the 12 variations for each of the two original industrial buildings models, a total of 24 models subjected to five earthquakes resulted in a total of 120 points for each PGA value. Figures 6.12 and 6.13 show the statistics for the industrial buildings combined. Figure 6.14 show the fragility curves for the combined industrial buildings.

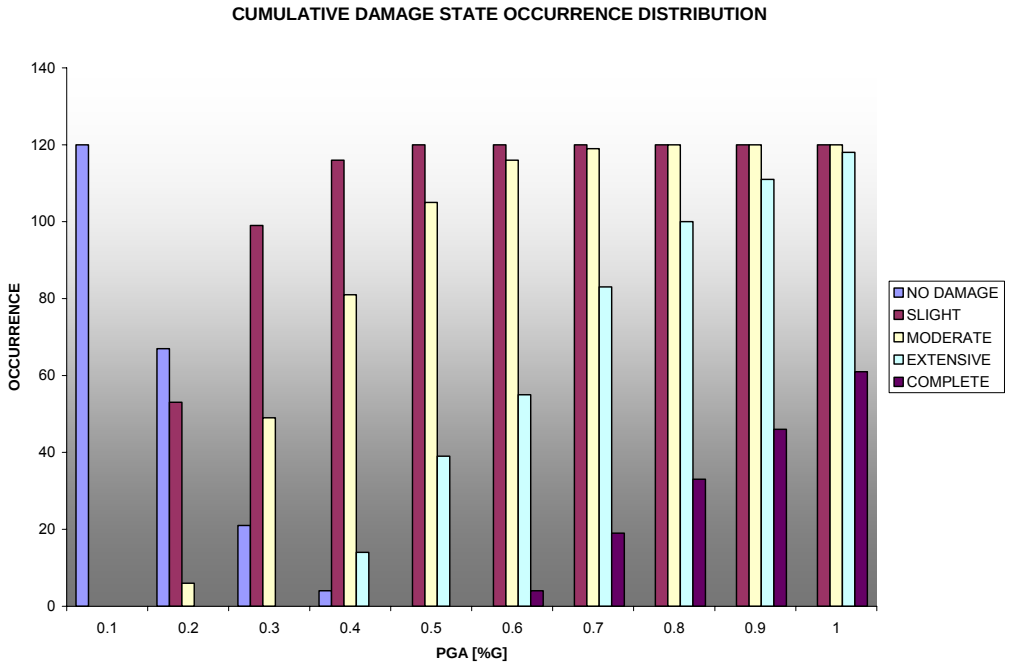

Figure 6.12 Cumulative damage state occurrence distribution for the combined industrial buildings.

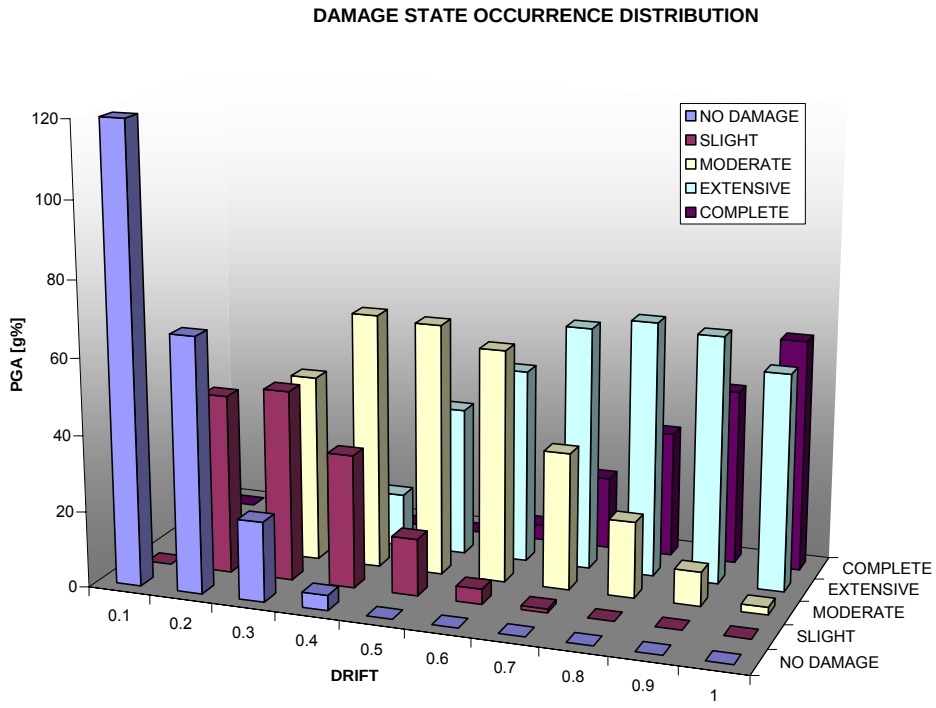

Figure 6.13 Damage state occurrence distribution

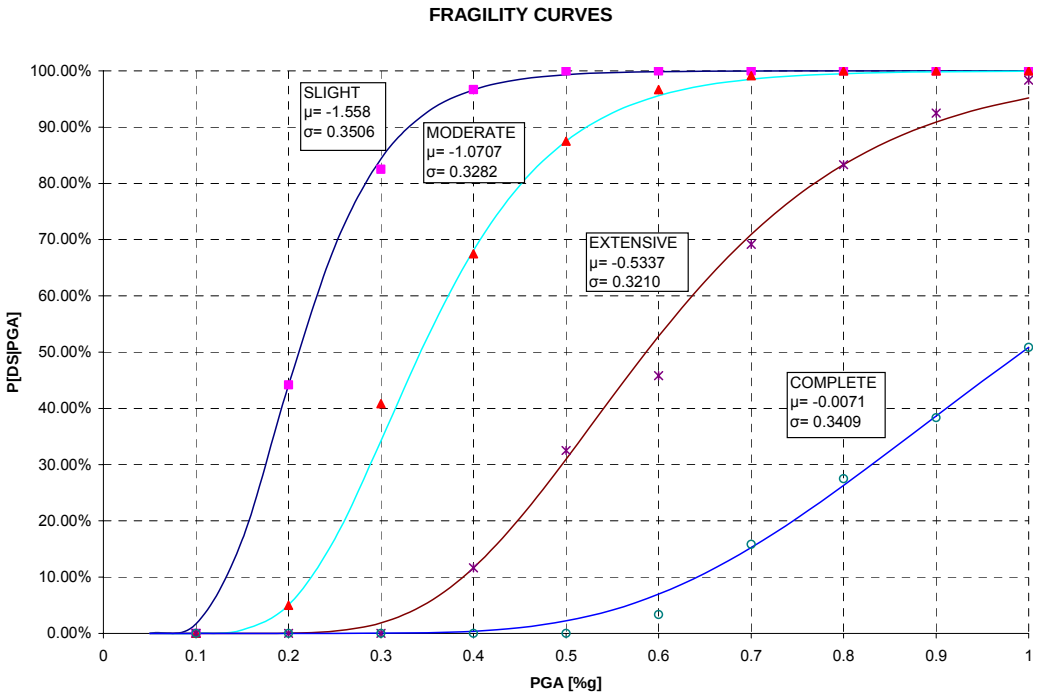

Figure 6.14 Fragility curve for industrial buildings

6.2.4 Offices and Commerce

Based in the information gathered from the survey conducted, it was observed that it is very common in Puerto Rico to construct buildings for offices and commercial spaces mixed. Having that in mind, both categories have been studied together.

6.2.4.1 Two Story Commercial/Office Building

A two story office building having the typical frame shown in Figure 6.15 was analyzed. The variations made to the model are shown in the flowchart of Figure 6.16. Table 6.6 shows the values of the parameters varied. The fundamental period for the analyzed buildings range from 0.47 seconds to 0.94 seconds. The maximum drift vs. PGA plot is shown in Figure 6.17. The damage state occurrence distribution at each PGA value is shown in Figure 6.18. Figure 6.19 shows the fragility curves obtained for the two story commercial/office buildings.

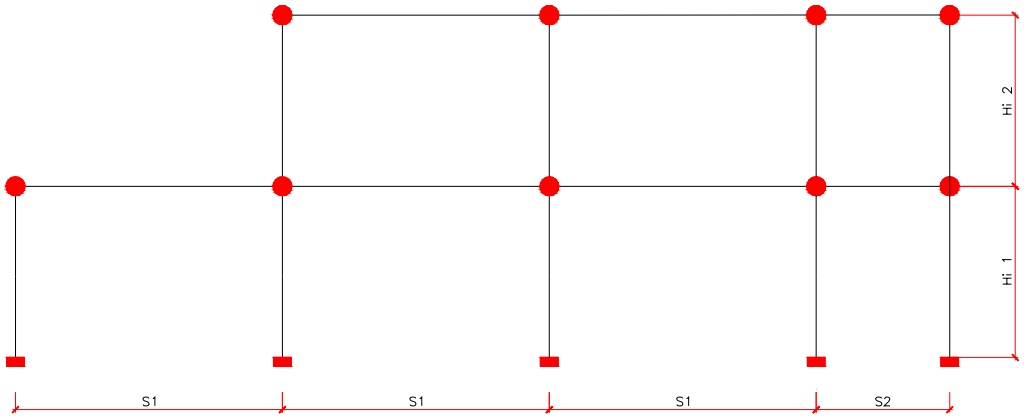

Figure 6.15 Two story commercial/office building geometry and mass distribution

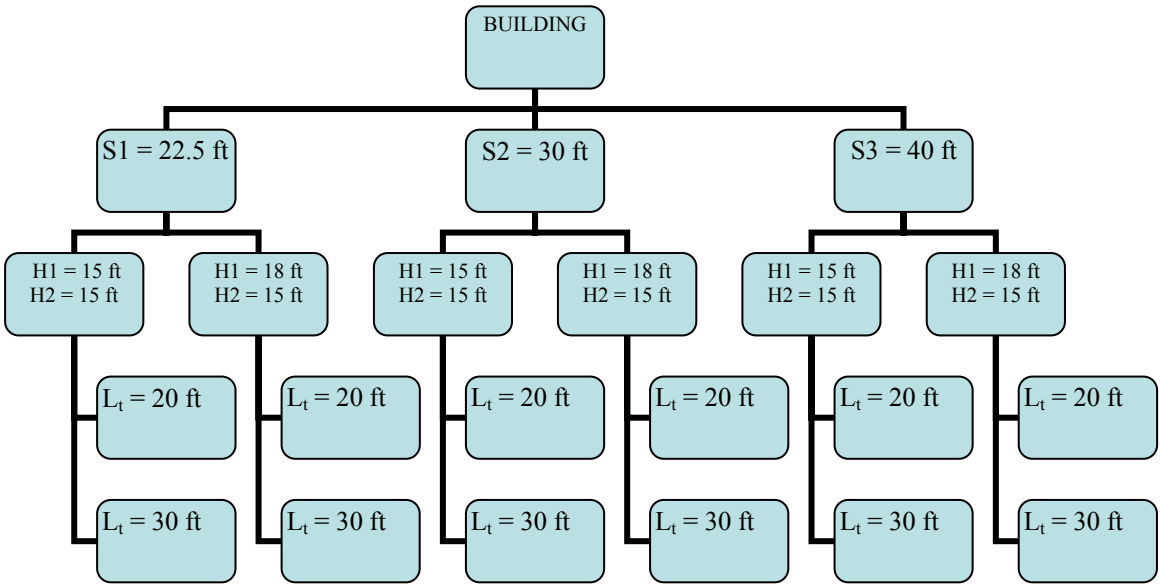

Figure 6.16 Flowchart of the parameter combinations for the 2 story commercial/office buildings.

Table 6.6. Parameters variation for the 2 story commercial/office building

	PARAMETERS VARIATION			
MODEL	S[ft]	H1 [ft]	H2 [ft]	Ltrib[ft]
1	22.5	15	15	20
2	22.5	15	15	30
3	22.5	18	15	20
4	22.5	18	15	30
5	30	15	15	20
6	30	15	15	30
7	30	18	15	20
8	30	18	15	30
9	40	15	15	20
10	40	15	15	30
11	40	18	15	20
12	40	18	15	30

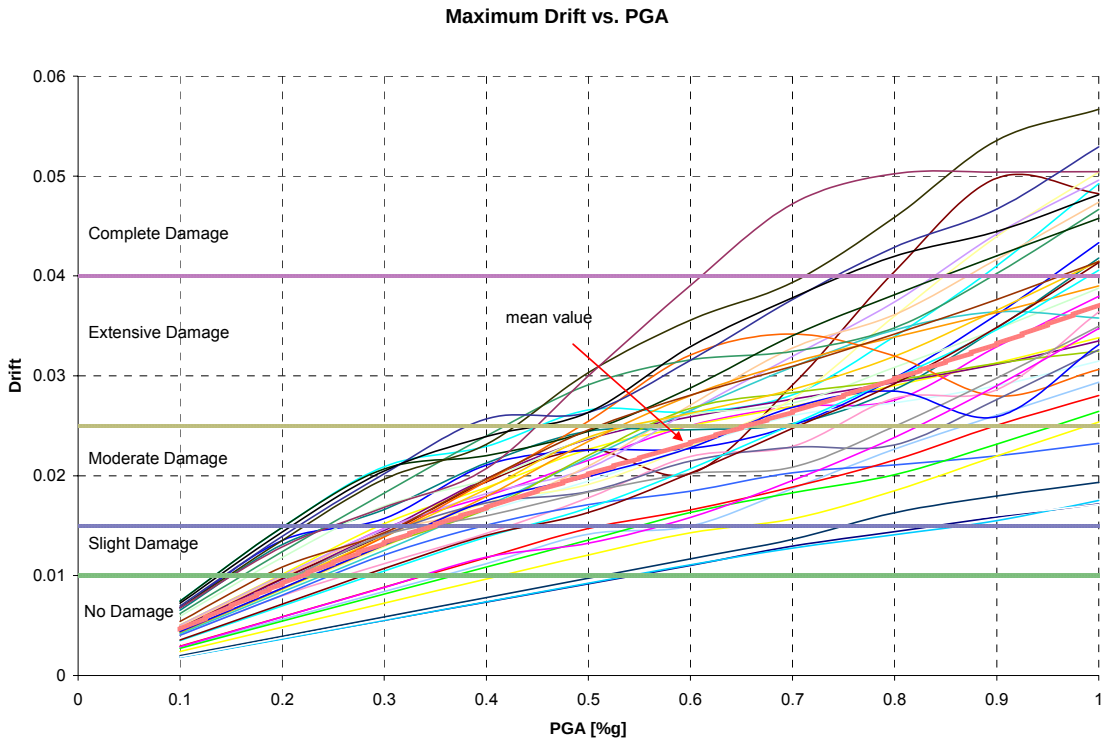

Figure 6.17 Maximum drift vs. PGA for the 12 models of the 2 story commercial/office building

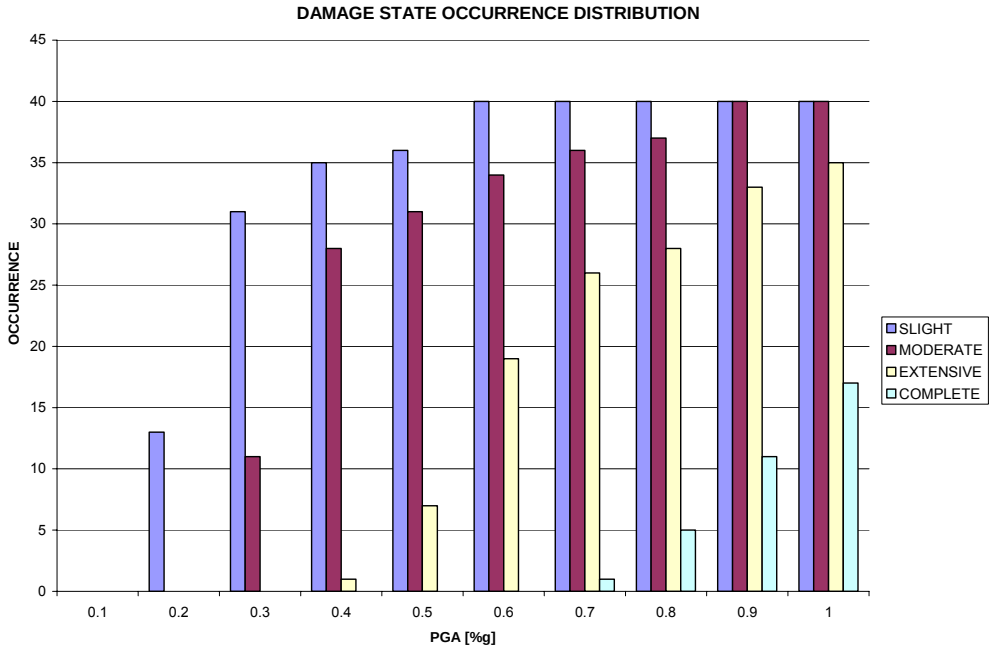

Figure 6.18 Cumulative damage state occurrence distribution for the two story commercial/office building.

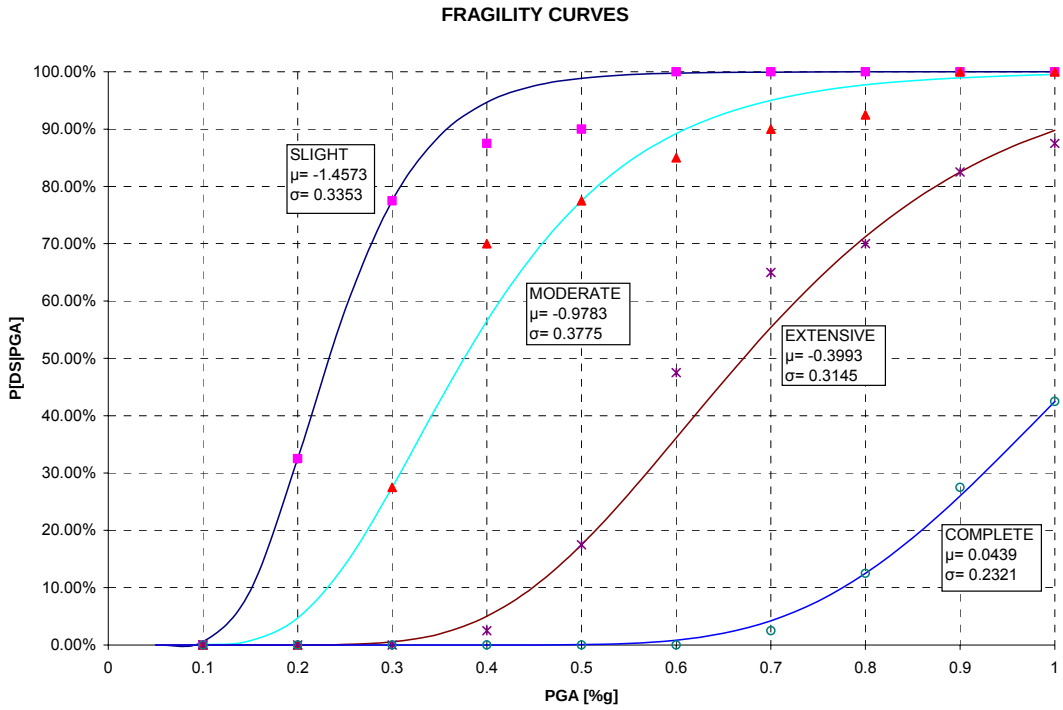

Figure 6.19 Fragility curve for a two story commercial/office building.

6.2.4.2 Three Story Commercial/Office Building

A three story commercial/office building was modeled (Figure 6.20). Nine variations were made to the original model. The fundamental period for the nine variations made range from 0.87 seconds to 1.45 seconds. The modifications were made to the span and the tributary length. A flowchart of the parameters in the models is shown in Figure 6.21. Figure 6.22 shows the maximum drift vs. PGA plot for the nine variations made to the original model. The cumulative occurrence of each damage state for each value of PGA is shown in Figure 6.23. Figure 6.24 shows the fragility curves created for the commercial/office occupancy.

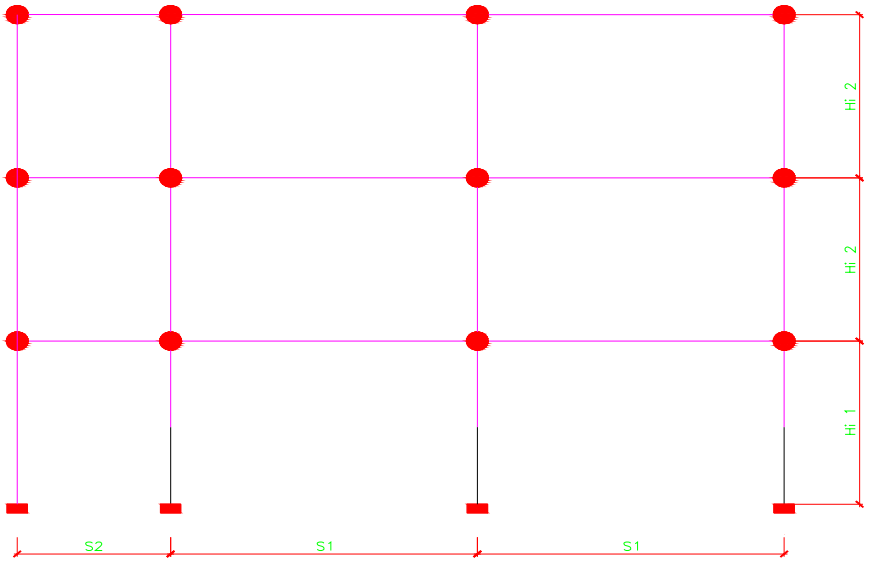

Figure 6.20 Elevation of a typical frame of a 3 story commercial/office building.

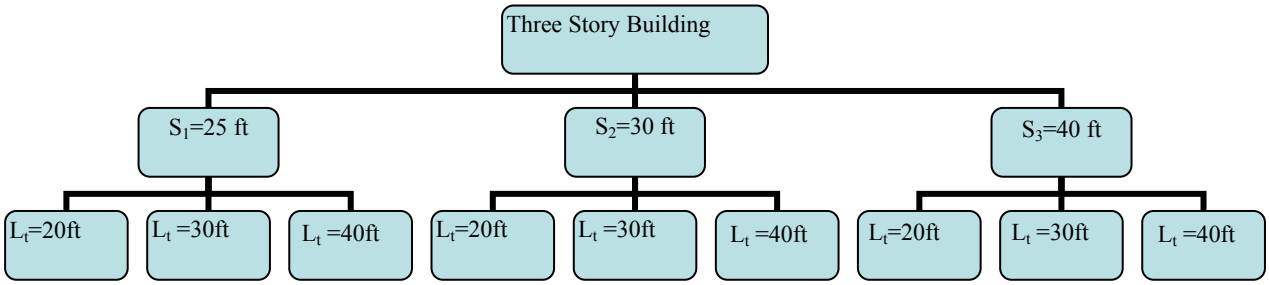

Figure 6.21 Flowchart of the building combinations for a 3 story commercial/offices buildings.

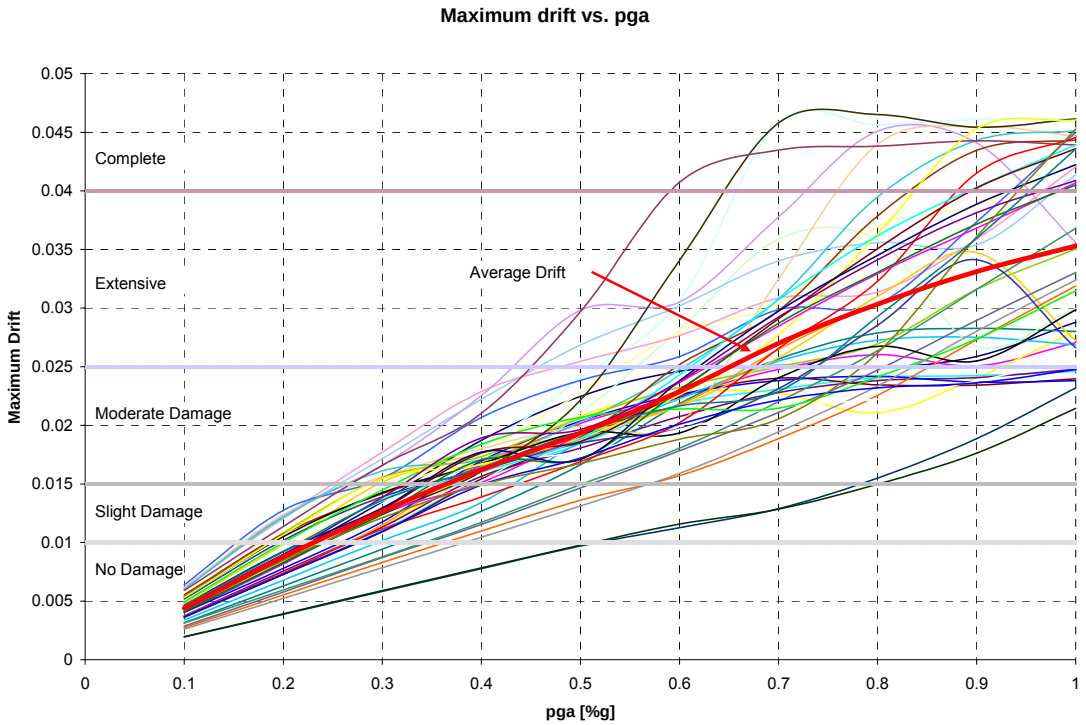

Figure 6.22 Drift vs. PGA plot for all 9 model variations of a 3 story commercial/office building.

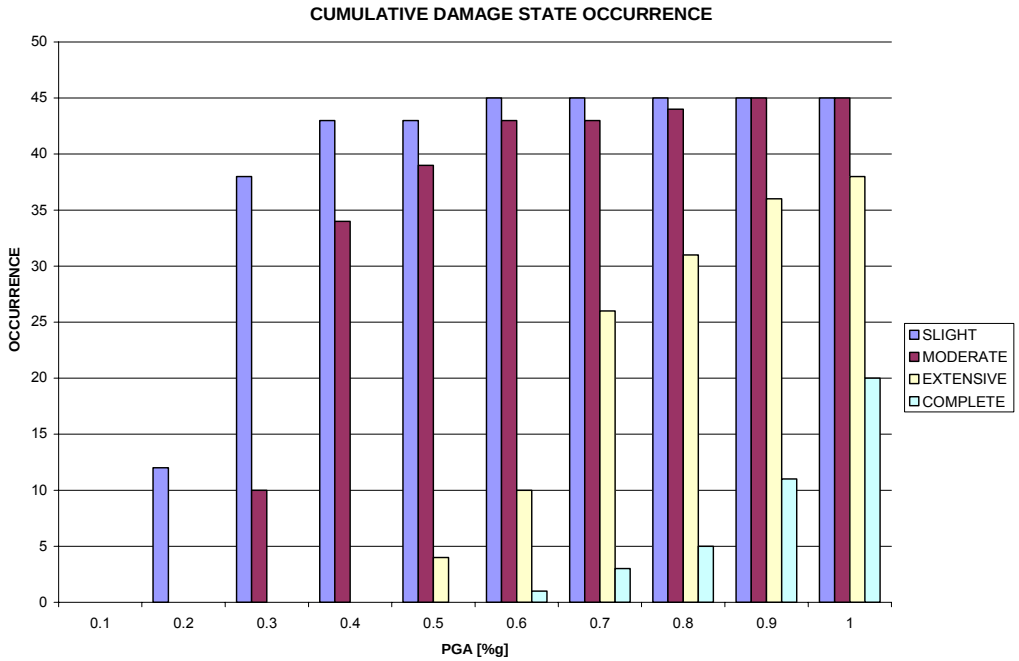

Figure 6.23 Damage state cumulative occurrence distribution for 3 story buildings.

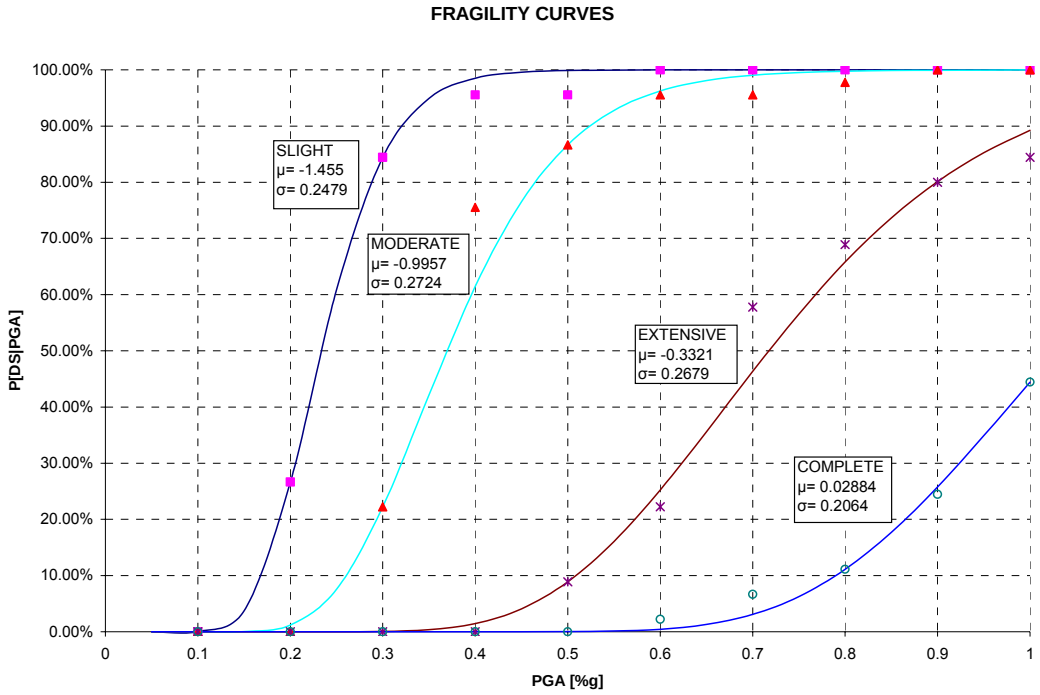

Figure 6.24 Fragility curves for 3 story commercial/offices building.

6.2.4.3 Four Story Commercial/Office Building

The following building studied is a four story building used for commerce and offices. Figure 6.25 shows a typical frame found in the analyzed building. Eight variations have been made to the building: the mass, the span and the story height. The fundamental period of the eight variations made range from 1.05 seconds to 1.52 seconds. Figure 6.26 shows a flowchart of the variations made to the original model. The parameters were varied accordingly to typical buildings observed (Table 6.7).

Figure 6.27 shows the maximum drift vs. PGA plot for the nine variations. Figure 6.28 shows the occurrence distribution of each damage state at each PGA intensity. The fragility curve for the 3 story commercial/office buildings is shown in Figure 6.29.

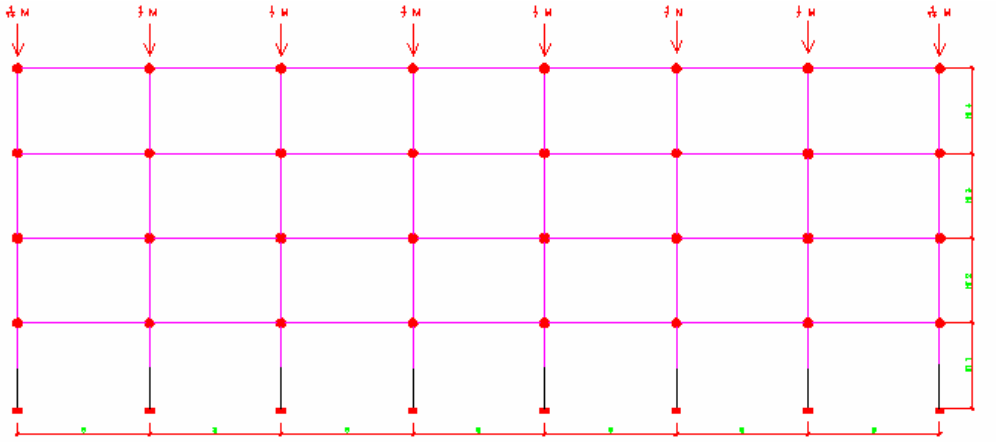

Figure 6.25 Four story commercial/office building

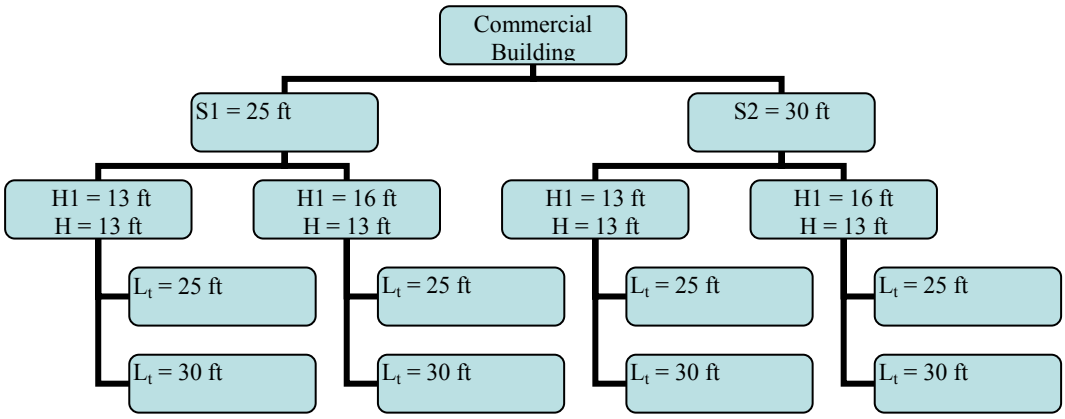

Figure 6.26 Flow chart showing the combinations for the 4 story building

Table 6.7. Parameters variations for the 4 story commercial/office building

	PARAMETERS VARIATION			
MODEL	S[ft]	Hi 1[ft]	Hi 2-4[ft]	Ltrib[ft]
1	25	13	13	25
2	25	13	13	30
3	25	16	13	25
4	25	16	13	30
5	30	13	13	25
6	30	13	13	30
7	30	16	13	25
8	30	16	13	30

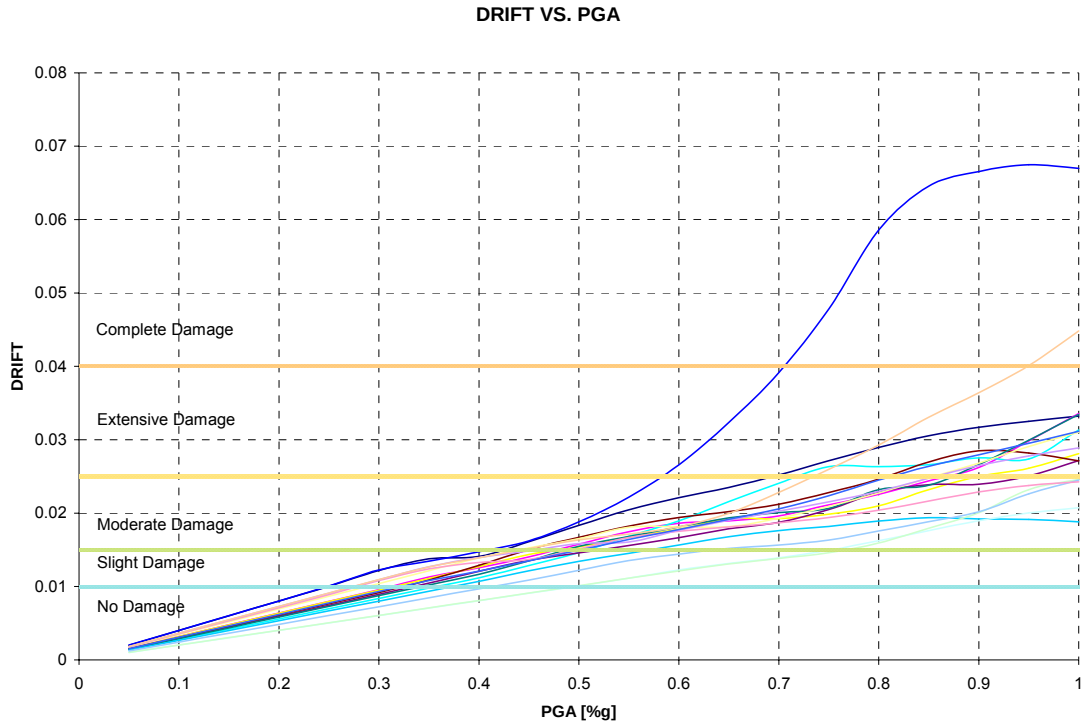

Figure 6.27 Maximum drift vs. PGA plot for the 8 models based on the 4 story commercial/office building.

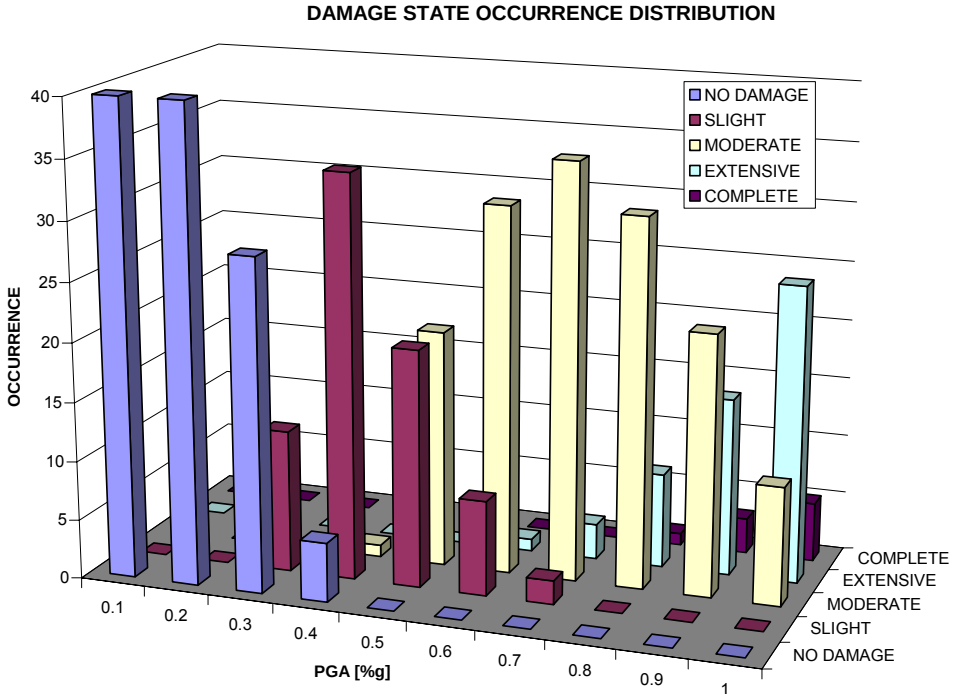

Figure 6.28 Occurrence distribution for 4 stories commercial/office buildings.

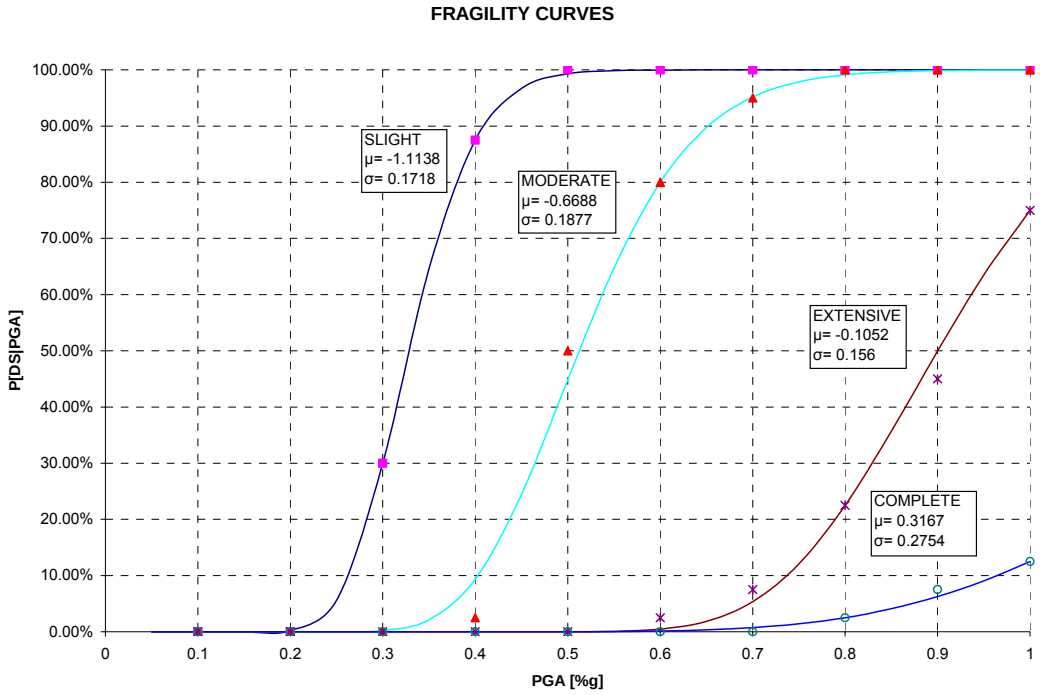

Figure 6.29 Fragility curves for 4 story commercial/office buildings.

6.2.4.4 Commercial/Office Buildings Combined Fragility Curves

After analyzing the statistics of each office/commercial building, the results were combined. The fragility curves for each damage state were created for the entire population of buildings dedicated to office and commercial activities; they are shown in Figure 6.30.

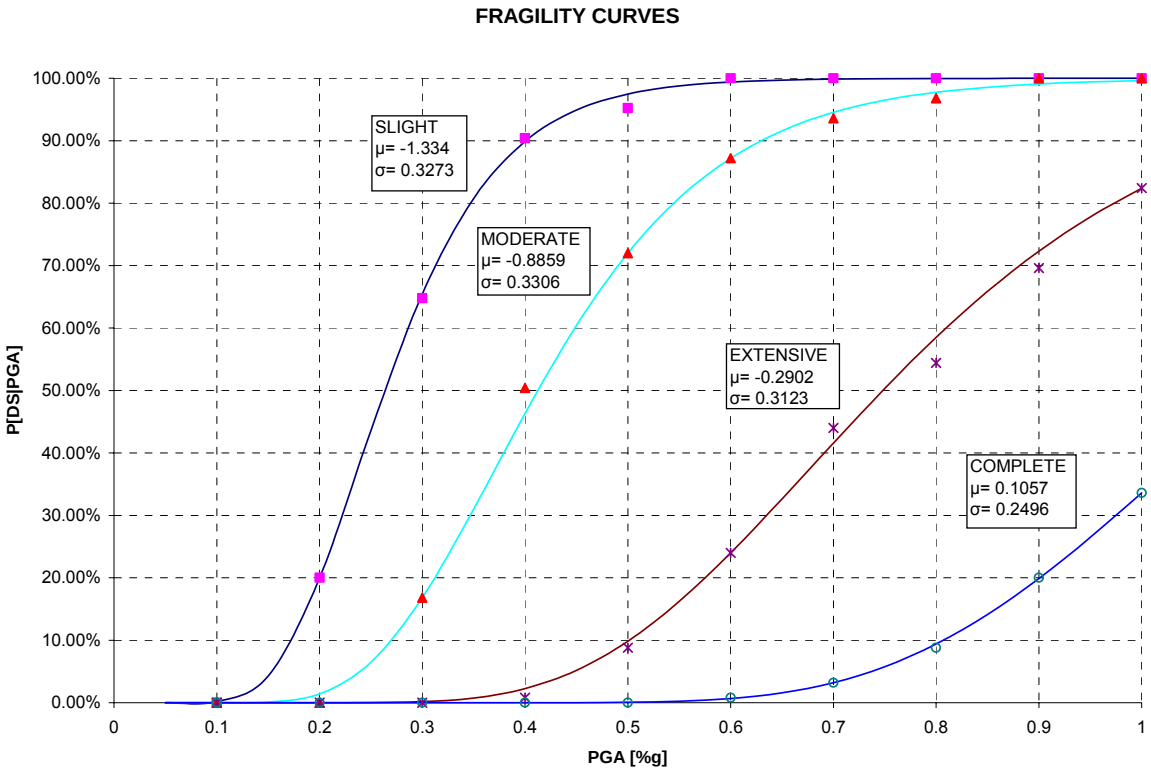

Figure 6.30 Fragility curves for commercial/office buildings.

6.2.5 Storage Buildings

6.2.5.1 One Story Storage Building

A one story storage building having an area of 3,000 square feet and a height of 26' – 6" was analyzed. Figure 6.31 shows a typical frame of the building.

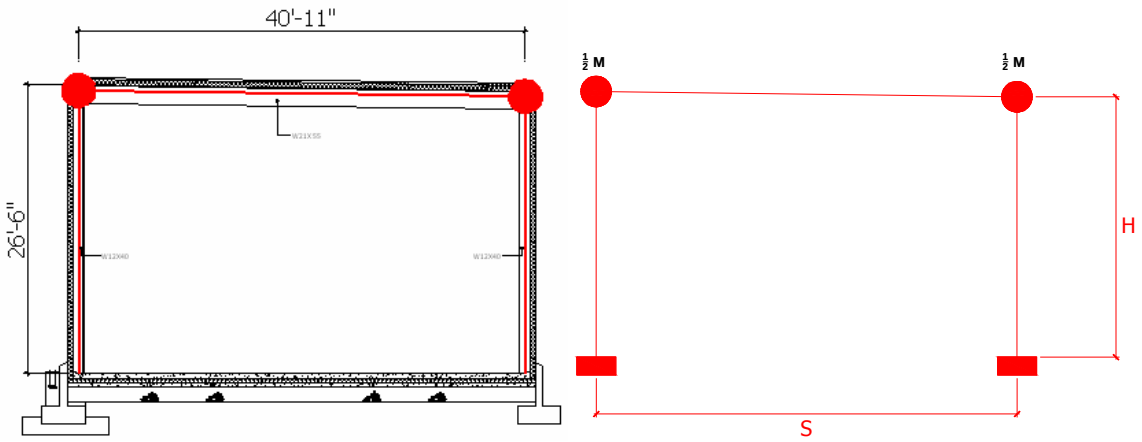

Figure 6.31 Building idealization for a 1 story storage building.

Table 6.8. Parameters variation for the Storage building

	PARAMETERS VARIATION		
MODEL	S[ft]	H [ft]	Ltrib[ft]
1	40	26.5	25
2	40	26.5	30
3	40	16	25
4	40	16	30
5	35	26.5	25
6	35	26.5	30
7	35	16	25
8	35	16	30
9	30	26.5	25
10	30	26.5	30
11	30	16	25
12	30	16	30

Twelve variations have been made to the original model. The fundamental period for the 12 variations made to the storage building range from 0.48 seconds to 1.02 seconds. The parameters that were varied are shown in Table 6.8. A flowchart of the twelve variations is shown in Figure 6.32.

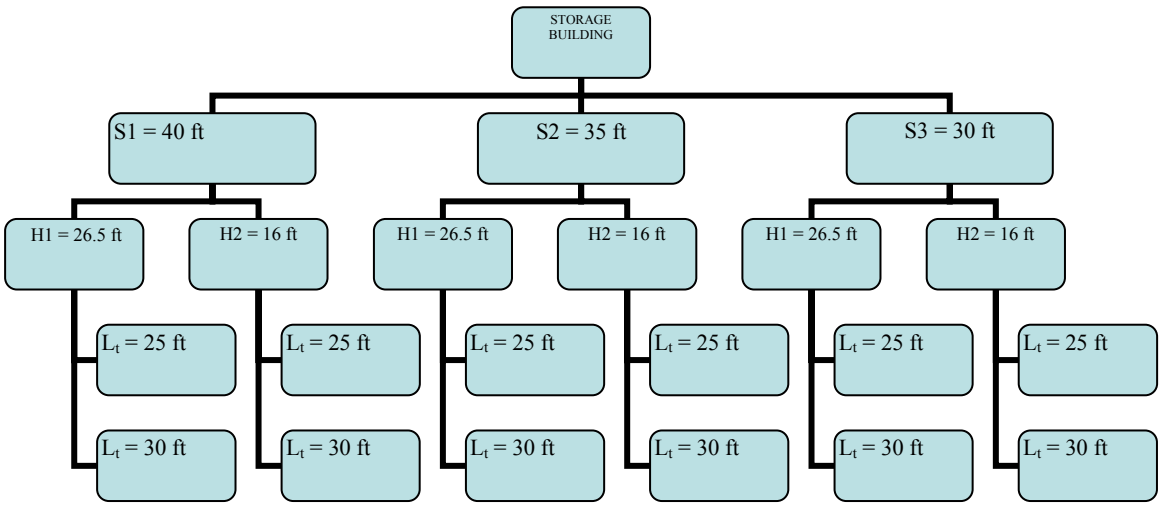

Figure 6.32 Flowchart for the 12 models generated for the storage building.

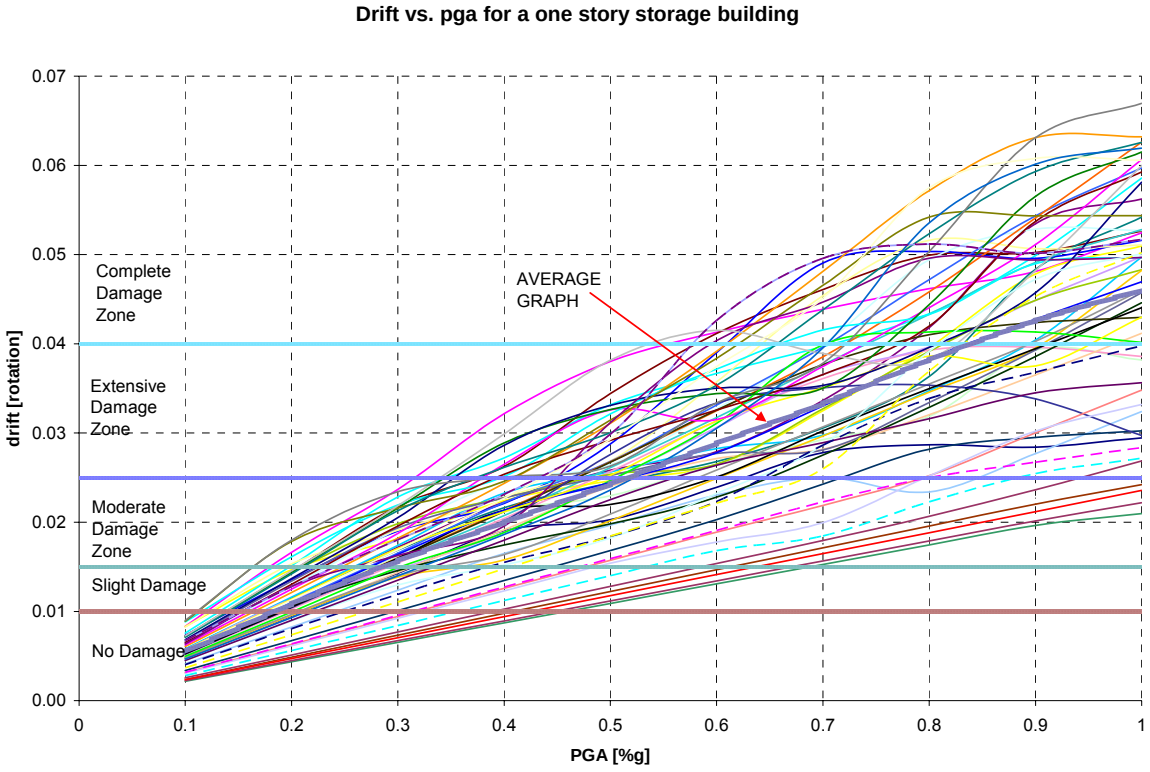

Figure 6.33 Maximum drift vs. PGA plot for all 12 models of the storage building.

Figure 6.33 illustrates the range of maximum drift values for the 12 models caused by the 5 different earthquakes. An average graph has been plotted to facilitate the comparison between the values. In general, it can be said that a building of this class would not suffer any damage until the earthquake has a PGA of 0.2g. Slight damage will occur for PGA values of 0.2 to 0.3g. Moderate damage will occur for a PGA ranging from 0.3g to 0.53g. PGA values of 0.53g to 0.83g will cause extensive damage. Complete damage of the building is expected for a PGA higher than 0.83g.

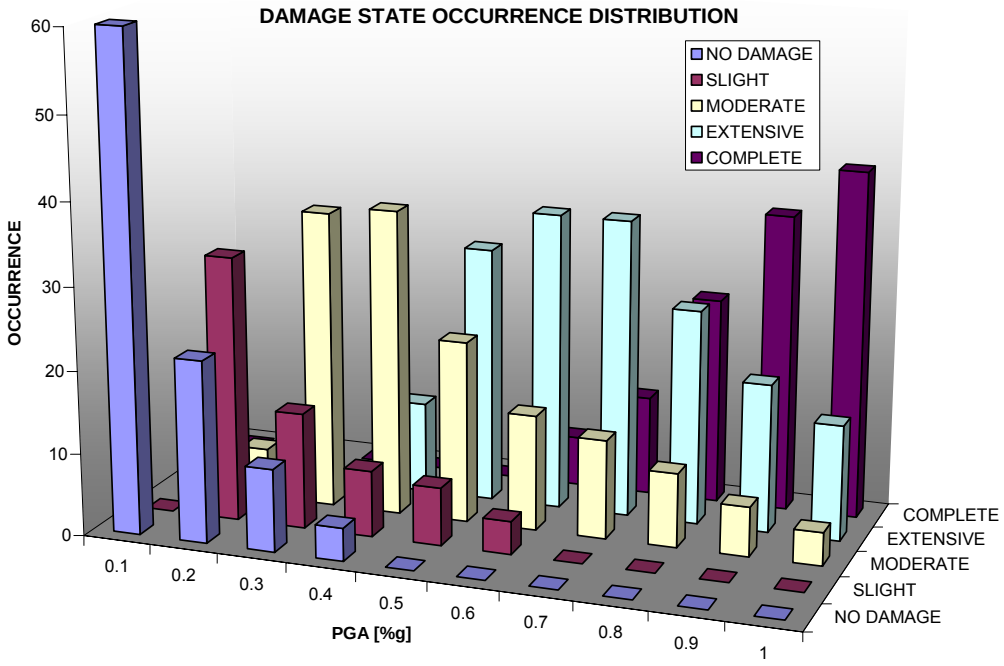

Figure 6.34 Damage state occurrence dist.

From figure 6.34 it can be seen that the number of occurrence plots have a similar shape to a log-normal distribution.

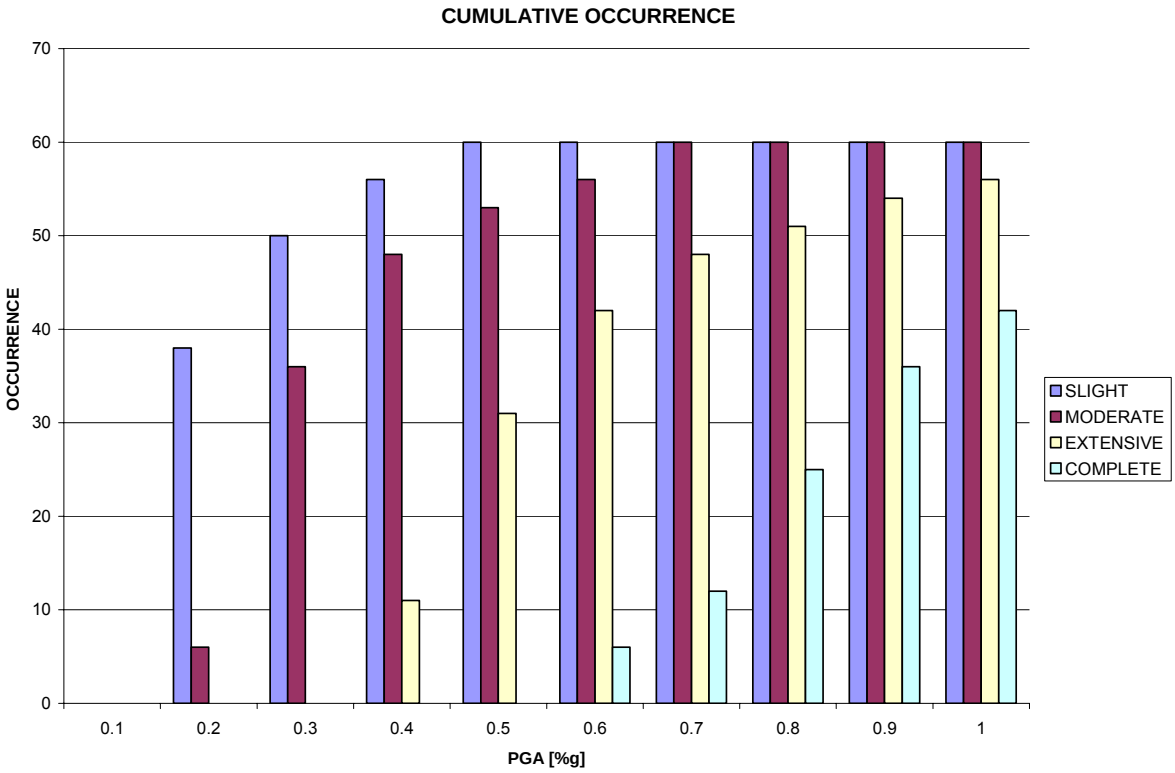

Figure 6.35 Cumulative occurrence for each damage state.

Figure 6.35 shows a bar graph indicating the number of times that each damage state occurs for all PGA values. As it is expected, the amount of times that each damage occurs increases with increasing values of PGA. Figure 6.36 shows the fragility curves for this type of buildings.

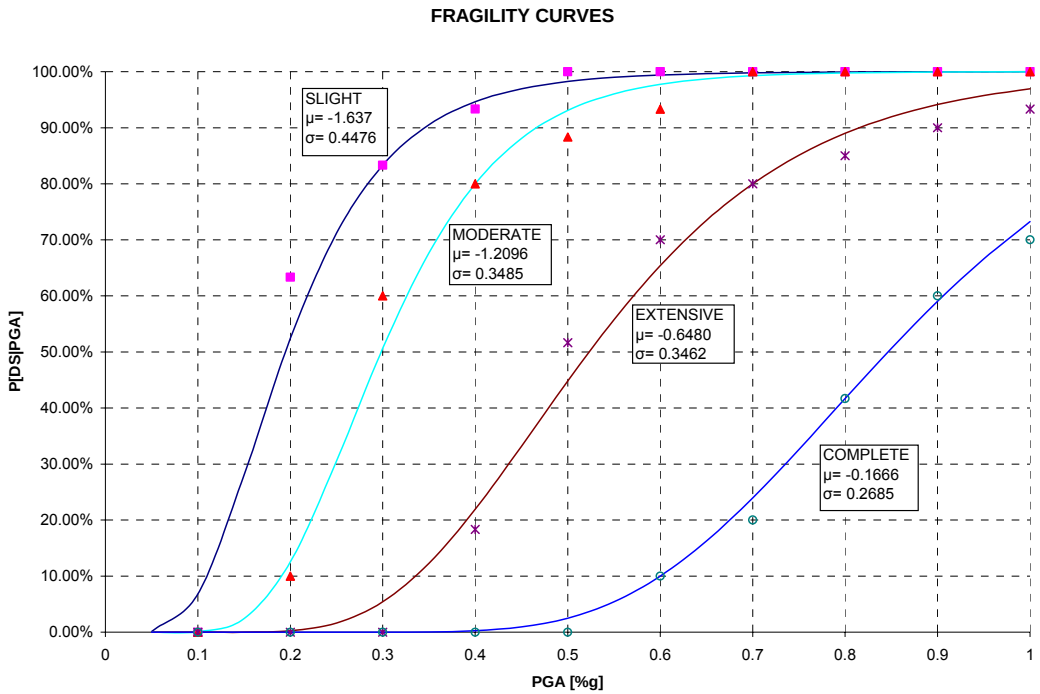

Figure 6.36 Fragility curves for a storage room

6.2.6 Low-Rise Buildings

Low-rise buildings are those buildings having 1 to 4 stories. In this section all low-rise building statistics were put together and fragility curves were created. Figure 6.37 shows the damage state occurrence distribution for this category, while Figure 6.38 shows the fragility curves obtained.

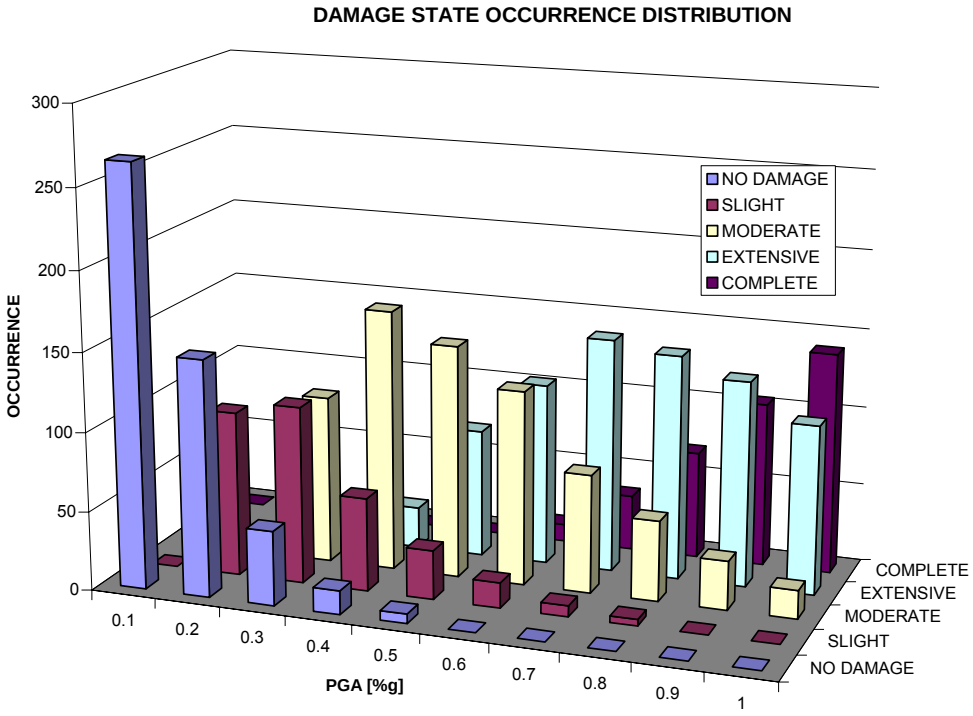

Figure 6.37 Damage state occurrence distribution for low-rise buildings.

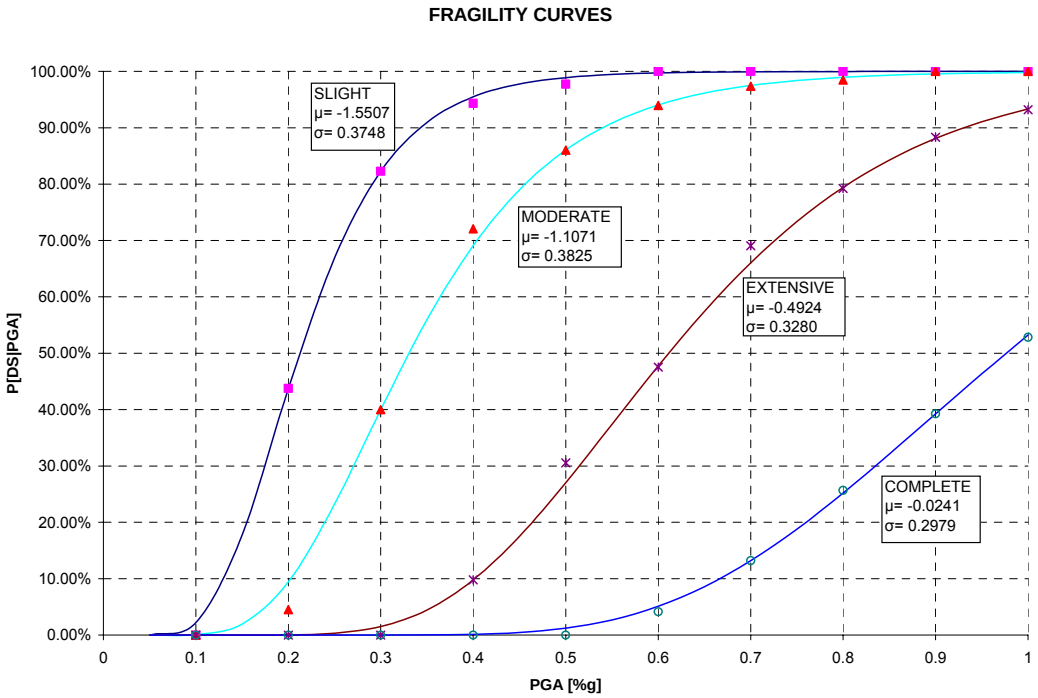

Figure 6.38 Fragility curves for low-rise buildings.

6.2.7 Mid-Rise Buildings

Mid-rise buildings are those having 4 to 7 stories. The frame of a typical six story building is shown in Figure 6.39. The variations made to the original model are shown in the flowchart of Figure 6.40. The fundamental period for the analyzed models range from 1.74 seconds to 2.19 seconds. A maximum drift vs. PGA plot is shown in Figure 6.41. Figure 6.42 shows the occurrence distribution for each damage state at each PGA value. The fragility curves for mid-rise buildings are shown in Figure 6.43.

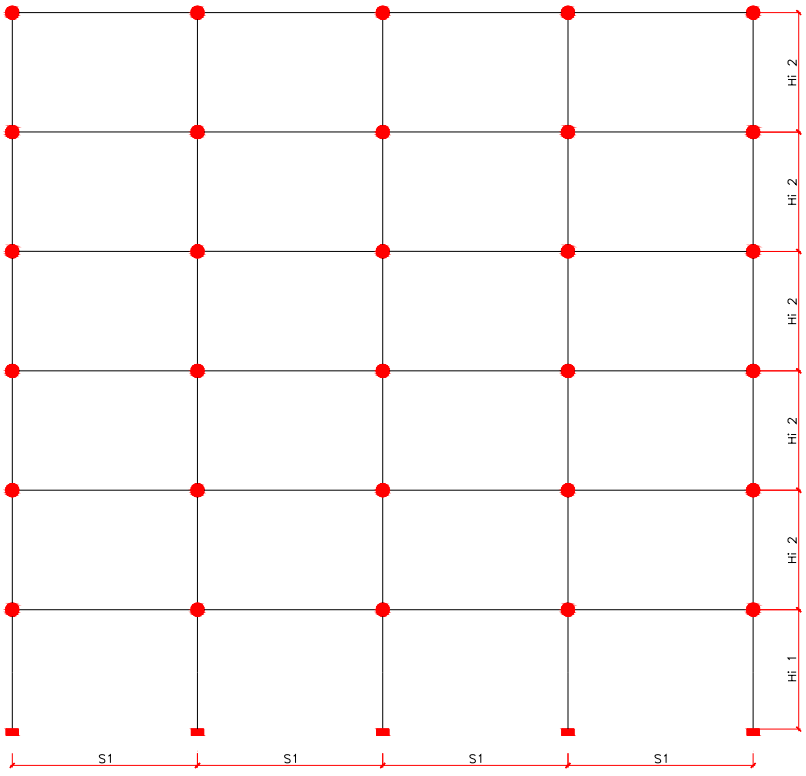

Figure 6.39 Six story building

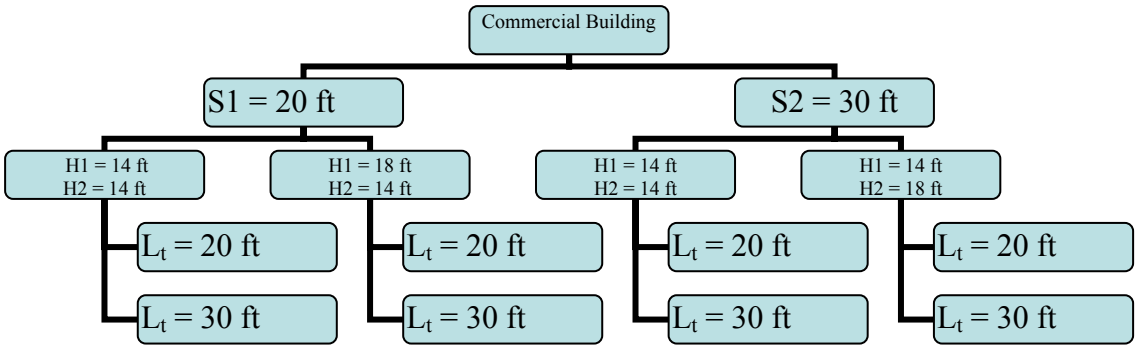

Figure 6.40 Flowchart for the eight variations made to the six story building.

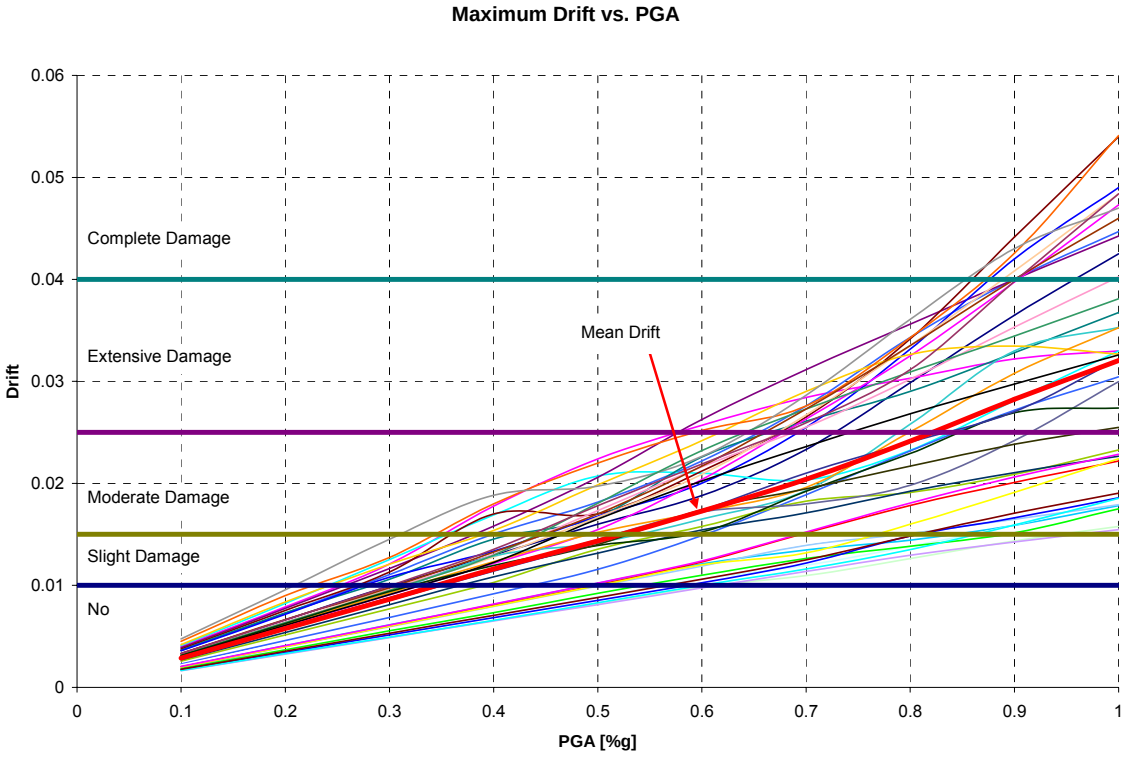

Figure 6.41 Maximum drift vs. PGA for the eight models of the six story building

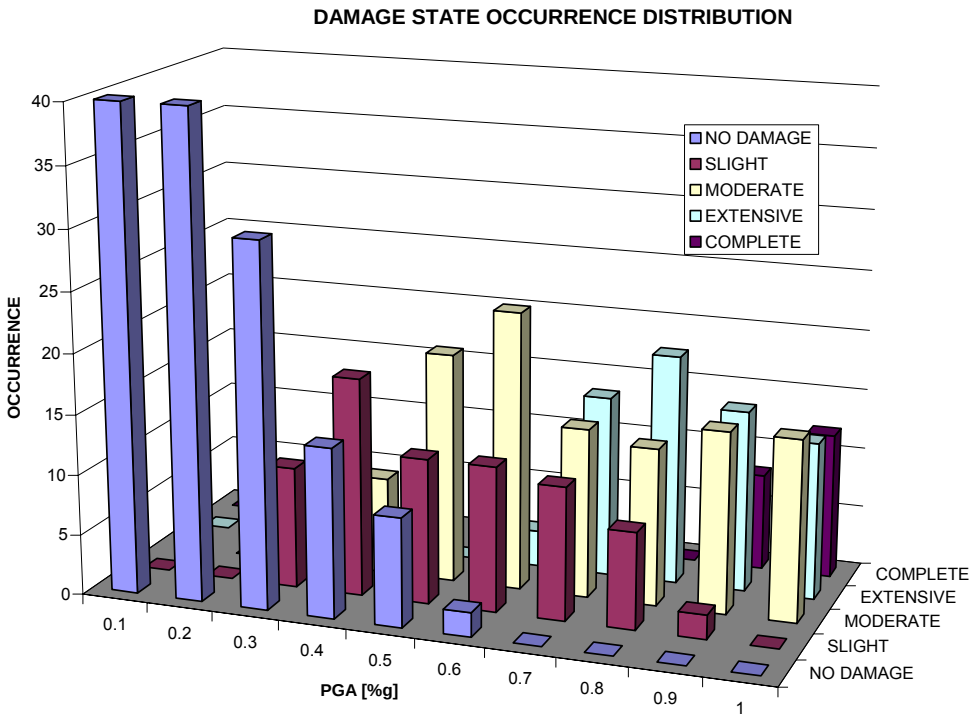

Figure 6.42 Occurrence distribution for the six story commercial building

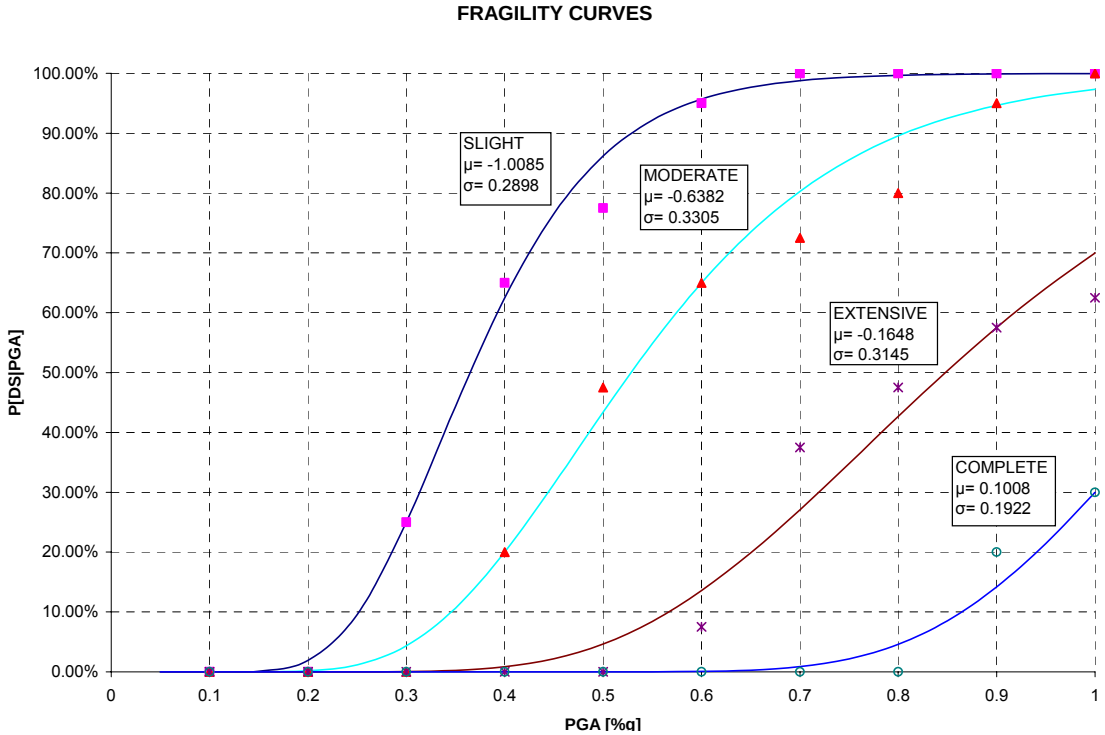

Figure 6.43 Fragility curves for the six story building

6.2.7.1 Combined Fragility Curves for Mid-Rise Buildings

The combined fragility curves for mid-rise buildings are obtained by combining the data from buildings having 4 to 7 stories.

The statistics obtained for the four stories office/commercial building shown in Section 6.2.4.3 are also used in this section, since that building is four stories high. Figure 6.44 shows the occurrence distribution of each damage state. The fragility curves are shown in Figure 6.45.

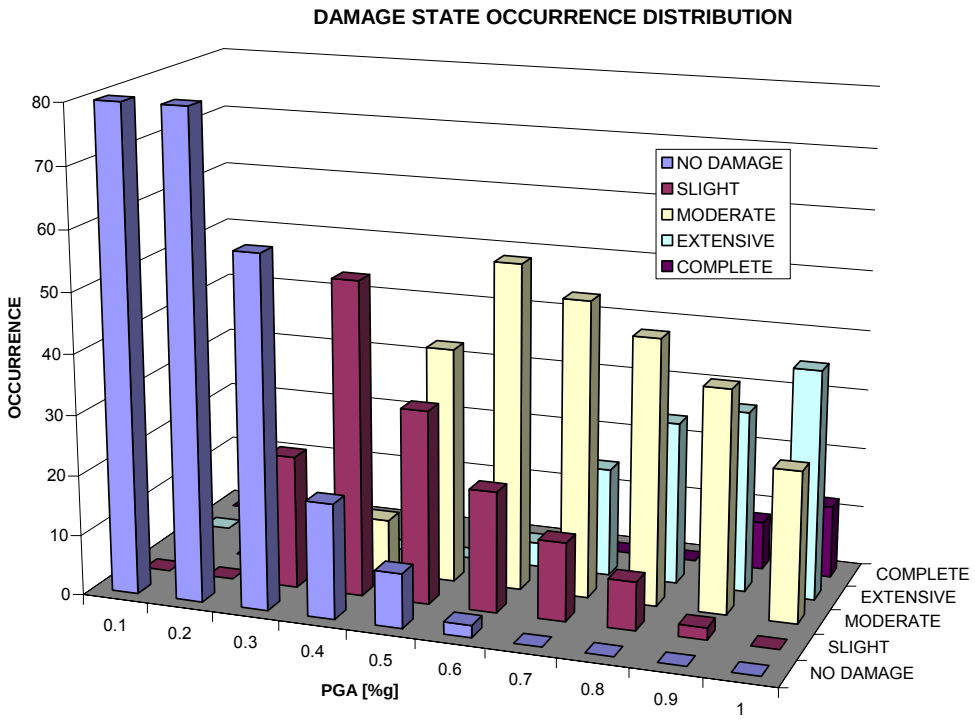

Figure 6.44 Occurrence distribution for mid-rise buildings.

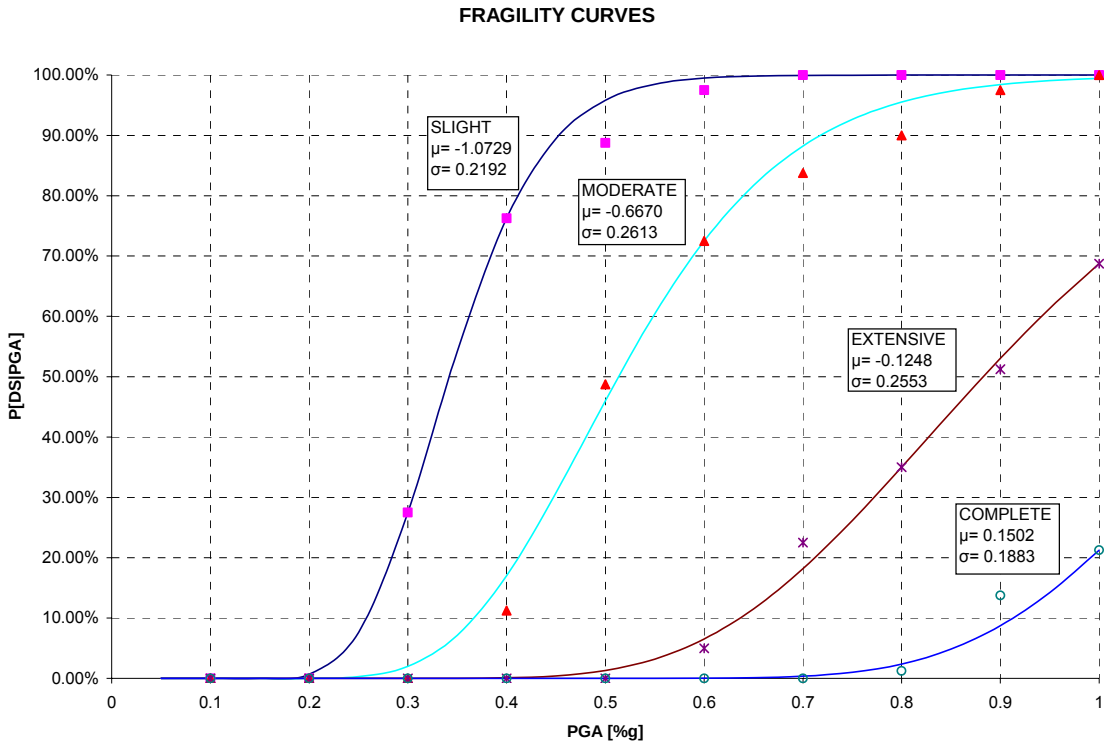

Figure 6.45 Fragility curves for mid-rise buildings

6.2.8 High Rise Buildings

In Puerto Rico there are not many high-rise steel buildings made with moment-resisting frames. Buildings were generated following the patterns observed in previously analyzed buildings. The four story office building was utilized as the base for the eight and the twelve story buildings that were created. The design of the generated buildings has been done according to the design code UBC 97 for a zone 3 region and a soil type Sd. A simple gravity loads analysis was initially performed, even though in high rise buildings, earthquake effects may control the design. Having that in mind, a linear response spectrum analysis was also performed. The design combinations utilized to perform the design are the following:

1. 1.4D
2. 1.2 D + 1.6 L

3. 1.2 D + 0.5 L ± 1.0 E

4. 0.9 D + 1.0 E

For the design procedure followed here, see section 5.3.2.

6.2.8.1 Eight Story Building

An eight story building was analyzed next. A typical frame is shown is Figure 6.46. The fundamental period for the variations made range from 3.13 seconds to 3.57 seconds. Figure 6.47 shows the maximum drift vs. PGA plot for all 8 story models. Figures 6.48 and 6.49 show the damage state occurrence and the fragility curves obtained for all variations of the models respectively.

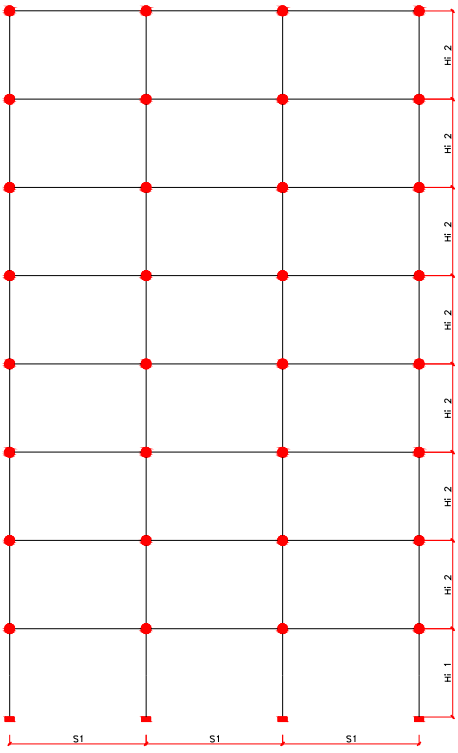

Figure 6.46 Eight story building.

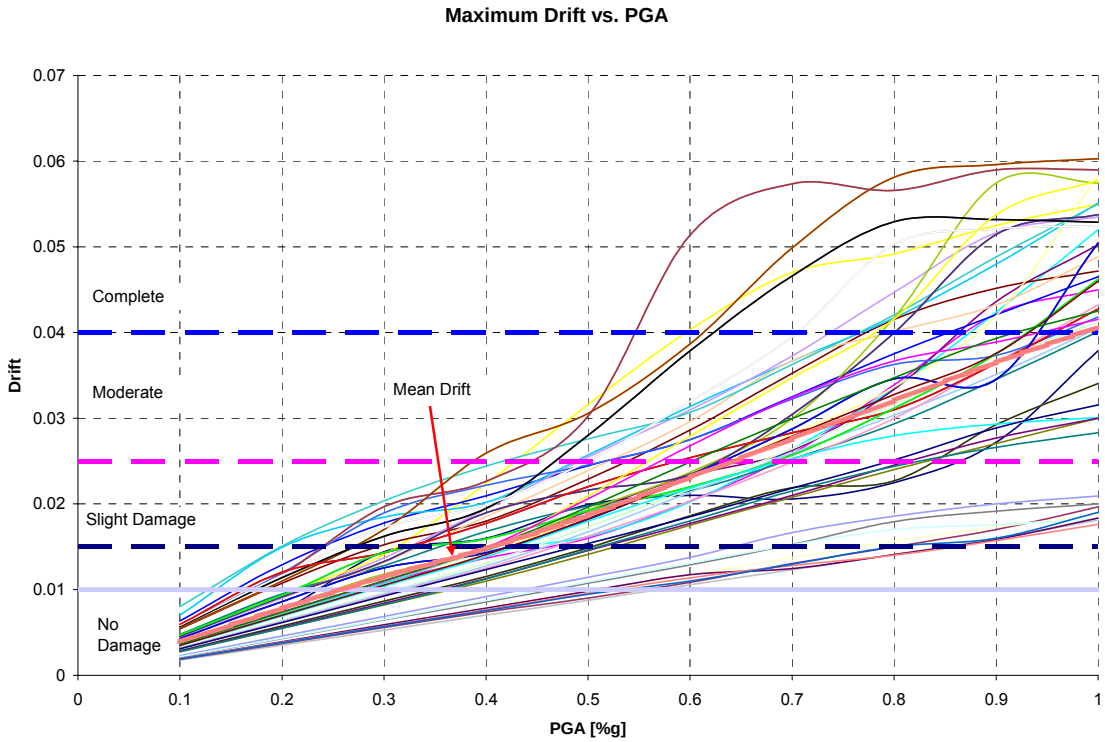

Figure 6.47 Maximum inter-story drift vs. PGA for the eight story building

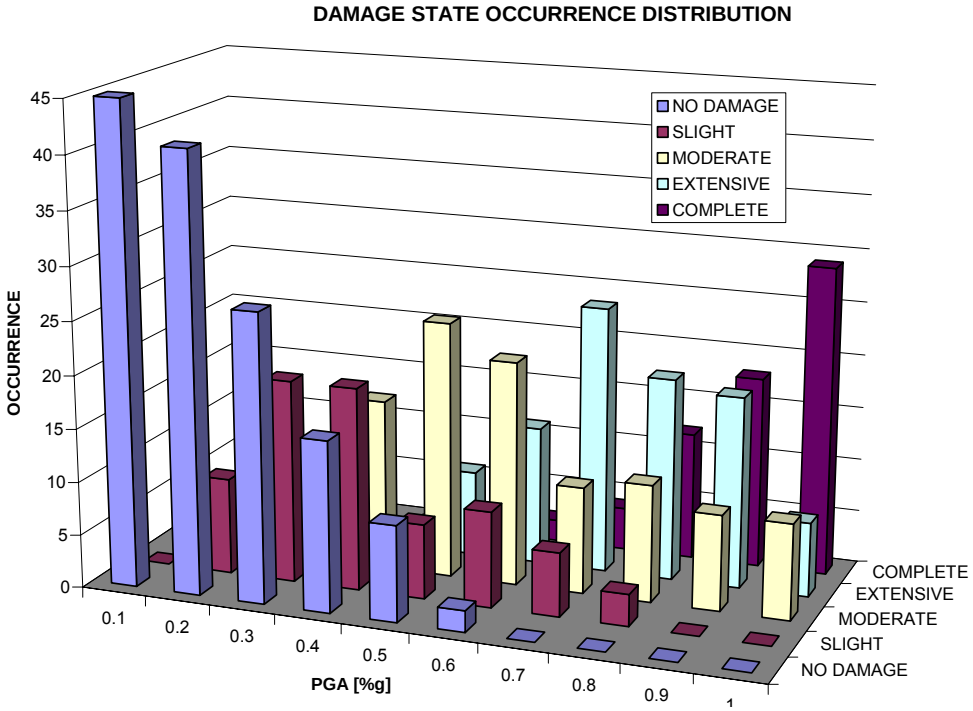

Figure 6.48 Occurrence distribution for the eight story building.

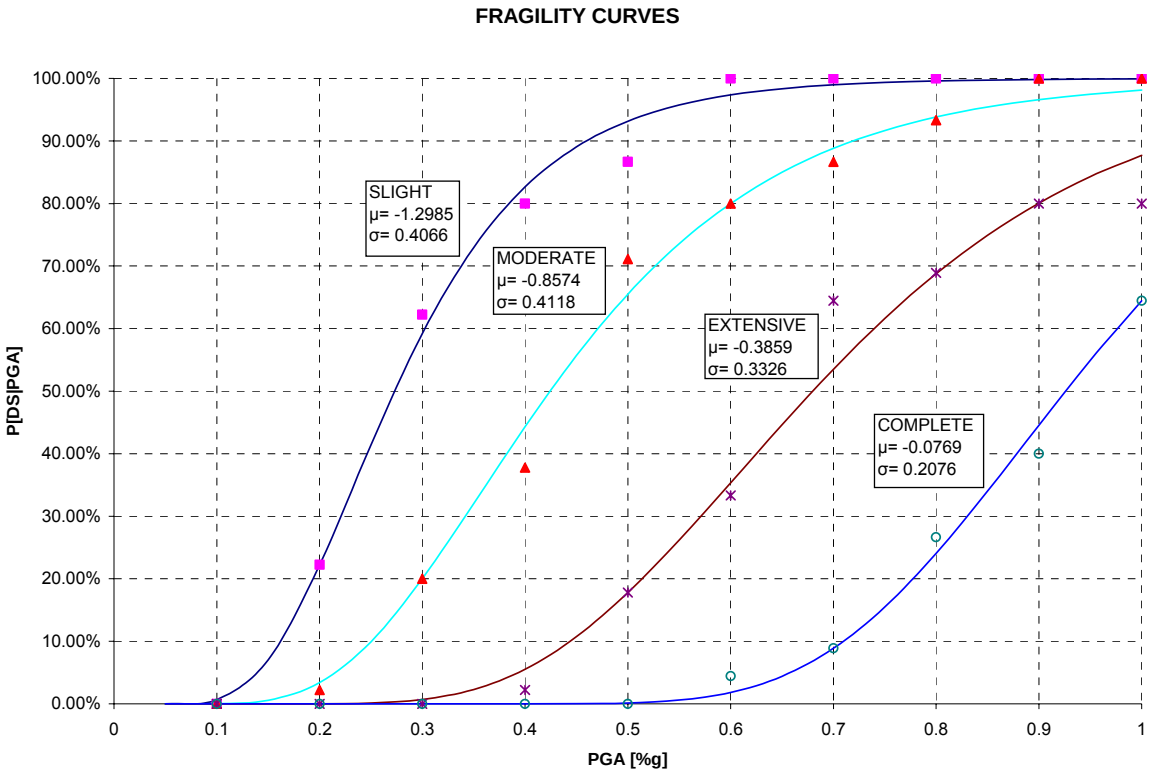

Figure 6.49 Fragility curve for the eight story high rise building

6.2.8.2 Ten Story Building

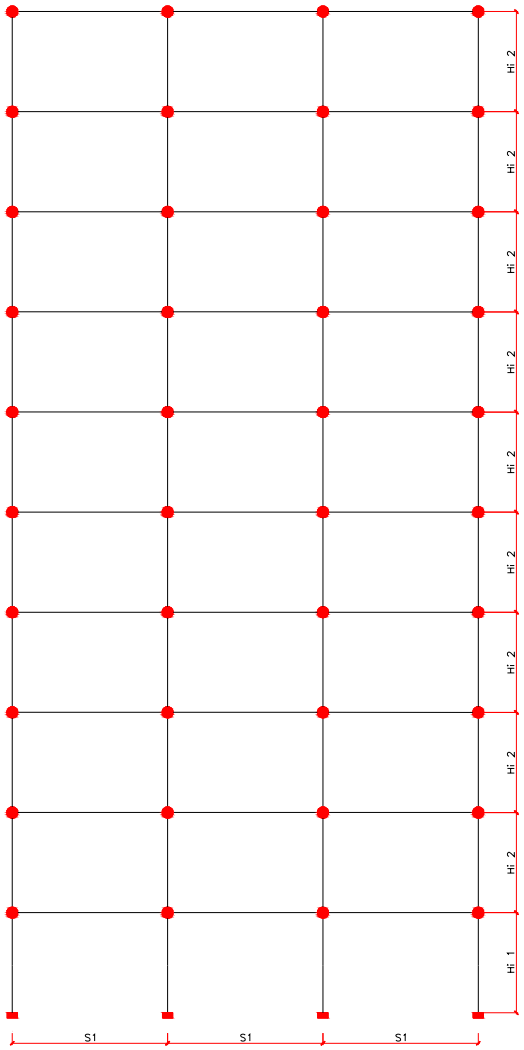

Figure 6.50 Ten story building frame

The ten story high-rise model representation is shown is Figure 6.50. Nine variations were made to this building. The fundamental period for the variations made range from 3.43 seconds to 3.89 seconds. These variations are shown in the flowchart in Figure 6.51.

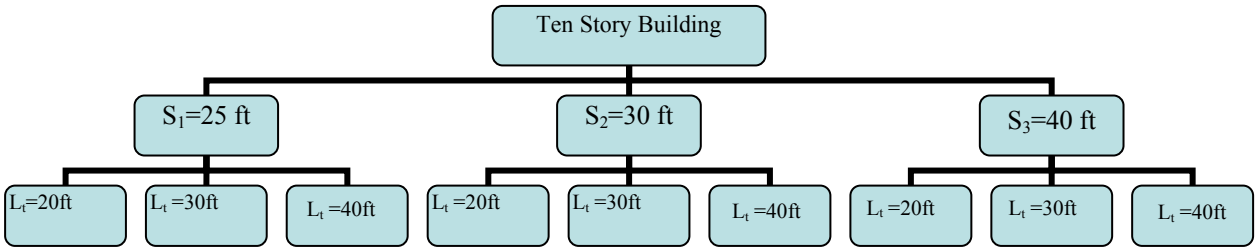

Figure 6.51 Flowchart showing the 9 model variations for the 10 story building.

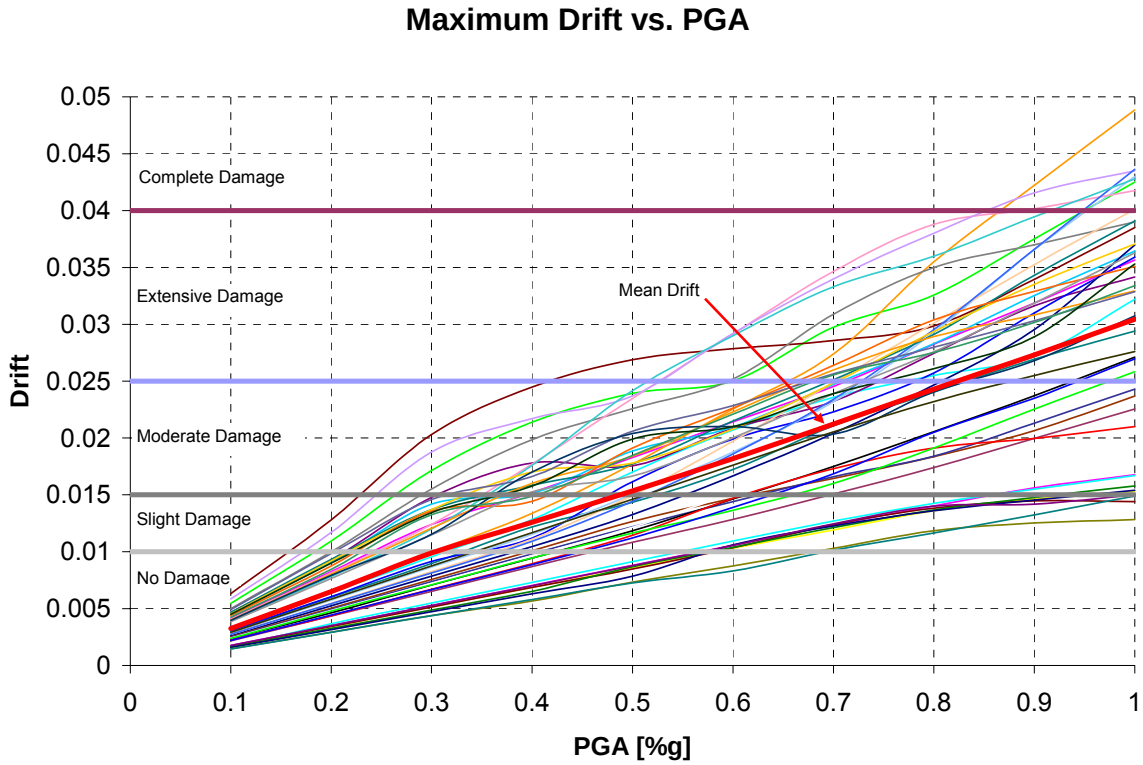

Figure 6.52 Maximum drift vs. PGA for the ten story building.

Figure 6.52 shows the maximum drift vs. PGA chart for the nine models subjected to the 5 earthquakes. Based on the mean drift curve shown in this figure, no damage is expected up to 0.30g. From 0.30g to 0.50g slight damage is expected. Moderate damage is expected from 0.50g to 0.83g. After 0.83g, extensive damage is expected.

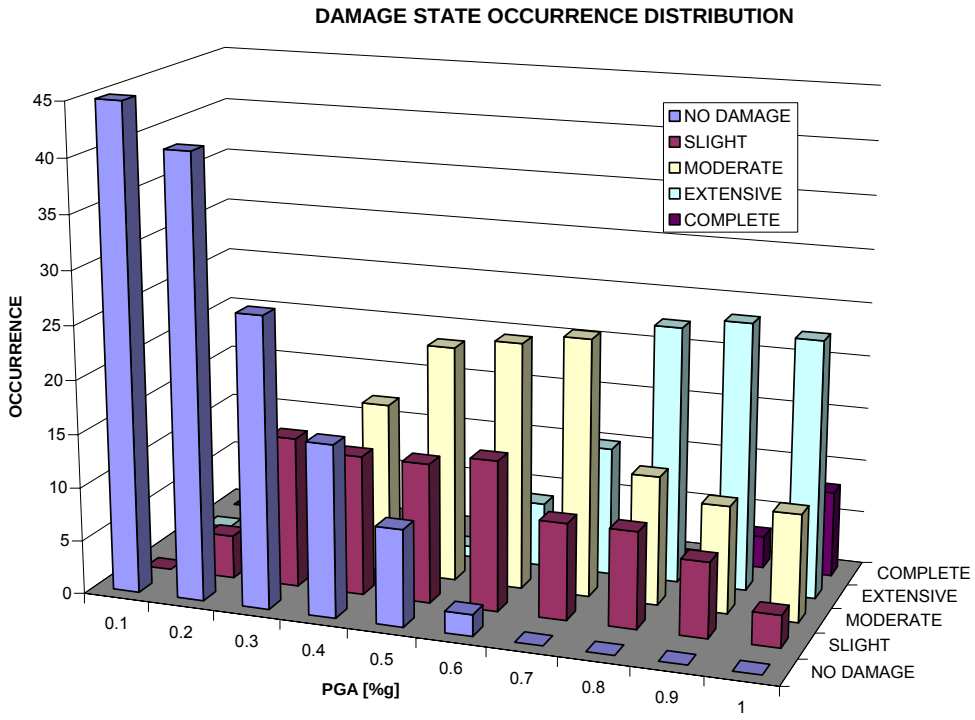

Figure 6.53 Damage state occurrence distribution.

Figure 6.53 shows the occurrence distribution for each damage state. Figure 6.54 shows the fragility curves for the ten story building and its variations.

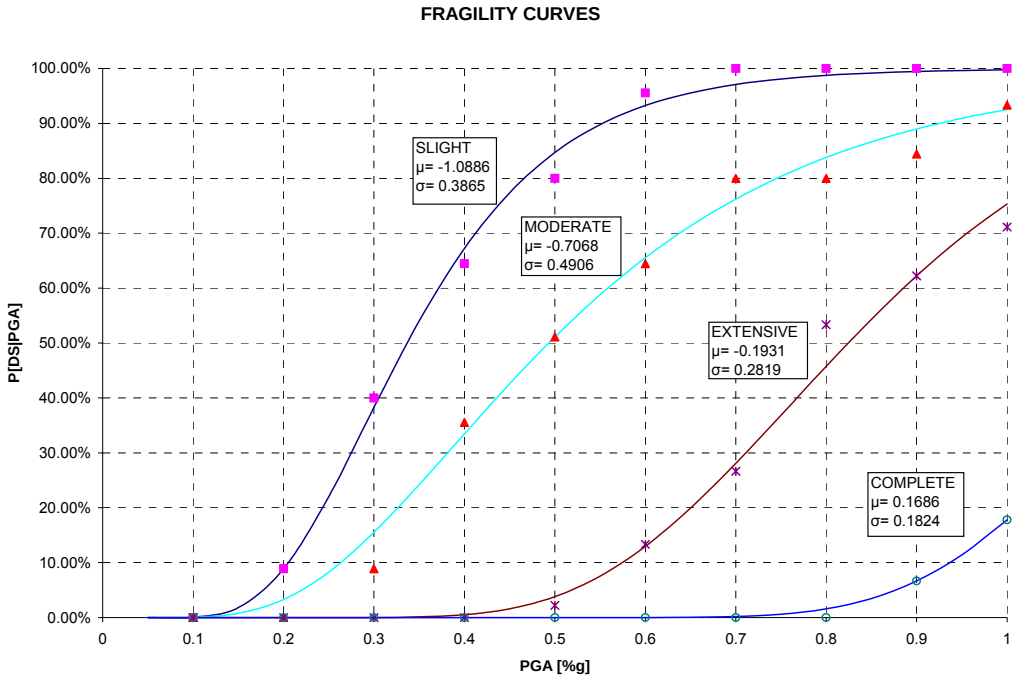

Figure 6.54 Fragility curve for a 10 story building.

6.2.8.3 Combined High Rise Buildings

After combining the high-rise buildings analyzed, the frequency distribution for this category was obtained and is shown in Figure 6.55. Figure 6.56 shows the fragility curve for all damage states for high-rise buildings.

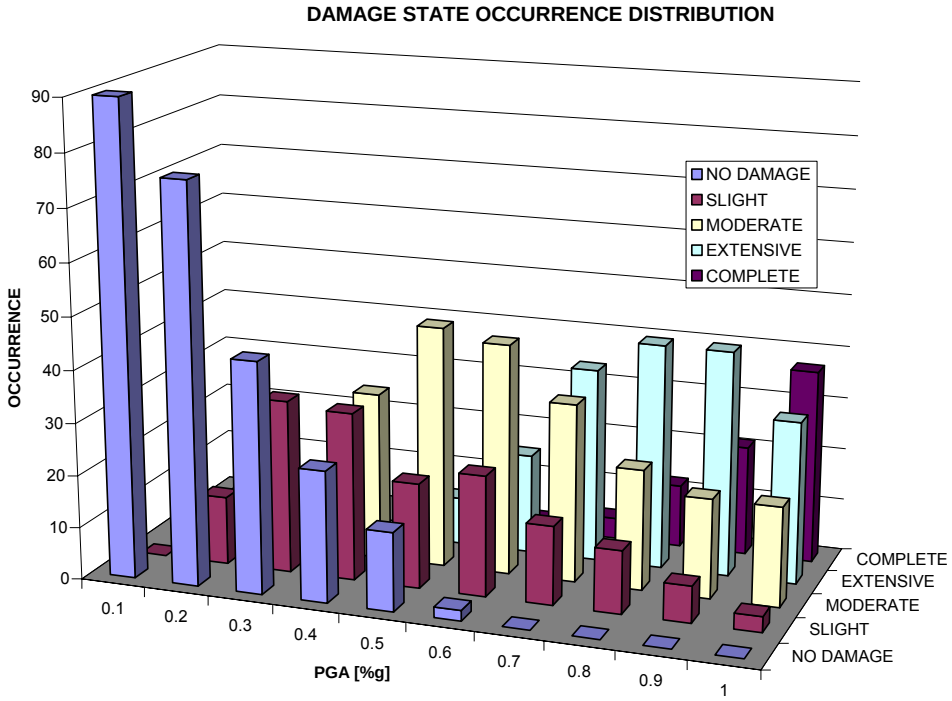

Figure 6.55 Damage state occurrence distribution for the 18 high-rise models analyzed

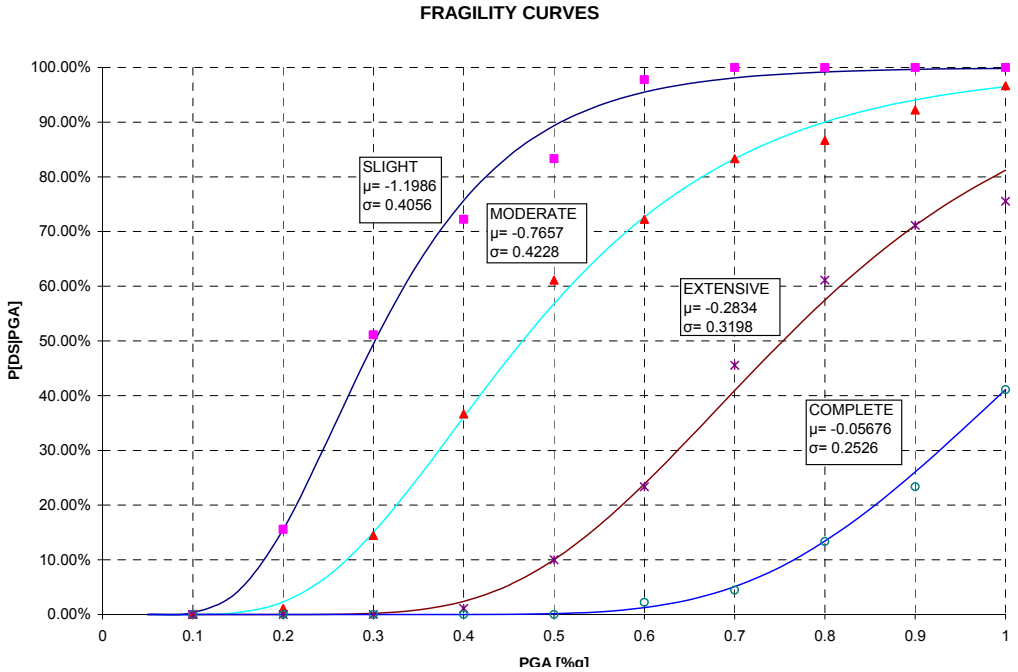

Figure 6.56 Fragility curves for high-rise buildings

6.2.9 General Fragility Curve for All Buildings

After analyzing all buildings, and obtaining all the statistics, a general fragility curve was created. The frequency distribution for the combined statistics of all models is shown in Figure 6.57. The fragility curve for all models is shown in Figure 6.58.

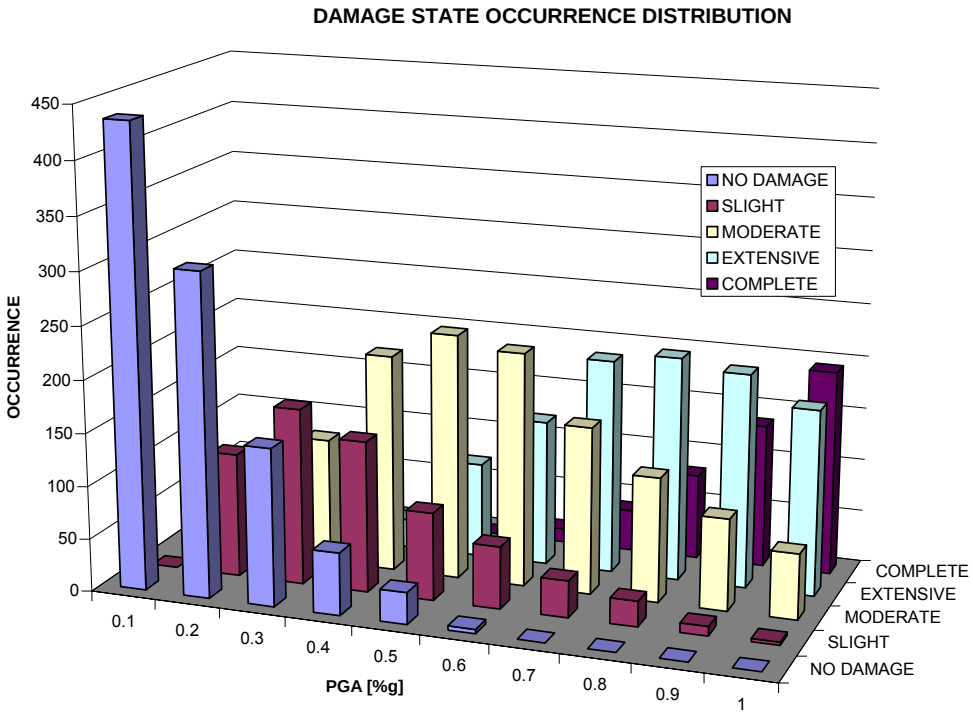

Figure 6.57 Frequency distribution for all 91 models

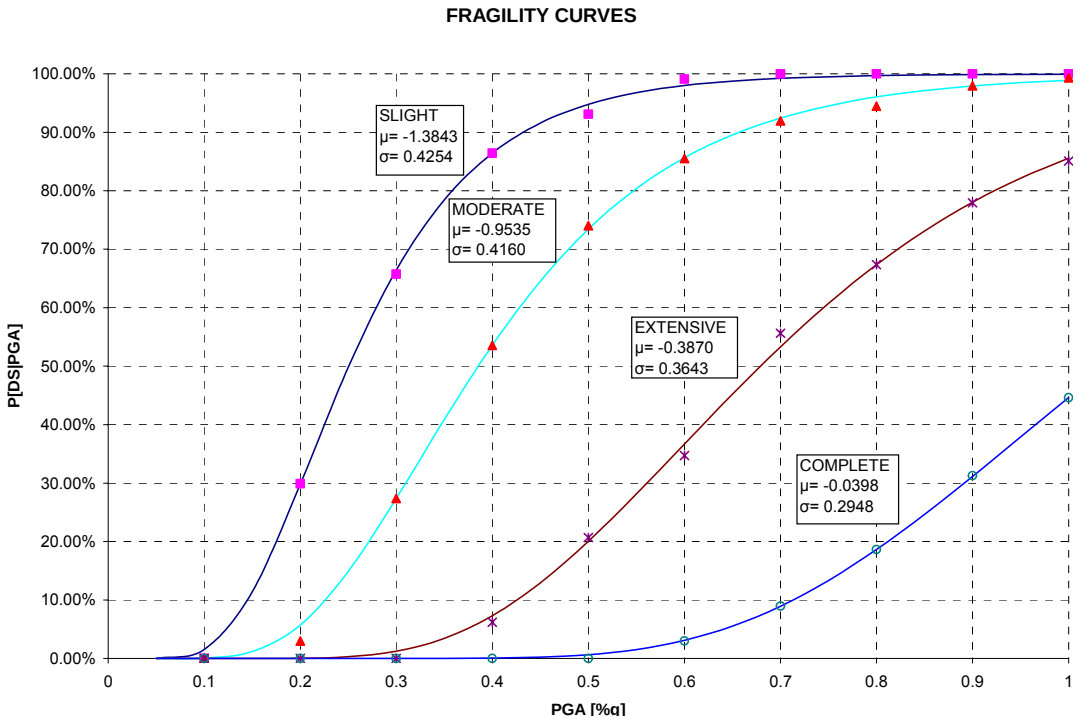

Figure 6.58 Fragility curves for all buildings

6.2.10 Fragility Curve Comparison

In this section the fragility curves are compared for the different building occupancies considered and explained in Chapter 3. Figures 6.59 to 6.62 show the different fragility curves for each damage state individually. From this figures it can be seen that storage building category is the most susceptible to damage, followed by the industrial building category, and finally, the commercial/office building category which is the least susceptible to damage.

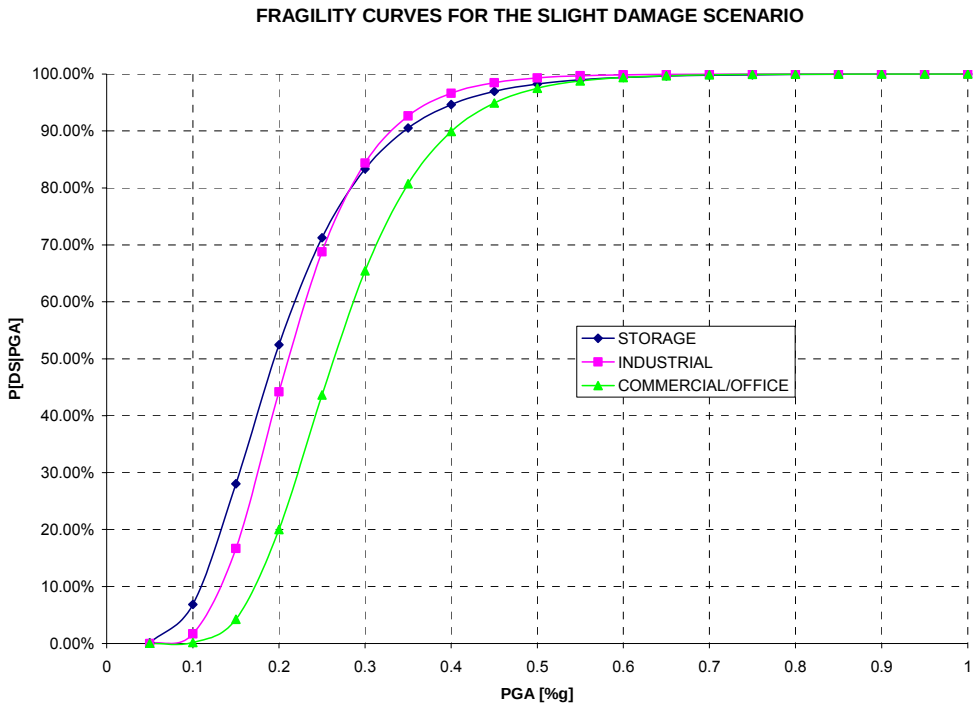

Figure 6.59. Fragility curves for the slight damage scenario of the different occupancy categories considered.

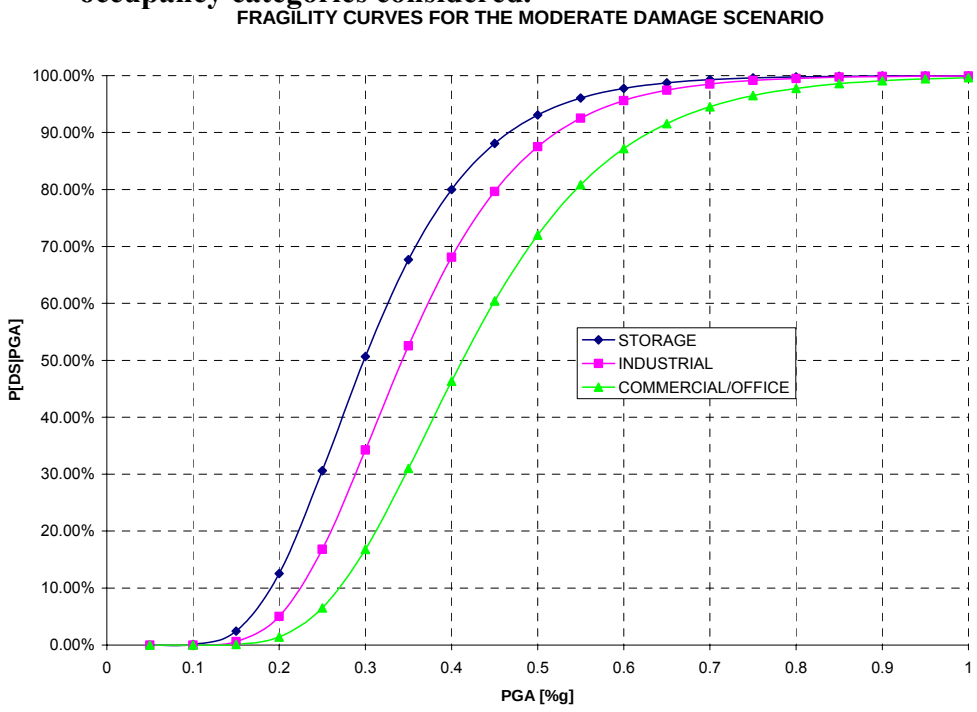

Figure 6.60. Fragility curves for the moderate damage scenario.

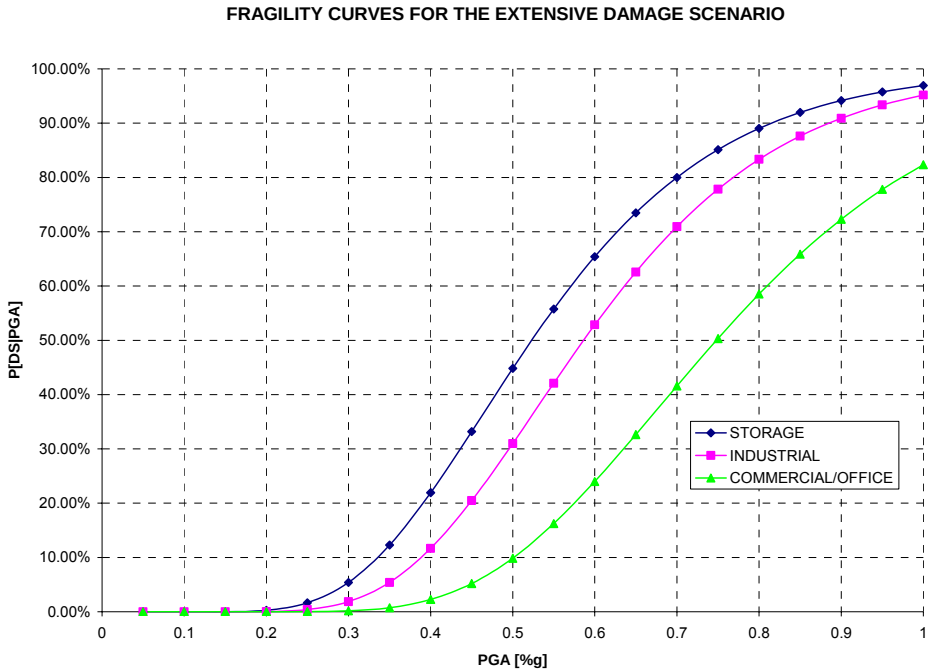

Figure 6.61. Fragility curves for the extensive damage scenario for the building occupancies considered.

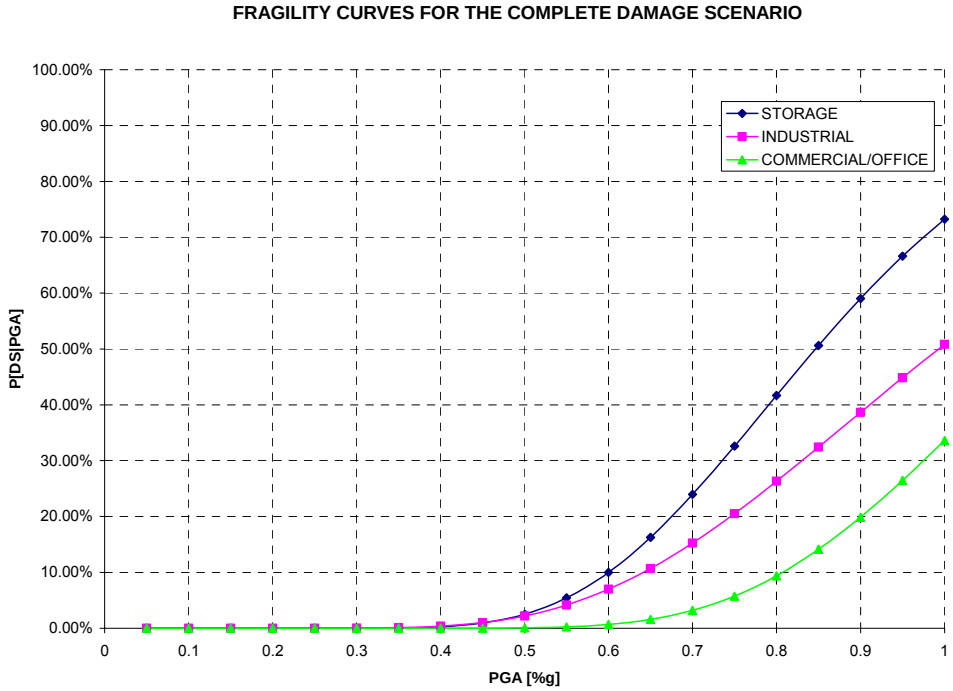

Figure 6.62. Fragility curves for the complete damage scenario for the building occupancies considered.

7 LOSS FUNCTIONS

7.1 Introduction

Loss functions are the link the damage probability and the expected monetary losses. This chapter does not pretend to fully explain the topic, only a brief explanation of the loss functions is given in the following section. Appendix B of FEMA-351 contains more information about the topic.

7.2 Loss functions development

Loss Functions are needed to estimate the economic loss. The damage probability of each damage state is multiplied by a relative cost assigned to each one. FEMA assumes a structural cost for steel buildings as 20% of the total building's cost (FEMA-351 2000). The relative cost of each damage state depends on the connection used in the building. If a Pre-Northridge connection was used, the costs are much higher. When a Post-Northridge connection is used, the repair cost of slight damage is assumed to be zero on the basis that any incidental damage under this category will not need to be repaired. For the Moderate and Extensive structural damage the cost of repair is assumed to be 10% and 50% of the structural cost, respectively, as recommended in FEMA-351. A 100% of the structural cost is assumed for the complete structural damage state. Table 7.1 shows the assigned cost for each damage state for buildings having Pre-Northridge connections and Table 7.2 shows the assigned cost for each damage state for buildings having Post-Northridge connections.

Following the FEMA-351 recommendations, the structural estimated cost per square foot is taken as \$25.00 (\$25.00/ft^2).

Table 7.1. Cost of Damage State (DS) for Pre-Northridge Connections (Table B-9, FEMA-351)[16]

	Structural Damage State			
Damage State	Slight	Moderate	Extensive	Complete
Mean Loss Ratio	8%	20%	80%	100%
Mean Loss Rate [\$/SF]	\$ 2.00	\$ 5.00	\$ 20.00	\$ 25.00

Figure 7.1 shows a graphical representation of the recommended mean loss ratio for the Pre-Northridge case for all damage states. Figure 7.2 contains the same information as Figure 7.1 but for the Post-Northridge connections case.

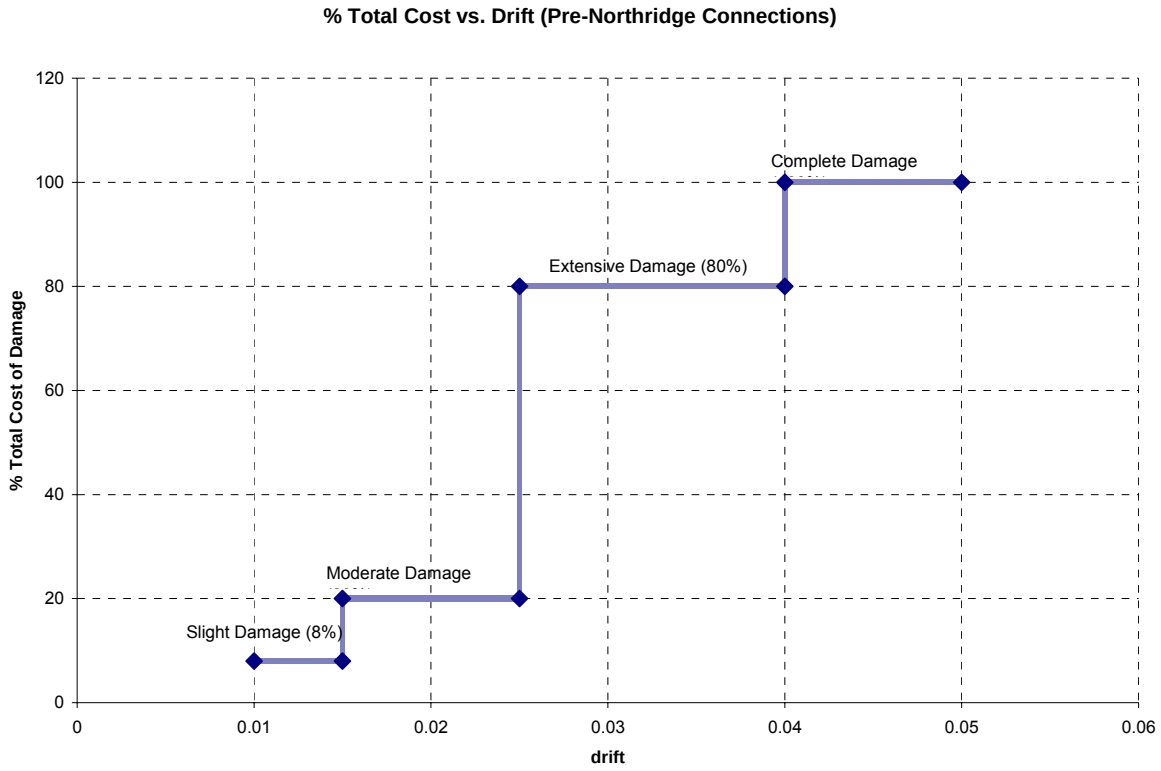

Figure 7.1 Percentage of damage cost for the Pre-Northridge condition

[16] SAC Joint Venture, 2000

Table 7.2. Cost of Damage State for Post-Northridge connections[17]

	Structural Damage State			
Damage State	Slight	Moderate	Extensive	Complete
Mean Loss Ratio	0%	10%	50%	100%
Mean Loss Rate [$/SF]	$ 0.00	$ 2.50	$ 12.50	$ 25.00

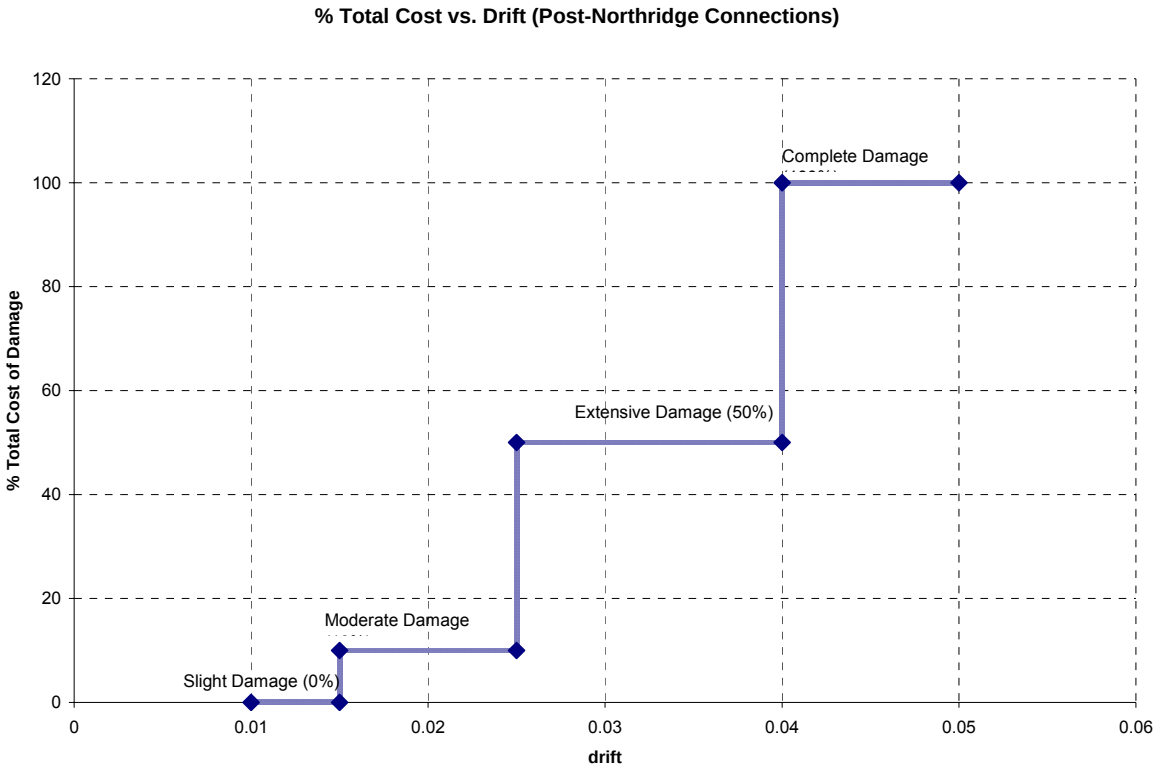

Figure 7.2 Percentage of the total cost for the Post-Northridge condition.

7.3 Loss Functions Example

This section presents an example of the monetary losses calculation for the same building whose fragility curves were created in Chapter 5. It is assumed that the four story building is located in a zone where the expected peak ground acceleration is 0.6g (19.32 ft/s^2). The four story building has plan dimensions 175 ft x 100 ft. The total area for the 4 stories is:

[17] SAC Joint Venture, 2000

$$A = 175\,ft(100\,ft)(4\ stories) = 70{,}000\,ft^2 \quad \textbf{(7.1)}$$

Assuming a cost of \$125.00/ft^{2,} the total replacement cost for this building is estimated to be:

$$Total\ Building\ Cost = Area(Cost / Area) = 70{,}000\,ft^2\,(\$125.00 / ft^2) = \$8{,}750{,}000.00 \quad \textbf{(7.2)}$$

$$Structural\ Cost = Total\ Building\ Cost(0.20) \quad \textbf{(7.3)}$$

$$Structural\ Cost = \$8{,}750{,}000.00(0.20) = \$1{,}750{,}000.00$$

From Figure 7.3 it can be seen that a ground intensity of 0.6 g causes only slight and moderate damage to this building. The amount of slight damage is 20%, while the amount of moderate damage is 80%. The next step in order to determine the monetary losses is to multiply the percentage of damage for each damage state by the cost associated to each damage state. This is done next, and is also shown in Table 7.3.

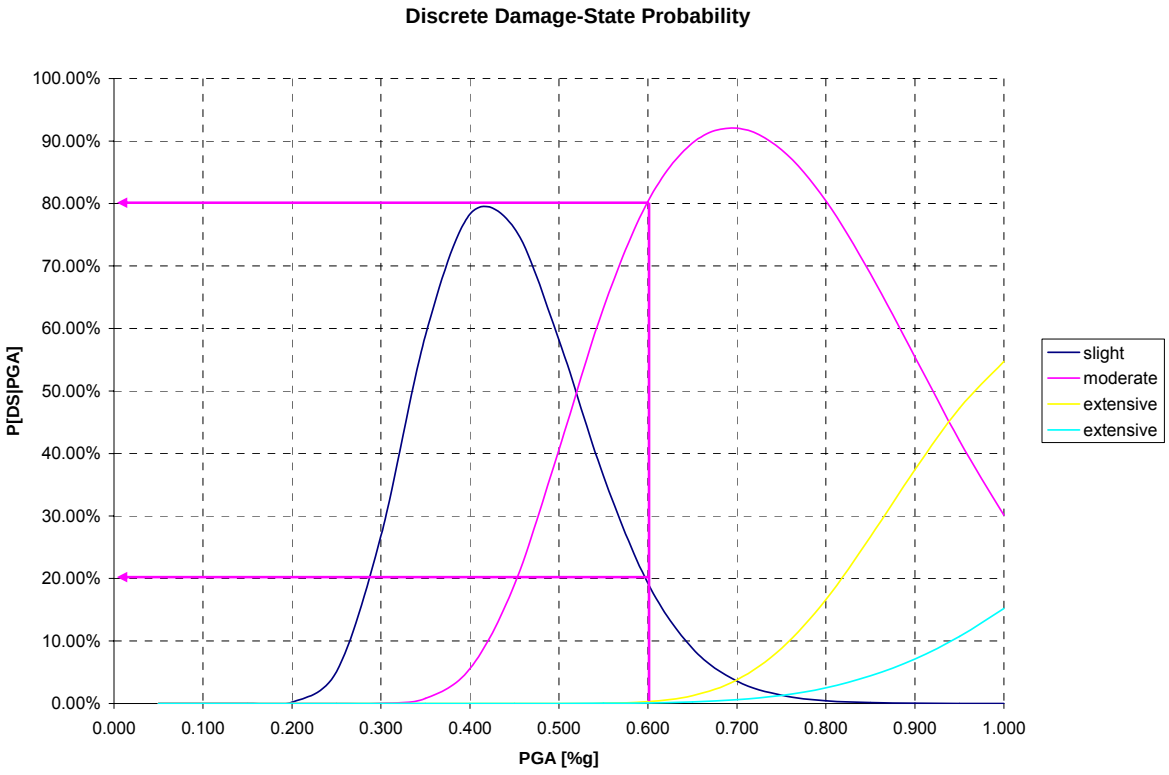

Figure 7.3 Discrete damage state probability for the four story office building.

$$
\begin{aligned}
&\textit{Monetary Losses} = \\
&\quad \$1{,}750{,}000.00 * 0\% * 20\% \\
&+ \$1{,}750{,}000.00 * 10\% * 80\% \\
&+ \$1{,}750{,}000.00 * 50\% * 0\% \\
&+ \$1{,}750{,}000.00 * 100\% * 0\% \\
&= \$140{,}000.00
\end{aligned}
$$

$$\textit{Monetary Losses} = \sum (\textit{structural cost} \cdot \textit{Percentage}(DS) \cdot P[DS \mid PGA] \qquad \textbf{(7.4)}$$

Where:

Percentage (DS) = percentage of loss expected at damage state DS (given in table 7.2)

P[DS|PGA] = discrete probability that a certain damage state will be reached for a specific PGA value.

Table 7.3. Monetary Losses for Post-Northridge Connections

SLIGHT	MODERATE	EXTENSIVE	COMPLETE
$ 0.00	$ 2.50	$ 12.50	$ 25.00
$ -	$140,000.00	$ -	$ -

The replacement value for an earthquake having a PGA of 0.6g is expected to be $140,000.00. This amount of money is about 8% of the structure cost, and about 1.6% of the total building's cost.

If the building was built using Pre-Northridge connections, the monetary losses would be as shown in Table 7.4.

Table 7.4 Monetary Losses for pre-Northridge Connections

SLIGHT	MODERATE	EXTENSIVE	COMPLETE
$ 2.00	$ 5.00	$ 20.00	$ 25.00
$ 28,000.00	$280,000.00	$ -	$ -

Therefore, the replacement value would be $308,000.00 if Pre-Northridge connections were used. The monetary losses represent 18% of the structure's cost, and 4% of the total building's cost.

The difference between the Post-Northridge connections and the Pre-Northridge connections cost is $168,000.00. In other words, the amount of losses expected is 2.2 times larger when Pre-Northridge connections are used.

7.4 Loss Functions Estimation from Charts

To simplify the estimation of damages one can use charts that indicate the amount of monetary damage. Table 7.5 shows the values needed to create such chart.

Table 7.5. Cost/ft^2 for the Pre-Northridge and Post-Northridge Conditions.

Discrete Fragility Curves					PRE	POST
PGA	Slight	Moderate	Extensive	Complete	COST/AREA	COST/AREA
0.05	0.00%	0.00%	0.00%	0.00%	$ 0.00	$ 0.00
0.1	0.00%	0.00%	0.00%	0.00%	$ 0.00	$ 0.00
0.15	0.00%	0.00%	0.00%	0.00%	$ 0.00	$ 0.00
0.2	0.20%	0.00%	0.00%	0.00%	$ 0.00	$ 0.00
0.25	5.63%	0.01%	0.00%	0.00%	$ 0.00	$ 0.11
0.3	29.78%	0.22%	0.00%	0.00%	$ 0.01	$ 0.61
0.35	62.43%	2.12%	0.00%	0.00%	$ 0.05	$ 1.35
0.4	78.14%	9.36%	0.00%	0.00%	$ 0.23	$ 2.03
0.45	72.21%	24.47%	0.00%	0.00%	$ 0.61	$ 2.67
0.5	54.45%	44.83%	0.00%	0.01%	$ 1.12	$ 3.33
0.55	35.14%	64.65%	0.03%	0.04%	$ 1.63	$ 3.95
0.6	19.98%	79.53%	0.33%	0.13%	$ 2.06	$ 4.48
0.65	10.23%	87.92%	1.51%	0.33%	$ 2.47	$ 4.99
0.7	4.82%	89.83%	4.63%	0.72%	$ 3.01	$ 5.69
0.75	2.12%	85.77%	10.70%	1.41%	$ 3.83	$ 6.82
0.8	0.88%	76.63%	19.99%	2.50%	$ 5.04	$ 8.47
0.85	0.35%	63.98%	31.58%	4.09%	$ 6.57	$ 10.55
0.9	0.13%	49.90%	43.69%	6.27%	$ 8.28	$ 12.80
0.95	0.05%	36.43%	54.44%	9.08%	$ 9.99	$ 14.98
1	0.02%	24.98%	62.49%	12.51%	$ 11.56	$ 16.87

Plotting the values in Table 7.5 results in the graph shown in Figure 7.4.

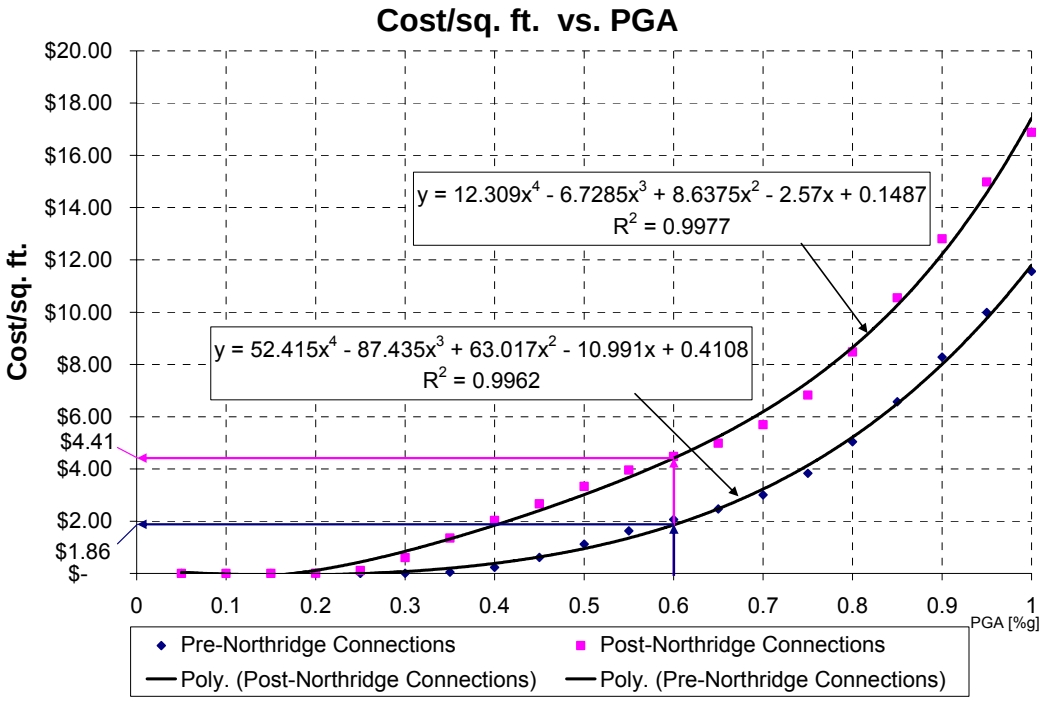

Figure 7.4 Graph of the cost per square feet vs. PGA.

The data obtained for each pair of ordinates has been plotted in Figure 7.4. A polynomial distribution of fourth degree has been fitted to the data in the figure, which results in a good approximation of the plotted points. For the Pre-Northridge Condition the equation is as follows:

$$Cost / Area = 12.30(PGA)^4 - 6.7285(PGA)^3 + 8.6375(PGA)^2 - 2.57(PGA) + 0.1487 \qquad \textbf{(7.5)}$$

For the Post-Northridge condition the equation is:

$$Cost / Area = 52.415(PGA)^4 - 87.435(PGA)^3 + 63.017(PGA)^2 - 10.991(PGA) + 0.4108 \quad \textbf{(7.6)}$$

Entering Table 7.5 with a 0.6g value, a $2.06 cost per square feet is obtained for the Post-Northridge condition. For the Pre-Northridge condition the cost per square feet is $4.48. These values can also be obtained using equations 7.6 and 7.7:

$$Cost / Area = 12.30(0.6)^4 - 6.7285(0.6)^3 + 8.6375(0.6)^2 - 2.57(0.6) + 0.1487 = \$4.41/ ft^2 \quad \textbf{(7.7)}$$

With this cost, the structural replacement cost can be estimated by multiplying the cost per square feet by the building area,

$$Cost = \$4.41/ ft^2 (70{,}000\, ft^2) = \$308{,}700.00 \quad \textbf{(7.8)}$$

In a similar way, for the Post-Northridge condition, the replacement cost is:

$$Cost / Area = 52.415(0.6)^4 - 87.435(0.6)^3 + 63.017(0.6)^2 - 10.991(0.6) + 0.4108$$
$$Cost / Area = \$1.86 / ft^2 \quad \textbf{(7.9)}$$

$$Cost = \$1.86 / ft^2 (70{,}000\, ft^2) = \$130{,}200.00 \quad \textbf{(7.10)}$$

A 0.23% and 5.7 % percent error is obtained for the Pre-Northridge condition and Post-Northridge condition, respectively. Although this error is small enough, it could be reduced by directly using the values from Table 7.5.

8 CONCLUSIONS AND FUTURE WORK

8.1 Introduction

This chapter describes the work and summarizes the findings of the thesis. It also describes the conclusions drawn from the project and presents recommendations for future work.

8.2 Summary and Conclusions

This thesis presented a method for estimating damages in steel buildings in Puerto Rico. A non-linear dynamic analysis was performed to the 91 models analyzed. The maximum inter-story drift was obtained for each of the earthquake records from the nonlinear analyses. With this, analytical fragility curves that describe the probability of damage to the buildings were created.

Fragility curves were created for steel buildings depending (1) on its occupancy, and (2) on the number of stories. Three occupancy classes were considered: offices and commercial buildings, storage buildings and industrial buildings. A fragility curve was created for each of these occupancies. Also, three categories based on the number of stories were used for the fragility curves: low-rise buildings, mid-rise buildings and high-rise buildings. Finally, a general curve which includes the statistics of all buildings was created. This general curve can give an overall idea of the general seismic behavior of steel buildings in Puerto Rico. Furthermore, it can be used to compare the general behavior of buildings made with different materials.

A simplified method was proposed as a qualitative way of describing the damage. This method serves to get an initial estimate of the expected damage by using a very simple linear equation. From this linear equation the average maximum drift value is obtained and this information is used to classify the building damage among the damage states.

Having in mind that the final desired output is to obtain the monetary losses that a certain building will suffer should an earthquake occur, plots that relate the cost per square foot of area with the peak ground acceleration were created. This plots allows one to very easily estimate the monetary damage in any steel building subjected to an earthquake with known intensity (PGA). In order to estimate the monetary losses, it is essential to know the cost of the building and what portion of the total building's cost corresponds to the structure. The plots generated can be easily changed to consider the specific cost of the building in different regions.

Based on the fragility curves obtained, the most significant conclusions are summarized below:

- Storage buildings are the most vulnerable, followed by the Industrial buildings and finally by the Office/Commercial buildings.
- An earthquake of 0.1g would not cause damage to any building
- Before 0.6g the complete damage scenario does not appears for any building
- Low-Rise buildings are the most vulnerable, followed by High-Rise buildings and by Mid-Rise buildings.

8.3 Recommendations for Future Work

After reviewing the plans of many steel buildings, it was observed that it is very common in Puerto Rico to use shear walls in mid-rise and high-rise steel buildings. Most of the time when this happens, the shear walls are designed to resists most, if not all, of the earthquake induced forces. This type of mixed buildings was not considered in this investigation, but it will be of much interest to study it since the expected behavior of such combined buildings could be very different to those studied here.

The response parameter used in this thesis was the inter-story drift. The maximum inter-story drift for the entire building subjected to a given ground acceleration intensity was recorded. However, the buildings could reach a maximum drift in a particular story while some other stories do not necessarily reach such a high drift. Having in mind that the drift value varies for each story, it will be interesting to study the building story by story, taking the inter-story drift of every story into account, not only the maximum value.

The soil–structure interaction was not considered in this research. The soil underneath the building could increase or decrease the system response. It would be subject of further study to include such effects.

The fragility curves in this research were calculated using analytical models. It will be helpful to do some experimental work. The beam to column connections could be studied and the rotations causing certain damage could be verified.

If an earthquake occurs, it could provide valuable data that would help in the validation of the analytical models. If such event occurs, it would be very important to conduct a survey

and gather the damage information. This information could be combined with the existing analytical data by using available Bayesian methods (Singhal and Kiremidjian 1998).

REFERENCES

AISC (2005). Steel Construction Manual, 13th Edition. American Institute of Steel Construction (2005). Chicago, IL.

Applied Technology Council (ATC), 1985, ATC-13, Earthquake Damage Evaluation Data for California. Report prepared for the Federal Emergency Management Agency, Washington, D.C.

Brookshire, D. S., S. E. Chang, H. Cochrane, R. A. Olson, A Rose, and J. Steenson, 1997, "Direct and Indirect Economic Losses from Earthquake Damage," Earthquake Spectra, Volume 13, No. 4, p. 683-701.

Chopra, A.K., 2001, "Dynamics of Structures, Theory and Applications To Earthquake Engineering", Second Edition, Prentice Hall, NJ.

Computers and Structures, Inc., 2002, "SAP2000 Analysis Reference Manual", Berkeley, California.

Ellingwood, B.R., Rosowsky, D.V., Li, Y., Kim, J.H., 2004, "Fragility Assessment of Light-Frame Wood Construction Subjected to Wind and Earthquake Hazards", Journal of Structural Engineering, Vol. 130, No. 4, p. 1921-1930.

Federal Emergency Management Agency, 2002, "NEHRP Guidelines for the Seismic Rehabilitation of Buildings, FEMA-273", Washington, D.C.

Irizarry, J., 1999, "Design Earthquakes and Design Spectra for Puerto Rico's Main cities Based on World Wide Strong Motion Records", Master of Science Thesis, University of Puerto Rico, Mayagüez, Puerto Rico.

Karim, K.R., Yamazaki, F., 2001, “Effect of earthquake ground motions on fragility curves of highway bridge piers based on numerical simulation”, Earthquake Engineering and Structural Dynamics, Vol. 30, page 1839-1856.

Kircher, C.A., Nassar, A.A., Kustu, O., Holmes, W.T., 1997, "Development of Building Damage Functions for Earthquake Loss Estimation," Earthquake Spectra, Vol. 13, No. 4, p. 663-682.

Kircher, C.A., Reitherman, R.K., Whitman, R.V. Arnold, C., 1997. "Estimation of Earthquake Losses to Buildings", Earthquake Spectra, Vol. 13, No. 4, p. 703-720.

Kircher, C.A., 2003, “Earthquake Loss Estimation Methods for Welded Steel Moment-Frames Buildings”, Earthquake Spectra, Vol. 19, No. 2, p. 365-384.

Kunreuther, H., 1999, “Insurance as an Integrating Policy Tool for Disaster Management: The Role of Public-Private Partnerships”, Earthquake Spectra, Vol. 15, No. 4, p. 725-745.

Murty, C.V. R., 2002, “IITK – BMTPC Earthquake Tip 01”, www.bmtpc.org.

National Institute of Building Sciences, 1997b, “Earthquake Loss Estimation Methodology HAZUS 97: Technical Manual”, Report prepared for the Federal Emergency Management Agency, Washington, D.C.

RAM International, L.L.C., 2002, “RAM Perform 2D-User Guide”

SAC Joint Venture, 2000, "Recommended Seismic Evaluation and Upgrade Criteria for Existing Welded Steel Moment-Frame Buildings, FEMA-351", Washington, DC.

Salmon, C. G., Johnson, J. E., 1996, Steel Structures, Design and Behavior, 4th Ed., Prentice Hall, New Jersey.

Shinozuka, M., Feng, M.Q., Kim, H., Uzawa, T., Ueda, T., 2001, "Statistical Analysis of Fragility Curves", University of Southern California, California.

Singhal, A., Kiremidjian, A.S.,1998, "Bayesian Updating of Fragility Curves with application to RC Frames", Journal of Structural Engineering, Vol. 124, No. 8, p.922-929.

Smyth, A.W., Altay, G., Deodatis, G., Erdic, M., Franco, G., Gülkan, P., Kunreuther, H., Luş, H., Mete, E., Seeber, N., Yüzügüllü, O., 2004, "Probabilistic Benefit-Cost Analysis for Earthquake Damage Mitigation: Evaluating Measures for Apartment Houses in Turkey", Earthquake Spectra, Volume 20, No. 1, p. 171-203.

University of California at Berkeley, 2000, "PEER Strong Motion Database", http://peer.berkeley.edu/smcat/

United States Geological Survey, 2003, "PGA Hazard Curves for Puerto Rico and the Virgin Islands", http;//earthquake.usgs.gov/research/hazmaps/products_data/Puerto-Rico-VI/puerto-rico/fig13b.pdf

Vázquez, D., López, R.R., and Suárez, L.E., 2002, "Comportamiento Sísmico y Rehabilitación de Residencias Soportadas en Columnas y Localizadas en Terrenos

Escarpados", Revista Internacional de Desastres Naturales, Accidentes e Infraestructura Civil, Vol. 2, No. 2.

Whitman, R.V., Anagnos, T., Kircher, C.A., Lagorio, H.J., Lawson, R.S., Schneider, P., 1997, "Development of a National Earthquake Loss Estimation Methodology", Earthquake Spectra, Volume 13, No. 4, p. 643-661.

APPENDICES

APPENDIX A. EXAMPLE OF THE PUSH OVER METHOD

A.1 Introduction

This appendix intends to demonstrate the methodology used in the Publication "*FEMA-351: Recommended Seismic Evaluation and Upgrade Criteria for Existing Welded Steel Moment-Frame Buildings"*. This procedure is applied here to quantify the expected losses in a one story building located in Moca, Puerto Rico.

A flowchart of the steps followed is shown below:

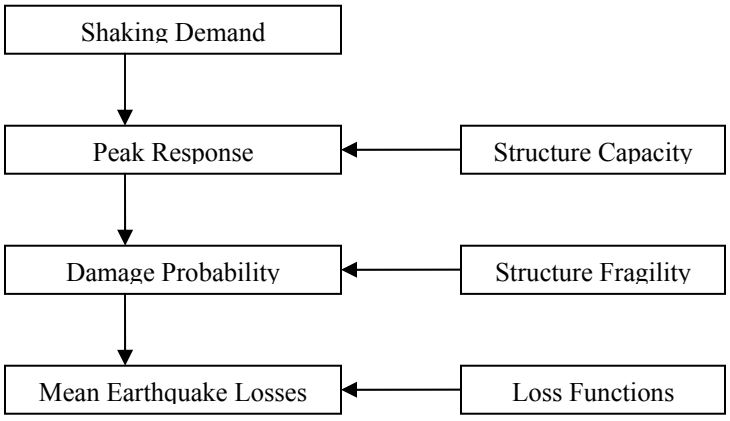

Figure A.1. Flowchart of the approach followed.

A.2 Description of the Building Analyzed

Type: Industrial Building

Area: 12,268 sq. ft.

Owner: Property of the Municipal Government of Moca

Location: PR 125 Street Industrial Zone, Moca, PR

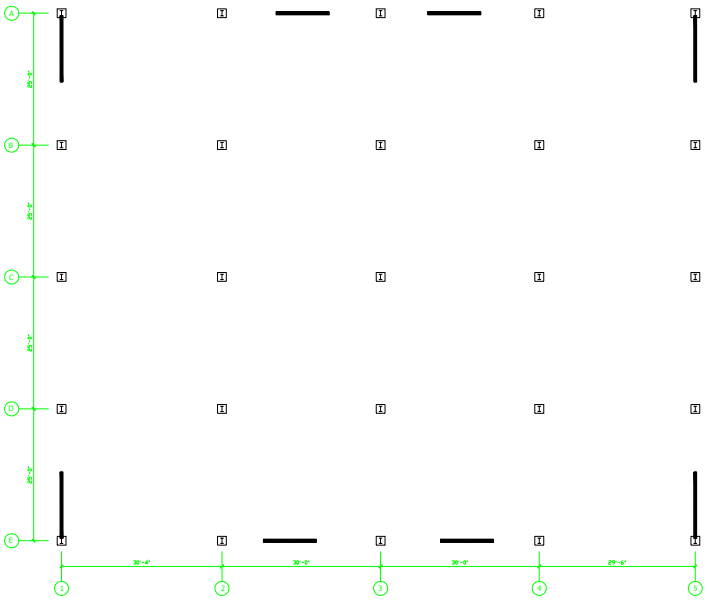

Figure A.2 Structural plan view of the industrial building analyzed.

A.3 **Description of the Building Analyzed**

The structure was modeled in the nonlinear version of SAP2000. A 3D finite element model of the structure was analyzed.

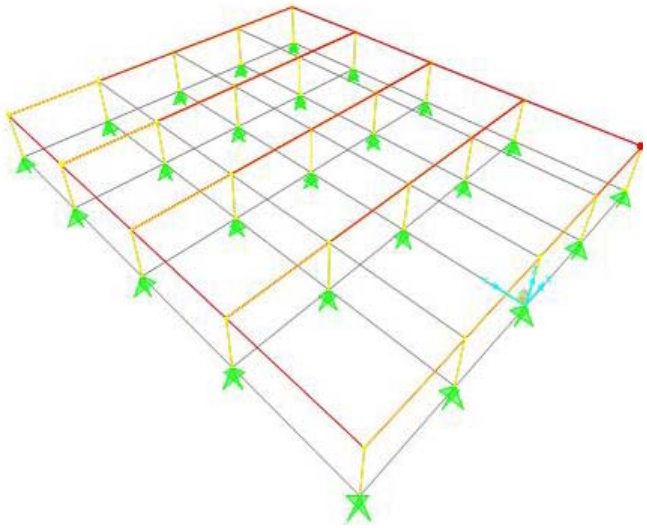

Figure A.3 3D model of the structure made in SAP2000.

After the building model was created (Figure A.3), a non-linear push-over analysis of the structure was run. The push-over analysis output is a spectral acceleration vs. spectral displacement graph. This graph gives the capacity curve and the demand curve which are needed to find the peak building response.

The push-over curve obtained from SAP2000 is shown in Figure A.4.

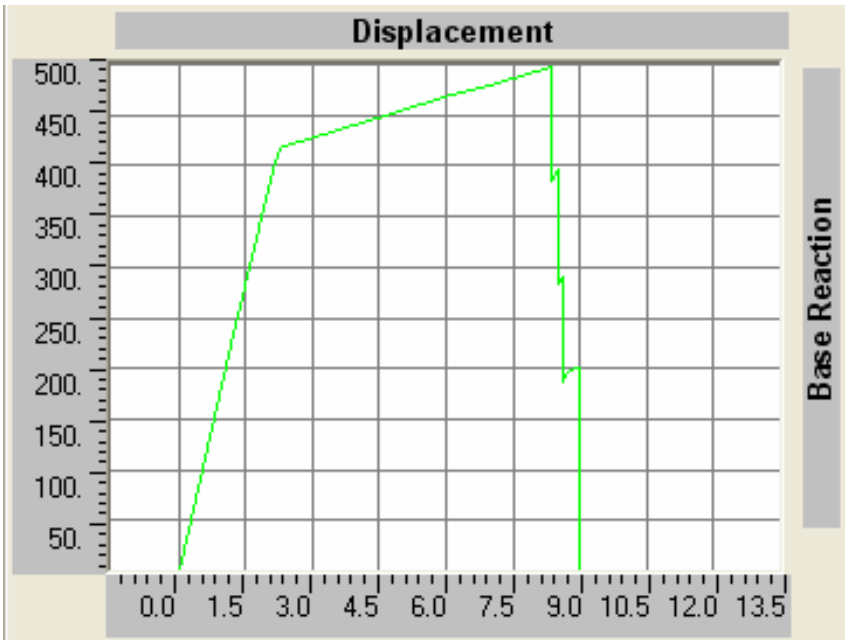

Figure A.4 Push-over curve, base reaction vs. displacement.

The capacity curve is obtained from the push-over graph. A coordinate transformation from base shear and roof displacement to coordinates of spectral acceleration and spectral displacement must be made. This coordinate transformation is done by using formulas A.1 and A.2 shown below.

$$S_{Di} = \alpha_2 \Delta_i \qquad \textbf{(A.0.1)}$$

$$S_{Ai} = \frac{\left(V_i / W\right)}{\alpha_1} \qquad \textbf{(A.0.2)}$$

Where:

α_1 = fraction of building weight effective in the fundamental mode in the direction under consideration

α_2 = fraction of building height at the elevation where the fundamental-mode displacement is equal to spectral displacement

Δ_i = displacement at point "i" on the pushover curve

V_i = base shear force at point "i" on the pushover curve

W = building weight [kips]

Once the coordinate transformation is performed, the graph shown on figure A.5 is created.

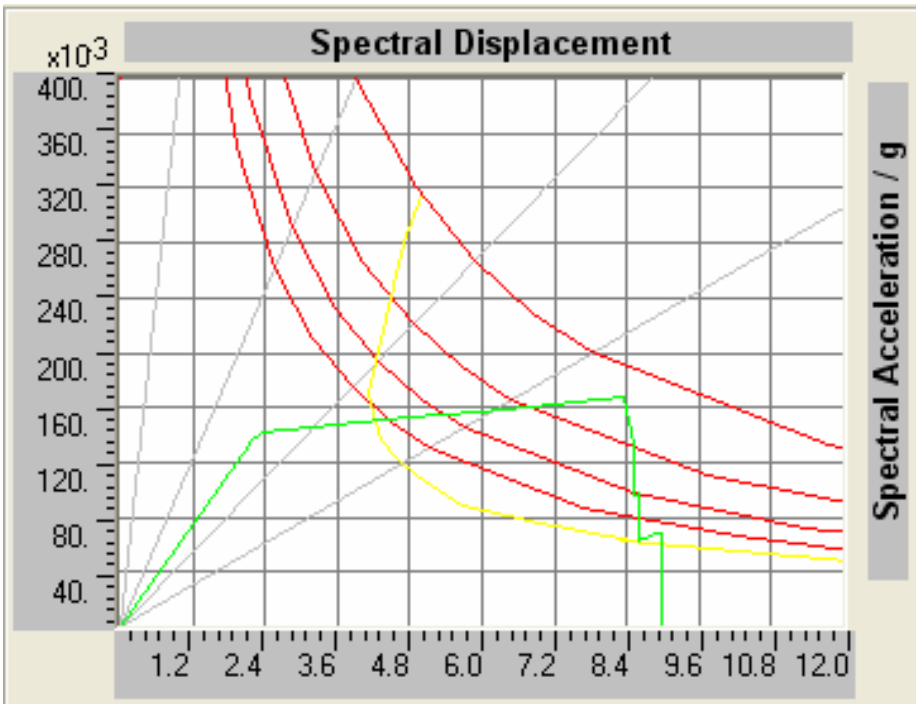

Figure A.5 Spectral displacement vs. spectral acceleration plot.

From Figure A.5, the point where the Capacity Curve intersects with the Demand Curve is obtained (4.214, 0.150). With that point the Discrete Damage Probability Curve (Figure A.6) is entered and the probability of damage for each of the damage states (slight, moderate, extensive, complete) is calculated.

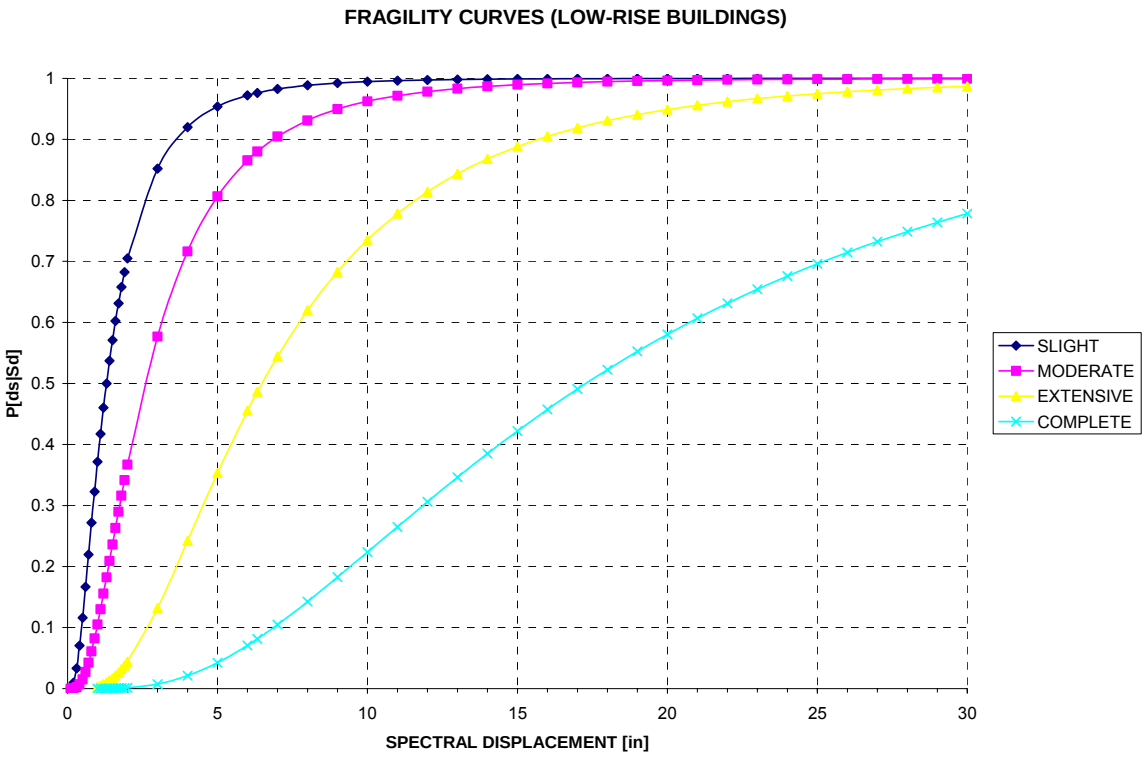

Figure A.6 Fragility curves for high-code seismic design level

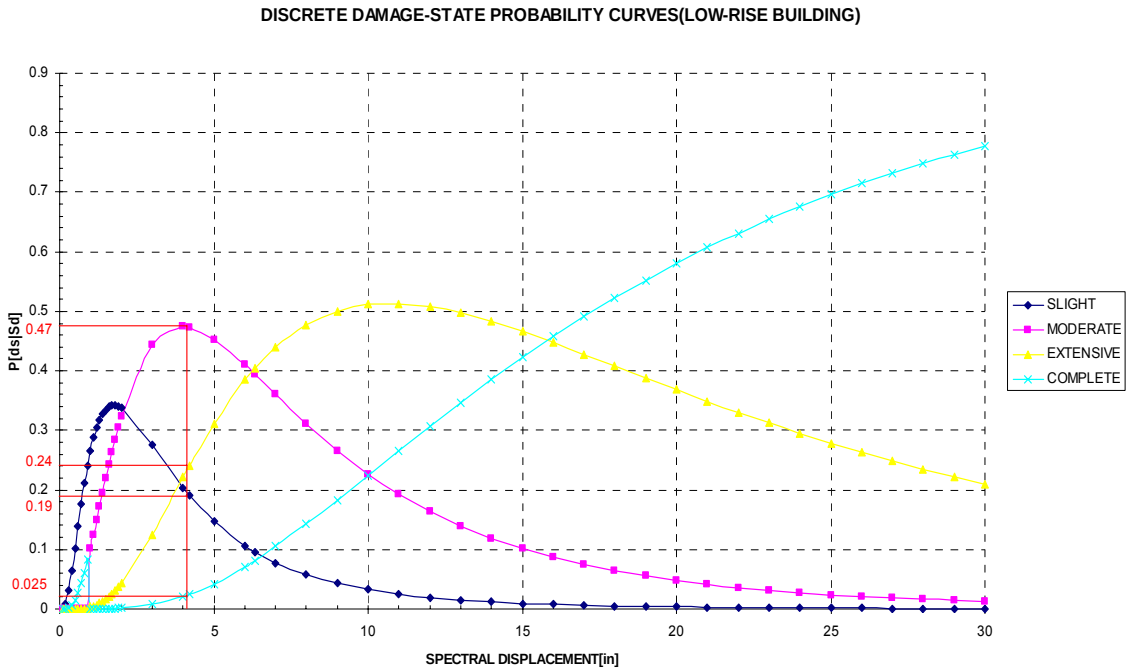

Figure A.7 Probability density functions for damage

The fragility curves relate the probability of reaching or exceeding a certain structural damage state. The following formula is used to create the fragility curves:

$$P[ds \mid S_d] = \Phi\left[\frac{1}{\beta}\ln\left(\frac{S_d}{S_{d,ds}}\right)\right] \qquad \textbf{(A.0.3)}$$

The values needed in equation A.3 are obtained from a representative data sample. The mean value ($S_{d,ds}$) and the standard deviation (β) were obtained from table 5.9a of the Hazus99-SR2 Technical Manual.

Now, having the damage probability we need the Loss Functions to finally estimate the cost. FEMA defines the structural cost of this type of buildings as 20% of the total cost. So for this example the cost/SF of the building is $125.00/SF so the structure will have a cost of $25.00/SF. The repair cost of slight damage is assumed to be zero on the basis that any

incidental damage under this category will not be required to be repaired. For the Moderate and Extensive structural damage the cost of repair is assumed to be 10% and 50% of the structural cost respectively.

Table A.1 Cost of Damage State DS

	Structural Damage State			
Damage State	Slight	Moderate	Extensive	Complete
Mean Loss Ratio	0%	10%	50%	100%
Mean Loss Rate [$/SF]	$0.00	$2.50	$12.50	$25.00

Table A.2 Cost Estimation for the analyzed building

DS	P[DS|4.2in]	Cost/SF	Cost	Cost for DS
slight	0.19016188	$ -	$ -	$ -
moderate	0.47263176	$ 2.50	$ 30,670.00	$ 14,495.62
extensive	0.24143068	$ 12.50	$ 153,350.00	$ 37,023.39
complete	0.0250029	$ 25.00	$ 306,700.00	$ 7,668.39
				$ 59,187.40

After the probability for each of the damage states is found, each probability is multiplied by its corresponding cost. The sum of each of the products obtained represents the total cost of replacement for the structure. For the industrial building studied in this example, an expected Spectral Displacement of 4.21 in will be translated into a total cost of $59,187.40. Table A.3 summarizes the cost for each of the damage states, as well as the total cost of repair for the structure being analyzed in this example.

In a similar way, plots of cost/SF vs. Spectral Displacement may be created and similar results are obtained. Figure A.8 shows the Cost/SF vs. Spectral Displacement [in] plots for the three categories of WSMF structures with Post-Northridge connections.

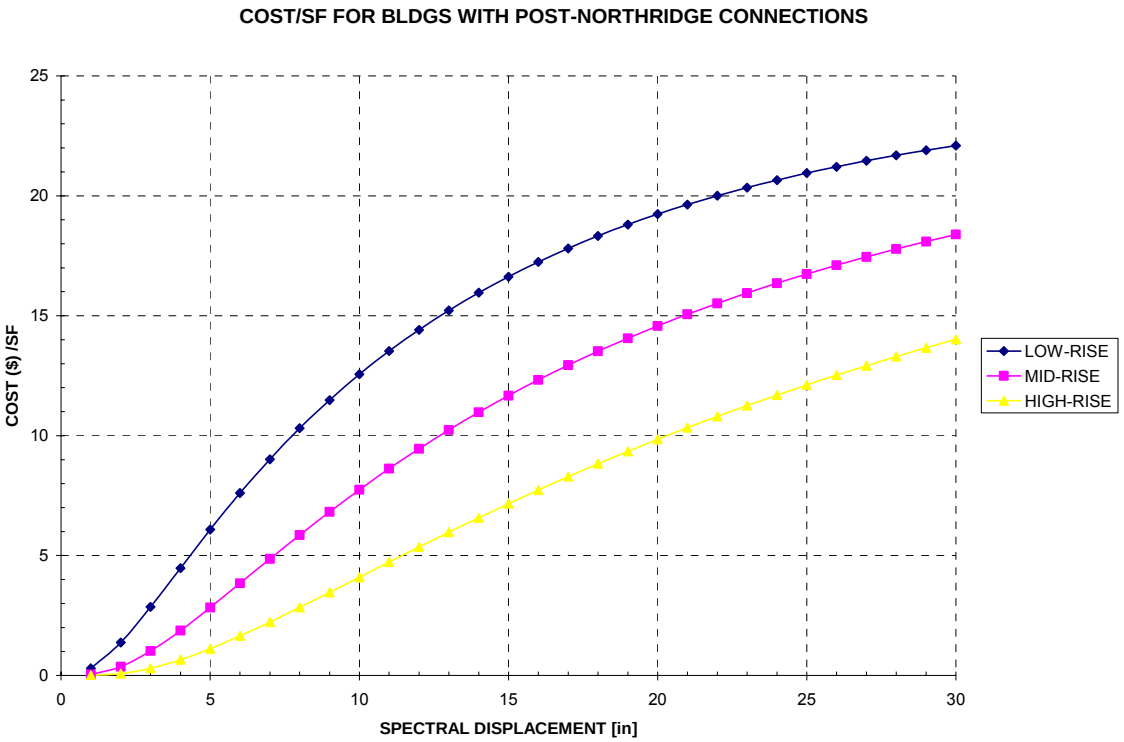

Figure A.8 Cost/SF vs. spectral displacement graph for buildings with Post-Northridge connections.

Table A.3 Costs associated for each Spectral Displacement.

LOW RISE BUILDINGS

	S	M	E	C
cost	$ -	$ 2.50	$ 12.50	$ 25.00

Sd	S	M	E	C	COST/SF
1	0.266221	0.10187	0.003344	3.79E-05	0.297418922
2	0.338003	0.322658	0.042844	0.001372	1.376495064
3	0.275398	0.444472	0.124679	0.007511	2.857439302
4	0.203674	0.474078	0.221162	0.021062	4.476258288
5	0.147276	0.453075	0.311043	0.042501	6.083234331
6	0.106539	0.409911	0.384699	0.070896	7.60591022
7	0.077728	0.360065	0.439807	0.104729	9.015986819
8	0.057351	0.311119	0.477566	0.142401	10.30738989
9	0.042826	0.266387	0.50053	0.182466	11.48424199
10	0.032358	0.227003	0.511532	0.223725	12.55477687
11	0.024725	0.193041	0.513204	0.265232	13.52844457
12	0.019092	0.164097	0.507807	0.306271	14.41459948
13	0.014888	0.139594	0.4972	0.346319	15.22195893
14	0.011716	0.118919	0.482872	0.385009	15.95842512
15	0.009298	0.101497	0.465989	0.422099	16.63107121
16	0.007437	0.086817	0.447456	0.457438	17.24619545
17	0.005993	0.074436	0.427967	0.490949	17.80939868
18	0.004862	0.063978	0.408044	0.522607	18.32566238
19	0.003969	0.055127	0.388078	0.552425	18.79942139
20	0.00326	0.04762	0.368358	0.580445	19.23463887
21	0.002693	0.041239	0.349089	0.606726	19.63485902
22	0.002236	0.035801	0.330419	0.631341	20.00325796
23	0.001866	0.031156	0.312444	0.65437	20.3426876
24	0.001564	0.027178	0.295228	0.675897	20.65571337
25	0.001317	0.023762	0.278804	0.696008	20.94464679
26	0.001113	0.020823	0.263186	0.714788	21.21157379
27	0.000945	0.018287	0.248374	0.73232	21.45837932
28	0.000805	0.016094	0.234355	0.748684	21.68676893
29	0.000688	0.014193	0.221109	0.763958	21.89828768
30	0.000591	0.012542	0.208609	0.778215	22.09433689

From Figure A.8 it would be easier to calculate the expected losses for a given building. Entering Figure A.8 with a spectral displacement of 4.21 inches for the structure analyzed we obtain a value of $5.80/SF. Multiplying this value by the total area of the building which is 12,268 SF, we get a total damage cost of $59,187.40.

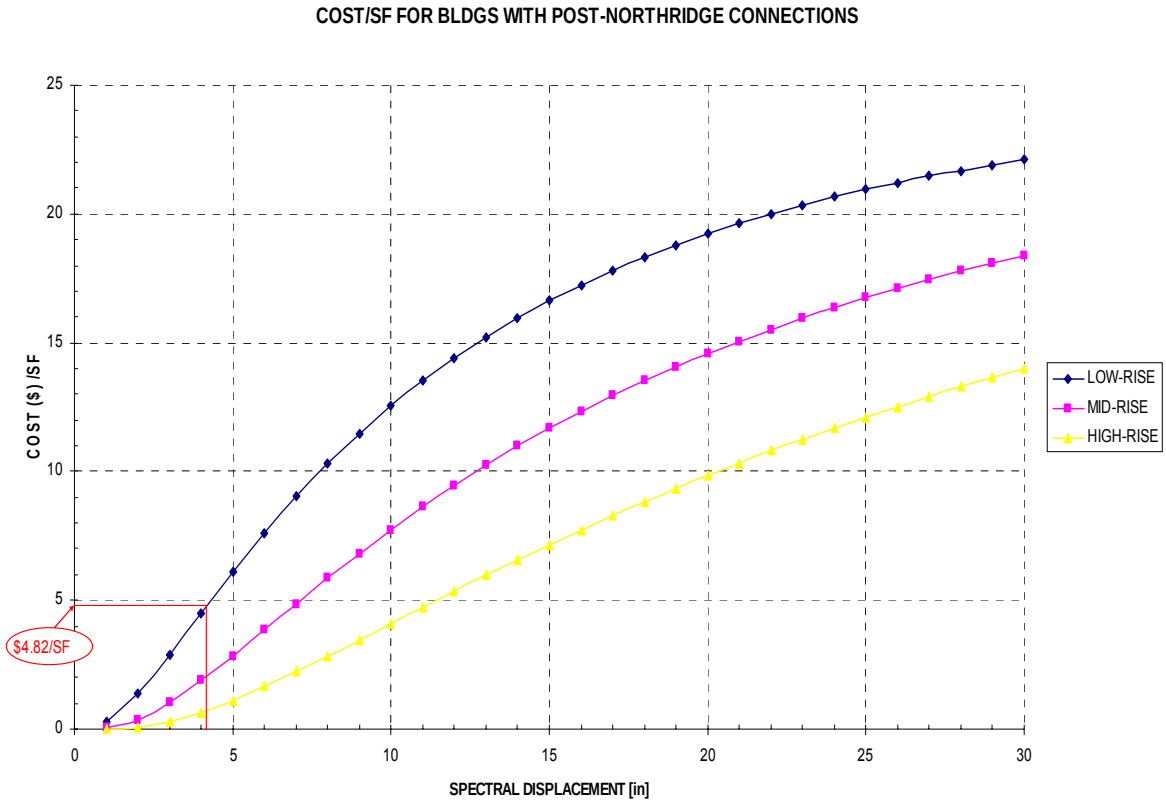

Figure A.9 Cost per area [ft^2] for a 6.33 in spectral displacement.

A.3 **Analysis of the Results**

The estimated total cost of the building is:

$$COST_{BUILDING} = {cost}/{SF} * (Area) = \left({\$125.00}/{ft^2}\right) * (12{,}268\,ft^2) = \$1{,}533{,}500.00$$

$$COST_{STRUCTURE} = {cost}/{SF} * (Area) = \left({\$25.00}/{ft^2}\right) * (12{,}268\,ft^2) = \$306{,}700.00$$

The structural loss obtained for a Spectral displacement of 4.214 inches is $59,187.40. This amount represents 19.3% of the total structural value, and a 3.86% of the building cost.

APPENDIX B. SIMPLIFIED METHOD TABLE

Table B.1 Simplified Method Coefficients

Description	a_0	b_0
Storage Room	0.0451	0.0017
Industrial Buildings	0.0413	0.0014
Commercial and Offices Building	0.0333	0.0014
Low-Rise Buildings	0.0401	0.0017
Mid-Rise Buildings	0.031	0.006
High-Rise Buildings	0.0354	0.0002

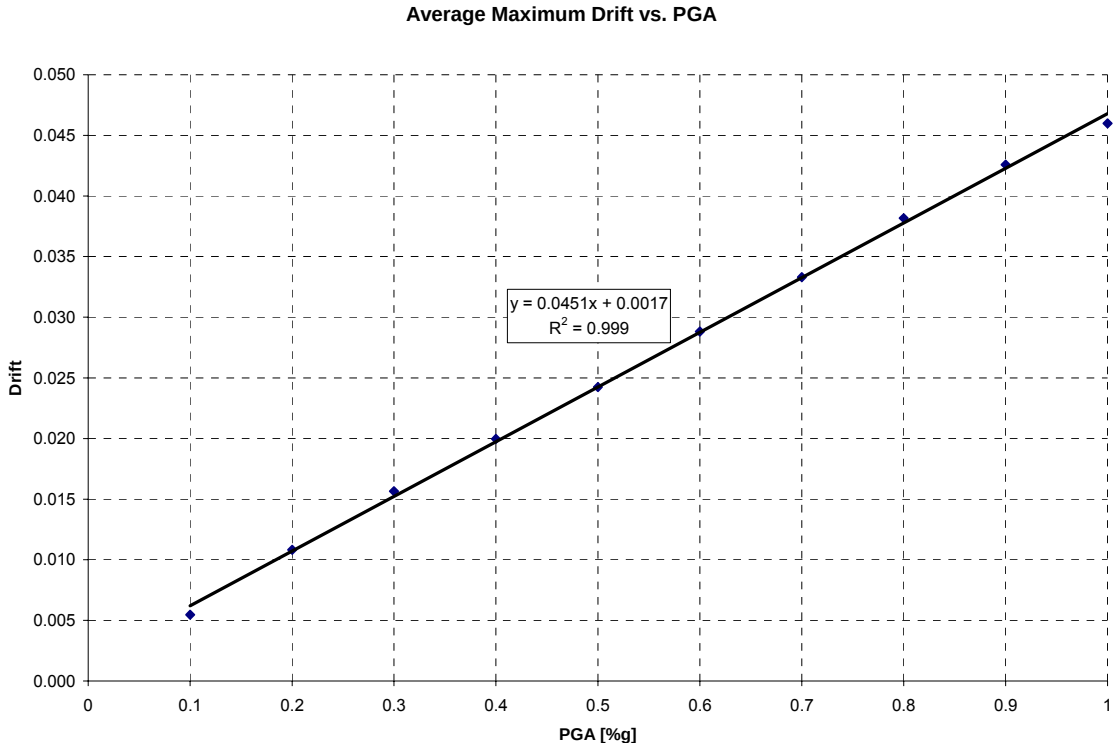

Figure B.1 Drift vs. PGA for storage room buildings

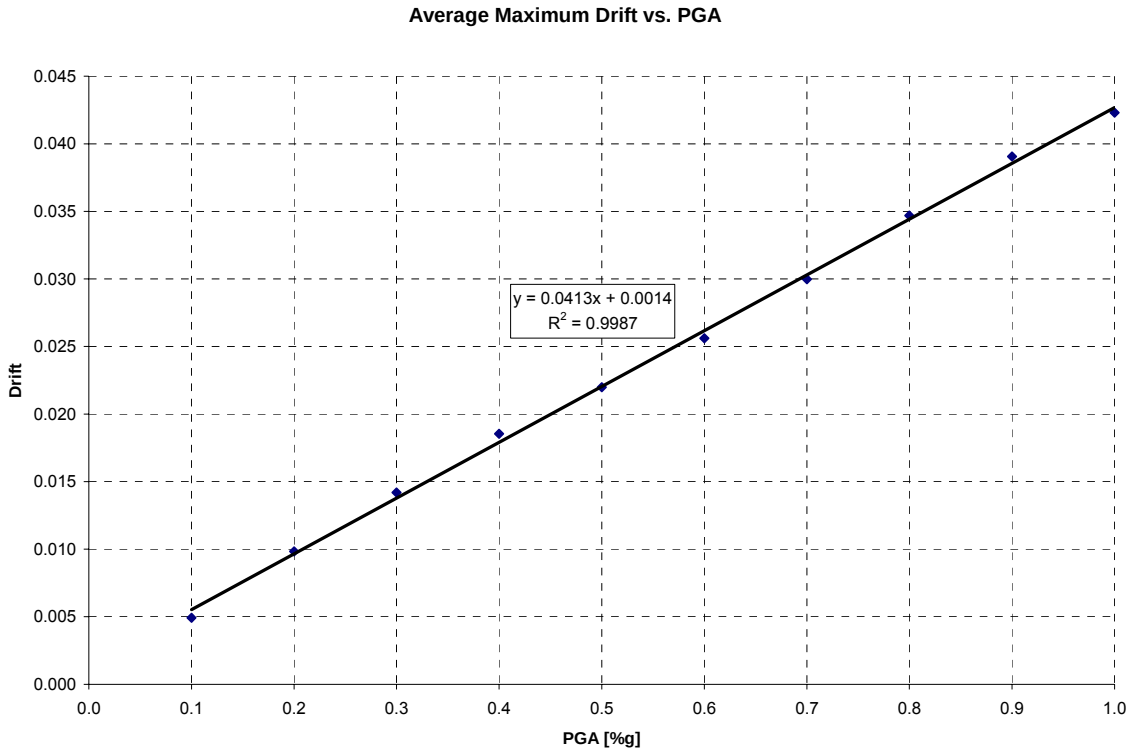

Figure B.2 Drift vs. PGA for industrial buildings

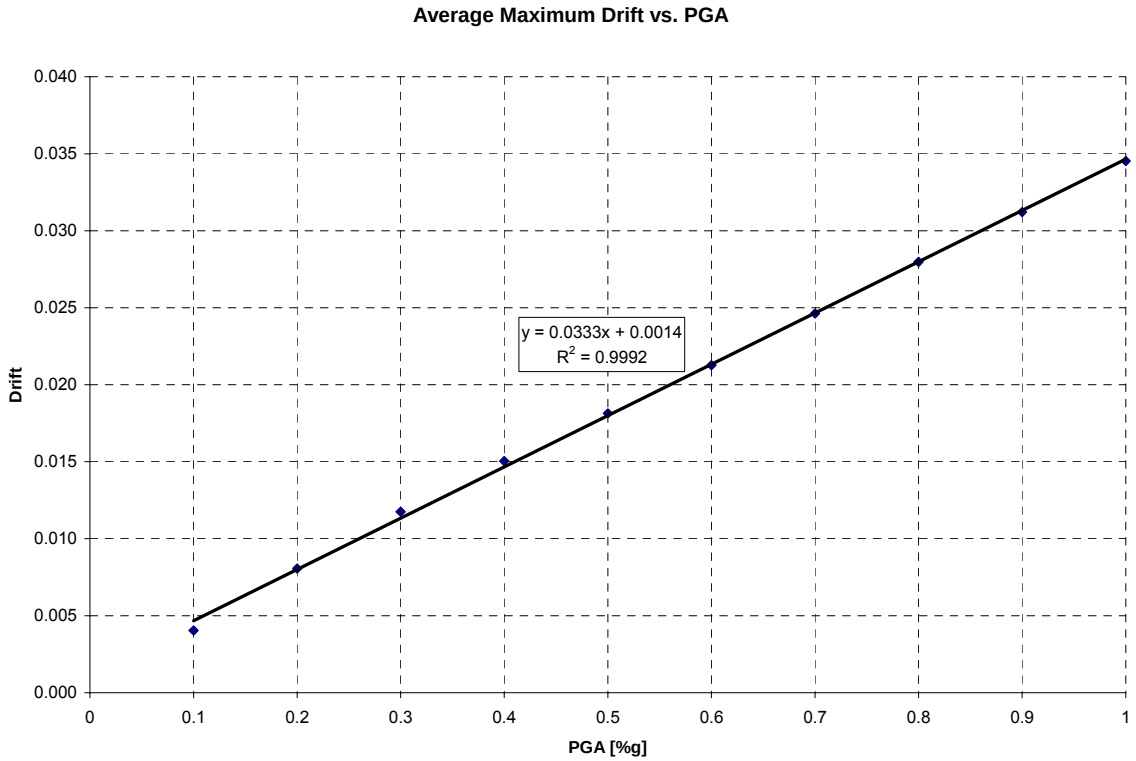

Figure B.3 Drift vs. PGA for commercial/offices buildings

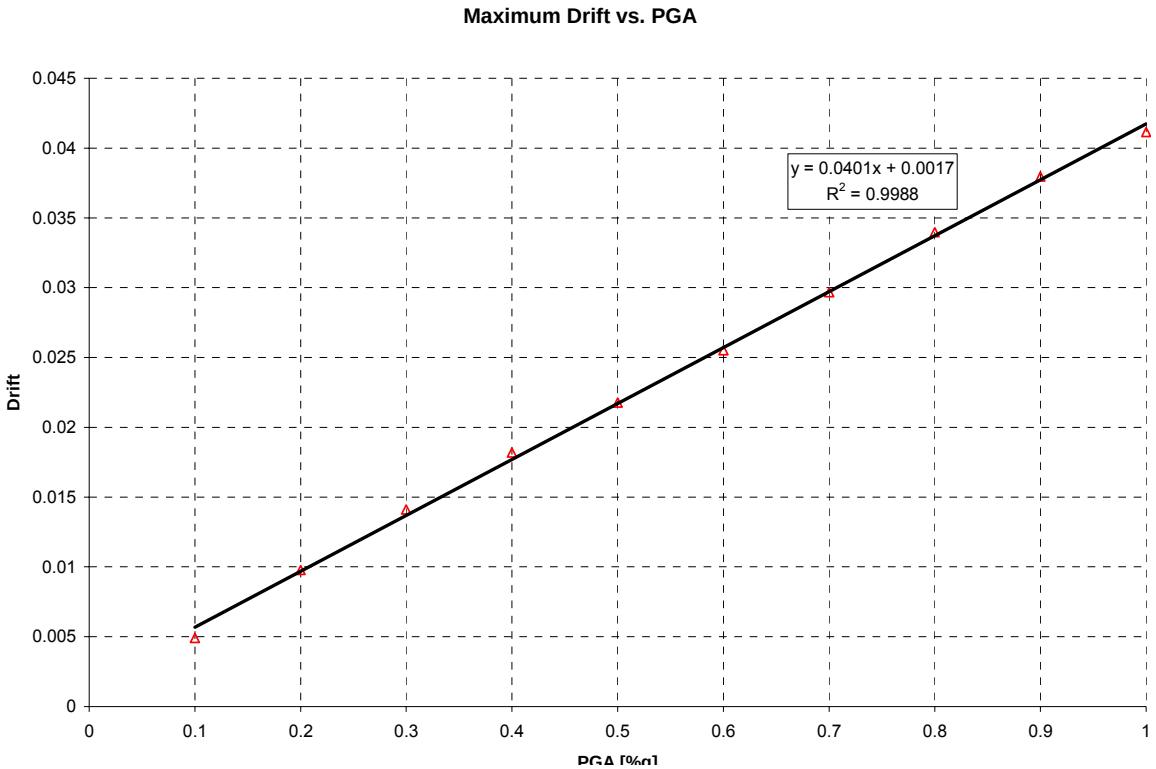

Figure B.4 Drift vs. PGA for Low-Rise buildings

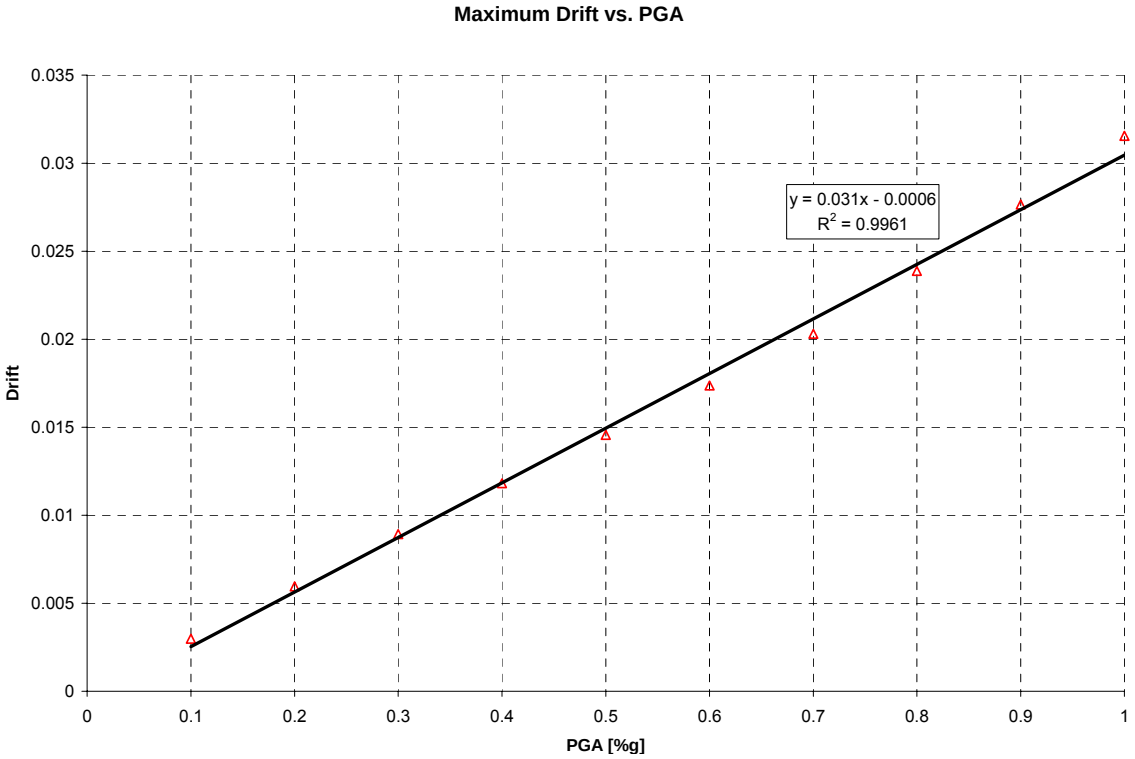

Figure B.5 Drift vs. PGA for Mid-Rise Buildings

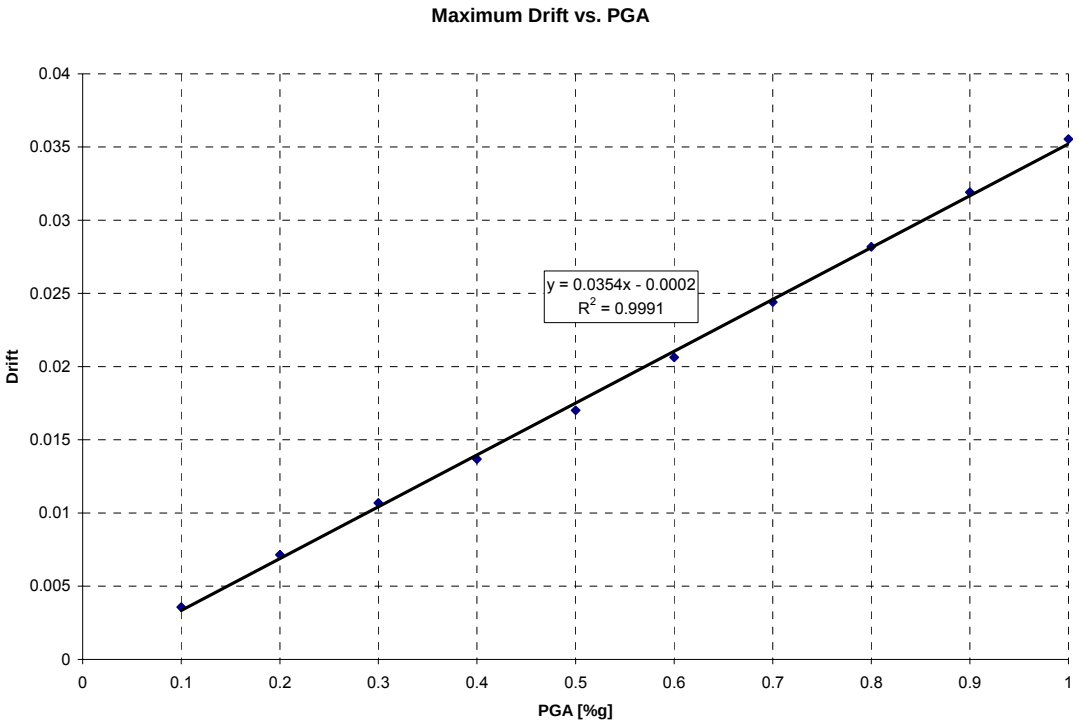

Figure B.6 Drift vs. PGA for High-Rise buildings

APPENDIX C. COST PLOTS

This appendix represents a set of charts giving the cost/area for a structure with assumed cost of $125.00/SF. The structural cost of the buildings was assumed to be 20% of the total building's cost, $25.00/SF.

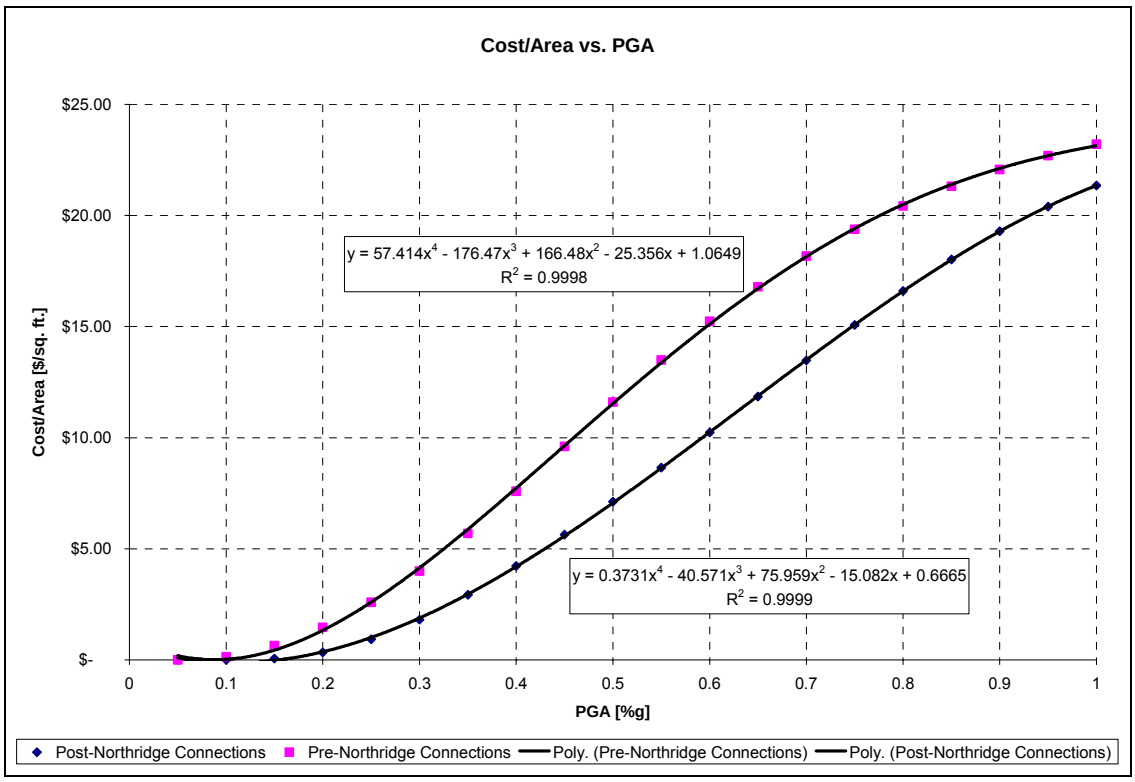

Figure C.1 Cost/Area vs. PGA for storage buildings

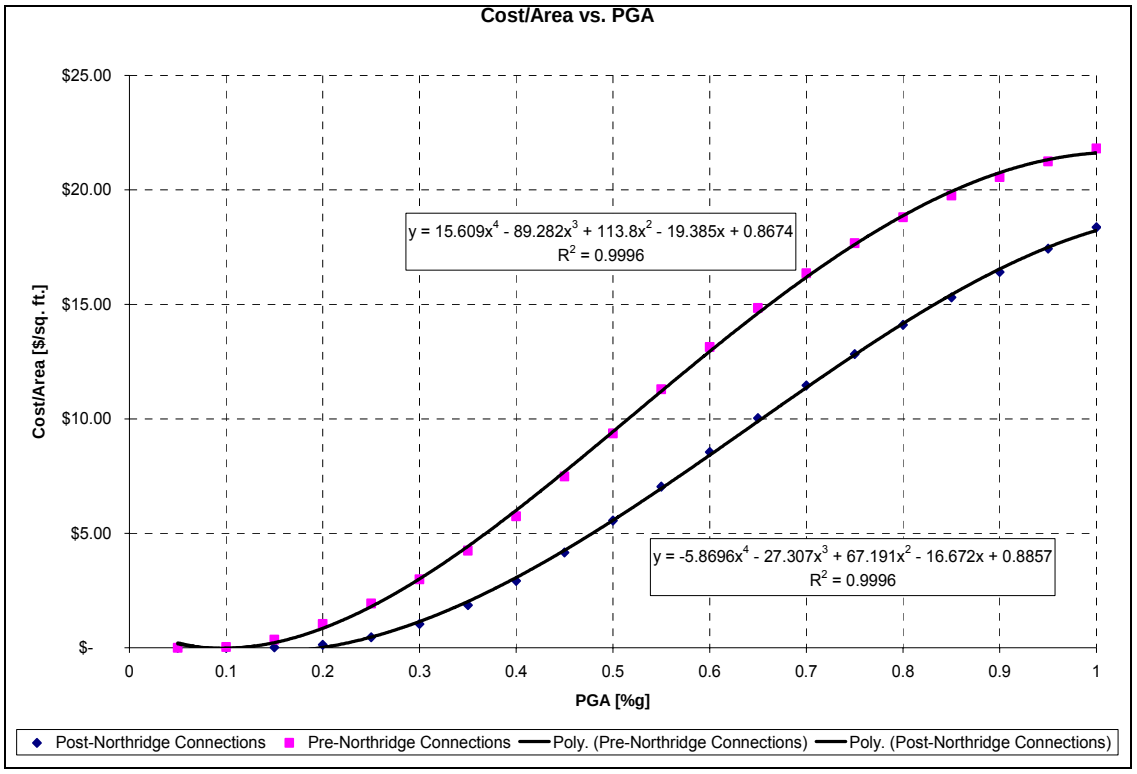

Figure C.2 Cost/Area vs. PGA for industrial buildings

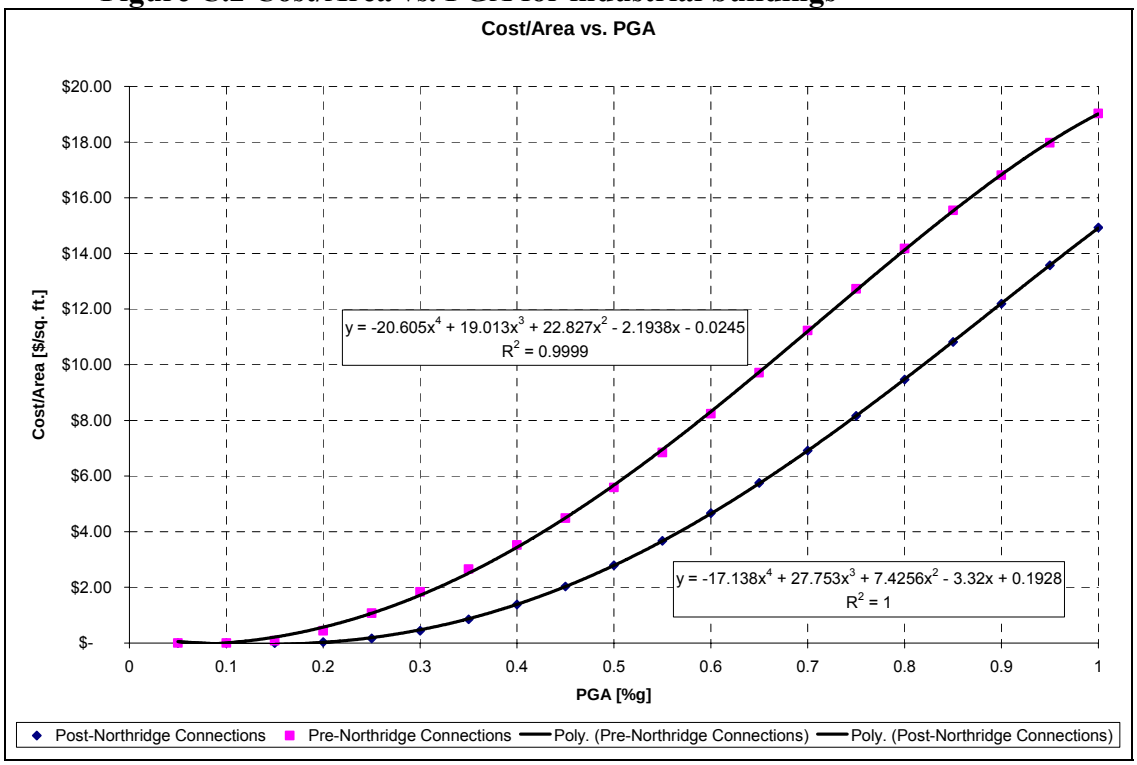

Figure C.3 Cost/Area vs. PGA for commercial/offices buildings

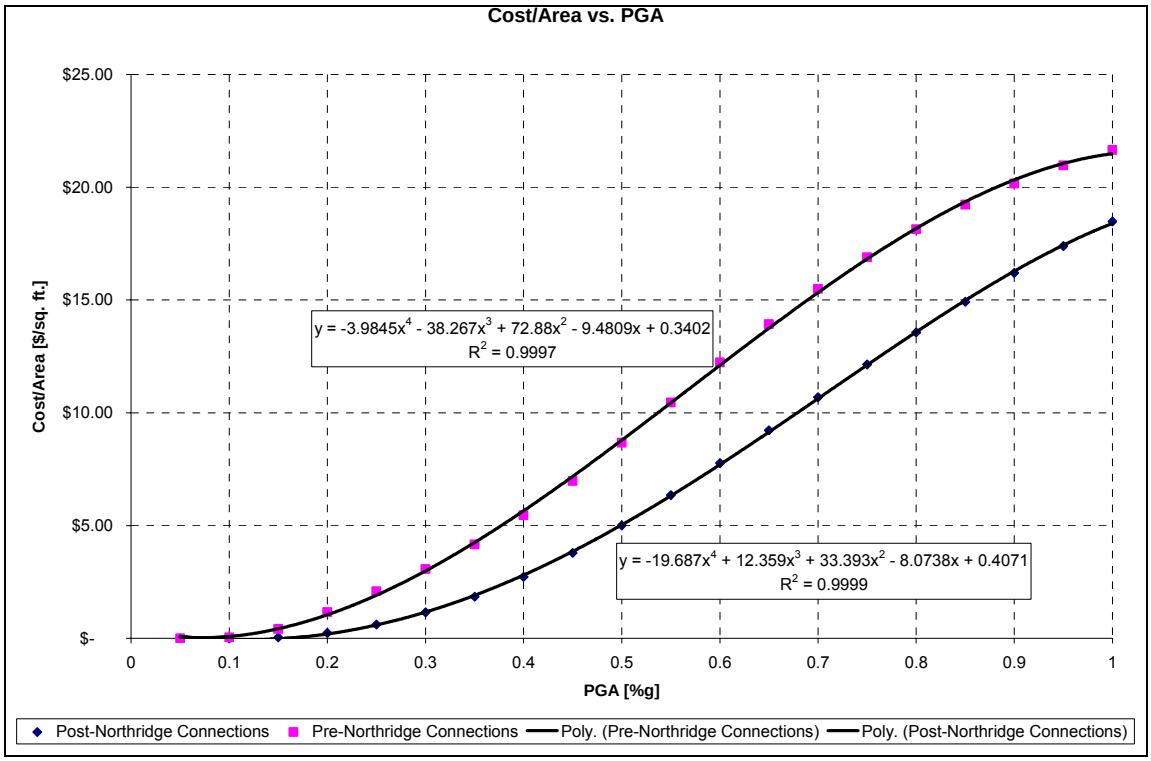

Figure C.4 Cost/Area vs. PGA for Low-Rise buildings

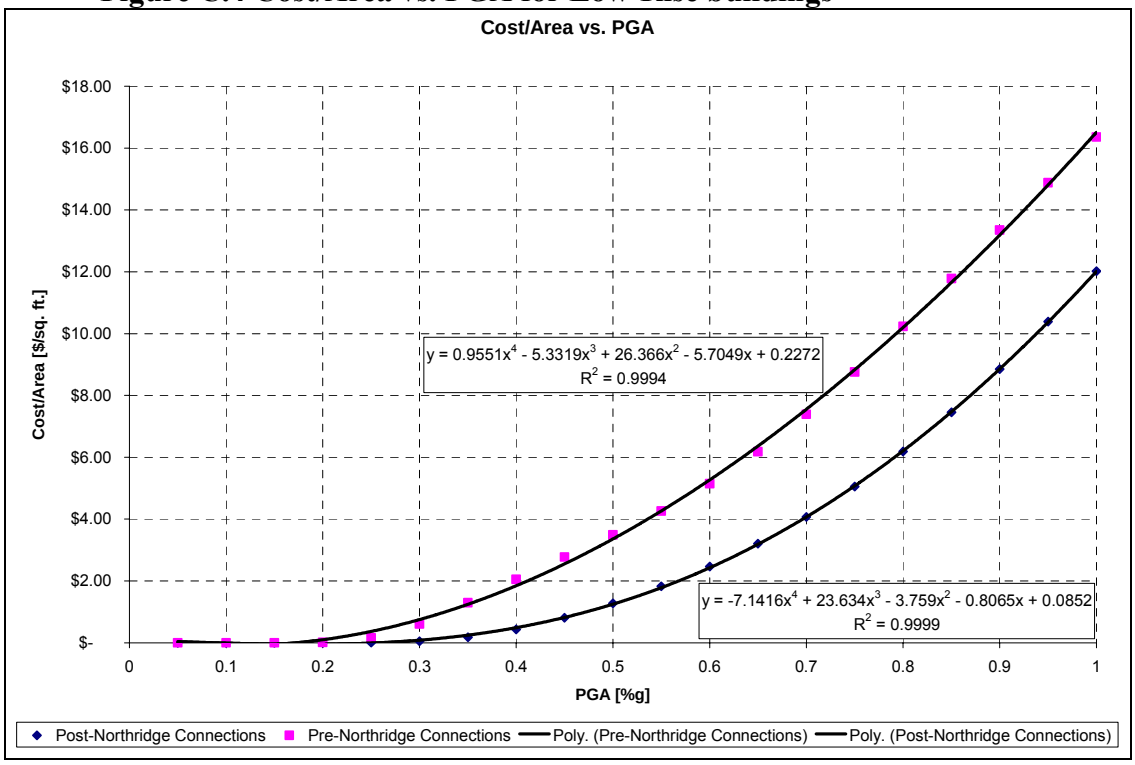

Figure C.5 Cost/Area vs. PGA for Mid-Rise buildings

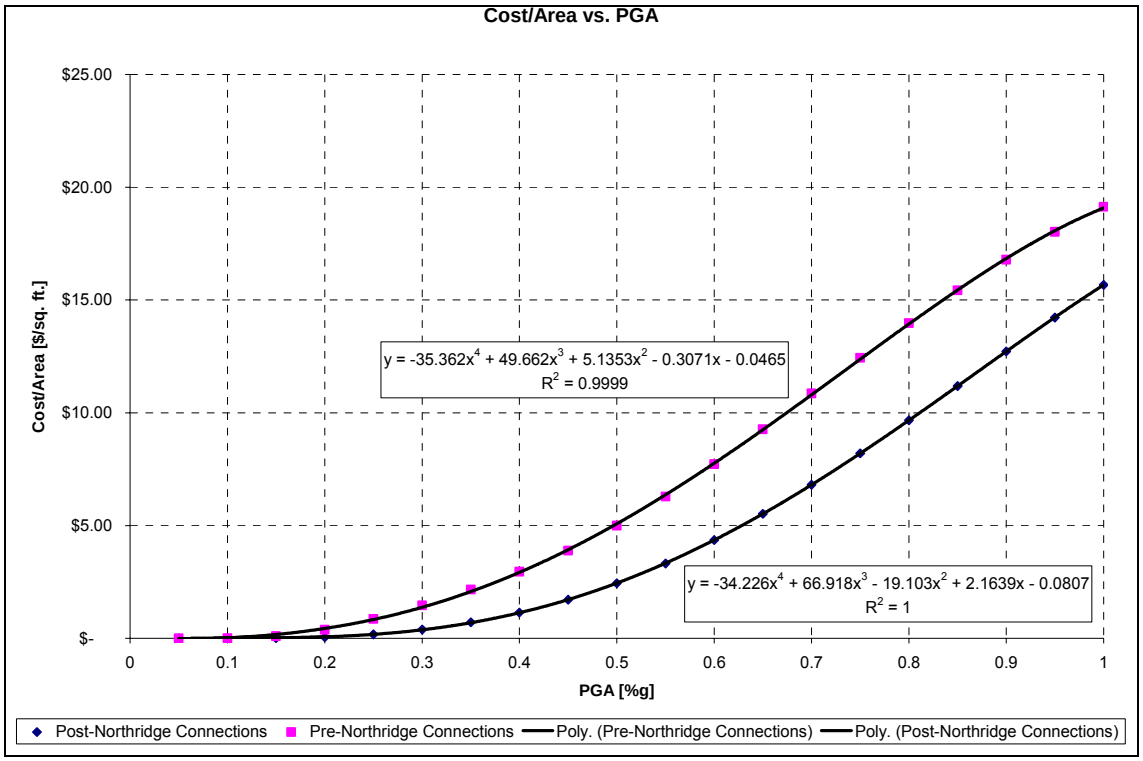

Figure C.6 Cost/Area vs. PGA for High-Rise buildings

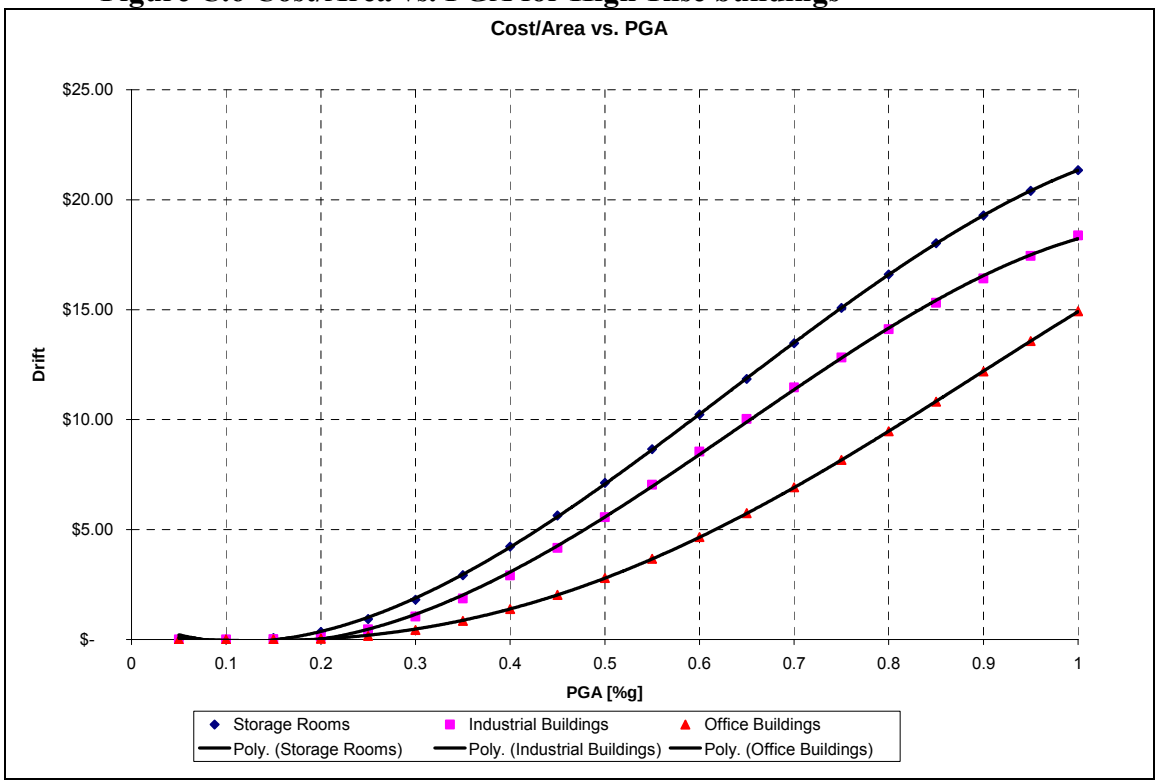

Figure C.7 Cost/Area vs. PGA for buildings depending on its occupancy